

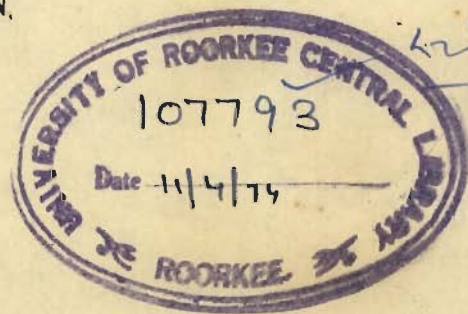
(T)
441-73
NAN

BEHAVIOUR OF RETAINING WALLS UNDER DYNAMIC LOADS

8977-78 ✓

A THESIS
submitted in fulfilment of the
requirements for the award of the degree
of
DOCTOR OF PHILOSOPHY
in
EARTHQUAKE ENGINEERING

By
P. NANDAKUMARAN,



SCHOOL OF RESEARCH AND TRAINING
IN EARTHQUAKE ENGINEERING
UNIVERSITY OF ROORKEE
ROORKEE (INDIA)

September 1973

SYNOPSIS

The current practice of considering the dynamic behaviour of retaining walls is to take into account an increase in the lateral earth pressure as calculated from the modified Coulomb formula. This has serious limitations.

In this study, model tests were conducted to study the effect of the flexibility of high retaining walls on the static and dynamic earth pressures. Also, the effect of the damage potential of different ground motions was studied by shock type loading.

Three types of 'small prototype' walls were used in this study; 1) a steel cantilever wall 1.0 m high to represent the effect of flexural bending of the wall only 2) a steel and brick wall 1.0 m high with provision for rotation, to separately investigate the effect of the movement of wall foundations and 3) a rigid wall 2.0 m high to study the problem at lower acceleration levels and steady-state vibrations. The walls 1 and 2 above, were housed in a horizontal shake table excited by the impact of a loaded pendulum. The wall 3 was placed in a pit dug in the ground and vibrations were caused by the fall of a heavy weight at some distance from the wall. Sinusoidal vibration of the system was also examined. This wall had a provision for varying its weight to study the inertial effects. The back was filled using air-dried medium coarse sand, and pressures were measured using suitable pressure cells.

The above tests were intended to remove some of the discrepancies of the Mononobe-Okabe formula widely in use to-day (1973). This theory is based on plastic equilibrium in soils and hence does not give any idea of the displacements suffered by a retaining wall

during an earthquake. It is obvious that a rational design of retaining walls should be based on the displacements, for, many walls can be permitted to undergo some displacements during an earthquake without constituting failure. This is more so because severe earthquakes are not very frequent and an engineering structure need be designed only for a few severe earthquakes. A mathematical model has been proposed here to determine the displacement of retaining walls in translation. Since it is rather difficult to assess the mass of soil participating in vibrations, an experimental set up was designed and fabricated for the purpose.

From these studies, it was concluded that

- i) The static earth pressure on cantilever retaining walls is given by Jaky's formula for at-rest pressures.
- ii) The dynamic earth pressures on all types of walls depend more on peak velocities of the ground motion than on accelerations.
- iii) The point of application of the dynamic increment is at about the mid-height of the flexible walls. On rigid walls it is lower and is at about 40 % height of the wall above its base.
- iv) The inertia force of the wall is also found to be a function of the energy input and hence the ground velocities because the resistance would be mobilised only at a finite displacement and some work has to be done.
- v) A mathematical model for predicting the earthquake induced displacement of a retaining wall in translation has been proposed based on the present day knowledge of the behaviour of the soil below and behind the wall under static loads.

ACKNOWLEDGEMENTS

This thesis is the result of four years of experimental and analytical investigations carried out at the School of Research and Training in Earthquake Engineering (S.R.T.E.E.), at the University of Roorkee. Expert guidance and suggestions from Dr. Jai Krishna, Vice Chancellor, University of Roorkee (formerly Director, S.R.T.E.E.) and Dr. Shamsheer Prakash, Professor of Civil Engineering, University of Roorkee (formerly Professor of Soil Dynamics, S.R.T.E.E.) have helped the author considerably in planning, execution and reporting this work.

Dr. A.S. Arya, Professor and Head, S.R.T.E.E. gave all possible help and encouragement during the time of these investigations.

Exchange of ideas with the author's colleagues specially Sri V. Chandrasekaran (now with C.B.R.I., Roorkee) and Sri Krishen Kumar proved helpful. The author also had useful discussions with Sri S.C. Sharda, on leave from M.R. Engineering College, Jaipur.

S/Sri J.P. Jaiswal, G.R. Agarwal, R.S. Messon, H.C. Dhiman and Laxmi Chand of the S.R.T.E.E. assisted the author in the experimentation.

Sri S.C. Sharma and Sri Deen Dayal have done a good job of the drawings and typing of the thesis respectively.

All help is acknowledged with thanks.

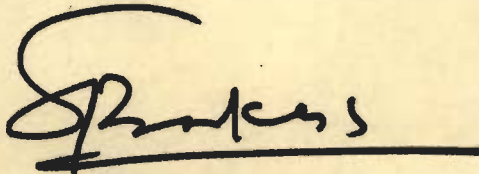
The investigation was partly supported by Beas Designs Organisation who sponsored the research work.

Finally the author would like to add a word of appreciation for Mrs Usha Nandakumaran for her patience and continued encouragement during the time of some of the experimental studies and the preparation of the manuscript.

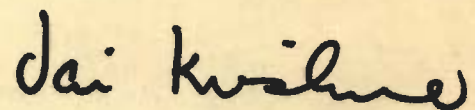
C E R T I F I C A T E

Certified that the thesis entitled, "Behaviour of Retaining Walls Under Dynamic Loads" which is being submitted by Sri P. Nandakumaran in fulfilment of the requirements for the award of the degree of Doctor of Philosophy in Earthquake Engineering of the University of Roorkee is a record of the student's own work carried out by him under our supervision and guidance. The matter embodied in this thesis has not been submitted for the award of any other degree or diploma.

This is to further certify that he has worked for a period of 48 months between September, 1969 and August, 1973 for preparing this thesis.



(SHAMSHER PRAKASH)
Professor of Civil Engineering
University of Roorkee
ROORKEE



(JAI KRISHNA)
Vice Chancellor
University of Roorkee
ROORKEE

TABLE OF CONTENTS

	Page
LIST OF ILLUSTRATIONS	xi
NOTATION	xivi
CHAPTER 1 INTRODUCTION	1
Current Solution	2
Scope of Present Investigation	5
CHAPTER 2 REVIEW OF LITERATURE	10
CLASSICAL EARTH PRESSURE THEORIES	11
EXPERIMENTAL INVESTIGATIONS	24
CHAPTER 3 TESTS ON FLEXIBLE WALLS	31
INTRODUCTION	31
TEST SET-UP	34
Test Bin	34
Test Wall	34
Design of Test Wall	36
Instrumentation	37
Method of Backfilling the Wall	39
Soil Properties	40
TEST PROCEDURE	43
Static Tests	43
Dynamic Tests	44
TEST RESULTS	45
DISCUSSION OF RESULTS	49
General	49

	Page
Testing Procedure	49
Static Earth Pressures	52
Rupture Surfaces	55
Dynamic Earth Pressures	56
Reproducibility of Results	60
SUMMARY	62
CHAPTER 4 TESTS ON RIGID WALLS	63
INTRODUCTION	63
TEST SET-UP	65
Instrumentation	67
Method of Backfilling the Wall	67
Soil Properties	68
TEST PROCEDURE	69
TESTS PERFORMED	71
TEST RESULTS	71
DISCUSSION OF RESULTS	74
General	74
Testing Procedure	75
Static Earth Pressure	77
Rupture Surfaces	78
Dynamic Earth Pressures	79
SUMMARY	82
CHAPTER 5 TESTS ON A LARGER RIGID WALL MODEL	84
INTRODUCTION	84

	Page
TEST SET-UP	86
The Wall	86
The Trough	87
The Pit	88
Facilities for Producing Forces	88
Impact Type Motion	89
Sinusoidal Motion	89
INSTRUMENTATION	89
Pressure Cells	89
Proving Rings	90
Other Measurements	91
BACKFILLING	91
Wall Filling	92
TESTS CONDUCTED	92
TEST PROCEDURE	93
Accelerations in the Pit	93
Static Tests	93
Dynamic Tests	94
Tests Under Steady State Vibrations	95
TEST RESULTS AND DISCUSSION	96
Accelerations in the Pit	96
Static Tests	96
Dynamic Tests	97

DISCUSSION OF RESULTS	100
Accelerations in the Pit	102
Static Earth Pressures	102
Dynamic Earth Pressures	103
Point of Application of the Dynamic Increment	106
Inertia Force of the Wall	106
SUMMARY	108
CHAPTER 6 DISPLACEMENT ANALYSIS	109
INTRODUCTION	109
MATHEMATICAL MODEL	111
Evaluation of Spring Forces	113
Analysis	115
Ground Motion	117
VARIABLES CONSIDERED	118
Yield Displacement	118
Behaviour of Foundation Soil	120
Natural Period of the Wall	123
Ground Acceleration Amplitudes	124
Period of Ground Motion	124
Ratio of Stiffnesses on the Compression and Tension Sides	125
Damping as Fraction of Critical Damping	125
RESULTS OF COMPUTATIONS AND RESULTS	126
Checks for the Computer Programme	126
Study of Response Characteristics of the System	127

Slip per Cycle	128
Effect of Damping	129
Effect of Ground Acceleration Amplitude	130
Effect of Natural Period of the System	130
Effect of Yield Displacement	131
Effect of η	132
USE OF THE RESULTS FOR ACTUAL PROBLEMS	133
Determination of Soil Mass	133
Test Procedure	135
ILLUSTRATIVE EXAMPLE	137
SUMMARY	141
CHAPTER 7 SUMMARY AND CONCLUSIONS	143
SUGGESTIONS FOR FURTHER RESEARCH	148
REFERENCES	150
FIGURES	155
VITA	213

LIST OF ILLUSTRATIONS

Figure No.		Page No.
3.1	PHOTOGRAPH OF TEST BIN	156
3.2	EARTH PRESSURE CELL	157
3.3	CALIBRATION CURVES FOR TWO CELLS	158
3.4	SET-UP FOR CALIBRATION OF WALL	159
3.5	CALIBRATION OF WALL - BENDING MOMENTS VS STRAIN	160
3.6	GRAIN SIZE DISTRIBUTION CURVE	161
3.7	STATIC EARTH PRESSURE DISTRIBUTION	161
3.8	PRESSURES AND BENDING MOMENTS, TEST 1	162
3.9	PRESSURES AND BENDING MOMENTS, TEST 2	162
3.10	PRESSURES AND BENDING MOMENTS, AND DEFLECTIONS, TEST 3	163
3.11	PRESSURES, BENDING MOMENTS AND DEFLECTIONS TEST 4	164
3.12	TYPICAL RECORD OF OBSERVATION, TEST 3	165
3.13	STATIC EARTH PRESSURE PROBLEM IN FLEXIBLE WALL	166
3.14	EFFECT OF ACCELERATION ON DYNAMIC PRESSURES	167
3.15	DISTRIBUTION DIAGRAM OF DYNAMIC INCREMENT PER UNIT OF ACCELERATION DUE TO GRAVITY WITH HEIGHT OF WALL	168
3.16	GROUND VELOCITY VS DYNAMIC INCREMENT COEFFICIENTS	169
3.17	VALUES OF DYNAMIC INCREMENTS IN THE SUCCESSIVE SHOCKS - TEST 4	170
3.18	VALUES OF DYNAMIC INCREMENTS IN REPRODUCIBILITY TESTS - TEST 3	170
4.1	CROSS SECTION OF TEST WALL	171
4.2	TEST SET-UP, RIGID WALL	172
4.3	AT-REST PRESSURES ON THE WALL	173
4.4	REDUCTION IN LATERAL PRESSURE WITH WALL MOVEMENT	174
4.5	ACTIVE EARTH PRESSURES MEASURED	175

4.6	ZONE OF RUPTURE SURFACES	176
4.7	DYNAMIC INCREMENT DISTRIBUTION TEST I AND IV	177
4.8	DYNAMIC INCREMENT DISTRIBUTION TEST II AND IV	178
4.9	DYNAMIC INCREMENT DISTRIBUTION TEST III AND VI	179
4.10	DYNAMIC INCREMENT AND CENTRE OF PRESSURE VS PEAK ACCELERATION	180
4.11	PEAK BASE VELOCITY VS COEFFICIENT OF DYNAMIC INCREMENT	181
5.1	TEST SET-UP SCHEMATIC DIAGRAM	182
5.2	TEST SET-UP WALL AND THE PIT	183
5.3	ACCELERATIONS IN THE PIT (PEAK VALUES)	184
5.4	AT-REST PRESSURES	185
5.5	ACTIVE PRESSURES	185
5.6	ACCELERATION VS DYNAMIC PRESSURES CELL 3,9,8,2,7,4,6, 1 AND 10	186 and 187
5.7	DYNAMIC INCREMENT DISTRIBUTION	183
5.8	PEAK ACCELERATION VS OVERTURNING MOMENTS	189
5.9	OVERTURNING MOMENTS VS PEAK ACCELERATION	190
5.10	PEAK ACCELERATION VS INCREASE IN OVERTURNING MOMENT	191
5.11	OVERTURNING MOMENT VS PEAK ACCELERATION STEADY STATE VIBRATION	192
5.12	PEAK VELOCITY VS COEFFICIENT OF DYNAMIC INCREMENT AND ITS POINT OF APPLICATION	193
5.13	INERTIA FORCES OF THE WALL	194
6.1	FORCE VS DISPLACEMENT	195
6.2	DETAILS OF MATHEMATICAL MODEL	196
6.3	FLOW CHART OF COMPUTER PROGRAM	197
6.4	RESPONSE OF ELASTIC SYSTEM BY LINEAR ACCELERATION METHOD	198

6.5	RESPONSE OF AN ELASTIC SYSTEM WITH DIFFERENT STIFFNESS ON TENSION AND COMPRESSION SIDES	199
6.6	DISPLACEMENT VS TIME	200
6.7	DISPLACEMENT VS NET SOIL RESISTANCE	200
6.8	NUMBER OF CYCLES VS SLIP	201
6.9	EFFECT OF DAMPING ON SLIP	202
6.10	EFFECT OF ACCELERATION AMPLITUDE ON SLIP	202
6.11	NATURAL PERIOD VS SLIP PER CYCLE	203
6.12	NATURAL PERIOD VS SLIP PER CYCLE	204
6.13	NATURAL PERIOD VS SLIP PER CYCLE	204
6.14	NATURAL PERIOD VS SLIP PER CYCLE	205
6.15	NATURAL PERIOD VS SLIP PER CYCLE	205
6.16	EFFECT OF YIELD DISPLACEMENT, ACCELERATION LEVEL AND FORCING FREQUENCY ON SLIP	206
6.17	NUMBER OF CYCLES VS SLIP	207
6.18	EXPERIMENTAL SET-UP	208
6.19	SCHEMATIC DIAGRAM OF EXPERIMENTAL SET-UP FOR FINDING SOIL VIBRATING WITH WALL	209
6.20	LOAD DEFORMATION CURVE EXPERIMENTALLY DETERMINED	210
6.21	FREQUENCY VS AMPLITUDE OF MODEL WALL	210
6.22	THE PROBLEM OF RETAINING WALL ANALYSED	211
7.1	COEFFICIENT OF DYNAMIC INCREMENT AT VARIOUS VELOCITIES	212

NOTATIONS

Symbol	
A	Ground Acceleration Amplitude, gals
C_u	Uniformity Coefficient
D_{10}	Effective Size of Soil
e	Void Ratio
e_{max}	Maximum Void Ratio
e_{min}	Minimum Void Ratio
g	Acceleration Due to Gravity
h	Height of Model Wall
i	Angle of Backfill Surface with Horizontal
k	Stiffness on Tension Side
k'	Stiffness on Compression Side
k_h	Horizontal Seismic Coefficient
k_v	Vertical Seismic Coefficient
K_A, k_a, K_a	Coefficient of Active Earthpressures, Static Case
K_{AE}	Coefficient of Active Earthpressure, Earthquake Case
K_o	Coefficient of Earthpressure at-rest
m	Mass
P_A	Dynamic Active Pressure at any Depth h
Q	= R/R_y
R	Resistance Offered by Soil
R_y	Yield Resistance
R_D	Relative Density of Soil

S_s	Specific Gravity of Solids
T	Period of Ground Motion
T_n	Natural Period of the System
V	Peak Velocity of Ground Motion
x	Displacement of System
y	Displacement of Ground
Z	$(x-y)$ = Relative Displacement
Z_y	Yield Displacement of System
α	Angle of Wall Back with Vertical
γ	Unit Weight of Soil
δ	Angle of Wall Friction
Δt	Time Increment
Δ_{KAE}	Coefficient of Dynamic Increment
ξ	Damping as Fraction of Critical
η	k'/k
θ	$\tan^{-1} \frac{k_h}{1-k_v}$
Φ	Angle of Internal Friction of Soil
ψ	Z/Z_y

CHAPTER 1

INTRODUCTION

Retaining walls are designed to resist the lateral thrust from the earth retained. The earth thrust could be due to its own weight and surcharge.

When a retaining wall is subjected to earthquake ground motion, the wall alongwith a part of the backfill vibrates. The wall can easily deform away from the backfill, whereas the resistance to its movement towards the backfill is considerably larger because the backfill offers much resistance if it is pushed by the wall. As a result of series of cycles of ground motion, the wall moves out and assumes a different position at the end of the earthquake. Such observations have been made in some past earthquakes; Chile 1960, Alaska 1964, Niigata 1964 etc. (Seed and Whitman, 1970). To account for the displacement of the walls during earthquakes, an added lateral thrust has been invariably assumed in the past. With this added thrust, the stability of the wall against sliding and overturning are checked with the help of a "pseudo" factor of safety. Also, the stresses in the foundation soil are kept within the safe values. It may however be mentioned here that very few countries specify such added seismic thrust in their building codes (Seed and Whitman, 1970) for retaining wall design.

However, damage to many bridges due to the

lateral shift of their abutments and devastation of harbour facilities due to total collapse of quay walls call for development of realistic design procedures for retaining walls in seismic zones.

Current Solutions

The first ever attempt to obtain additional earth pressures under earthquake conditions was made by Sano (1916). The increased earth pressure was calculated by a reduction in the value of Φ , the angle of internal friction by an amount equal to an angle θ , which equals $\tan^{-1}(k_h/1-k_v)$ where k_h is the horizontal seismic coefficient and k_v is the vertical seismic coefficient. Seismic earth pressures are computed for this reduced value of Φ , using either Rankine's or Coulomb's earth pressure theory. The method is not popular because it indirectly considers a reduction in Φ whereas no laboratory tests have shown such a reduction. The most popular method of computing the dynamic earth pressure is the modified Coulomb's theory due to Mononobe (1929) and Okabe (1924). Here, in addition to the static forces on the rupture wedge, an inertia force is also considered and from statics the earth pressure on the wall is computed. The Japanese practice is to consider this dynamic pressure to have a hydrostatic distribution. But some codes including the Indian Standard IS: 1893-1970 specify the static component

of the earth pressure to have a hydrostatic distribution and the dynamic component (dynamic earth pressure minus static earth pressure) is considered to have a triangular distribution with its apex at the base of the wall.

In this procedure, the type of the wall displacement and the consequent strain pattern in the soil have not been accounted for. Instead, a plane rupture surface in the soil under dynamic condition is assumed. This rupture surface is different from the one assumed to develop under static conditions. Also, the effect of the strain pattern on the distribution of the earth pressure has not been taken into account in these theories.

Also, for high retaining walls which are likely to bend during backfilling and which neither rotate bodily nor translate at the foundation level, the existing procedures for determining earth pressures are not applicable since their basic assumptions are not satisfied. The process of backfilling would cause the wall to deform beginning with the start of the backfill and ending on the completion of backfilling operations. No further deformations of the wall are likely to take place afterwards under static conditions. Such cases of backfill conditions are not covered by any of the earth pressure theories available today (1973). On such walls, the added earth thrust due to ground motions cannot be

computed with the available theories since the initial conditions are different from those assumed in these theories. Thus a need exists to investigate the problem of static as well as dynamic earth pressures when the backfill is strained due to the bending of the wall only.

A further point which needs investigation is the total overturning moment about the toe of the wall during earthquakes. This consists of two parts, namely, that due to the dynamic earth pressures and that due to the inertia of the wall itself. No study has so far been reported on the second aspect. The existing procedures are entirely based on engineering judgement. Indian standard (1993-1970) recommends the inertia forces as the product of the wall weight and the seismic coefficient while TVA (1951) had recommended only half this value. The difference between the two Standards calls for some experimental studies in this regard.

The present method of computing the dynamic earth pressures also suffers from the fact that it does not take into account the frequency characteristics of the ground motion and the natural frequencies of the retaining walls. These factors play a very important role in the response of the system. It is necessary to investigate how the above factors affect the dynamic earth pressures.

All the above studies aim to modify the present design procedures by considering such important factors like the strain pattern in the back fill and the ground motion characteristics. The modified procedure will, it is hoped, account for the actual field conditions in a more realistic way.

The above arguments notwithstanding, the problem cannot in reality be reduced to one of added earth pressures. It has been pointed out by Seed (1966) that the concept of a factor of safety in the seismic stability of slopes would be misleading. Almost the same conditions apply to retaining walls. Thus the solution of the problem is to determine displacements a retaining wall would suffer on being subjected to a probable earthquake at a site and then to see whether those are within the permissible limits. For this, either the concept of 'yield acceleration' suggested by Newmark (1965) or a dynamic analysis with the actual soil behaviour and the masses involved will have to be performed. The latter has definite advantages that the actual behaviour of the soil can be approximated in a much better way.

To sum up, it can be stated that

- i) Earth pressure theories, generally in use, cannot be used for the case of high retaining walls where bending of the wall rather than

its rotation or sliding is a marked phenomenon.

- ii) Mononobe-Okabe formula which is a modified version of Coulomb's formula to take into account the earthquake effects has some inherent disadvantages. Caution needs be exercised in using the formula for all types of retaining wall problems. On the other hand further studies are necessary to get quantitative data regarding the magnitude and distribution of earth pressures so as to use the principle of increased earth pressures under earthquake conditions.
- iii) The present method of computing dynamic earth pressures lack in the proper evaluation of the ground motion characteristics and the dynamic characteristics of the structure.
- iv) A dynamic analysis for the retaining wall problem in seismic areas has not been worked upon in detail yet.

Scope of Present Investigation

In this work, the following investigations have been carried out.

1. Model tests on a steel cantilever wall 1.0m high backfilled in layers with dry sand.

This would simulate the case of a high concrete wall with a rigid foundation wherein the strains in the backfill are caused entirely due to bending of the wall and the backfilling conditions are also simulated. Using sophisticated instrumentation data has been obtained on the static pressure and by impact loading on the dynamic pressure and its distribution.

2. Model tests on a rigid wall 1.0m high backfilled in layers with dry sand.

The wall was made to yield to bring about active conditions in the backfill. Data obtained on static pressures as well as dynamic pressures during impact loading.

3. Model tests on a rigid wall 2.0m high with variable wall weights to study the inertia properties.

Data on static earth pressures and dynamic pressures during impact type of loading were obtained.

4. A mathematical model has been proposed to consider the case of wall translation under earthquake conditions. It is difficult to evaluate the behaviour of the soil when the wall rotates even under static conditions. Therefore as a starting point the simplest case of translation has been considered. Sufficient qualitative and quantitative data are available to properly evaluate the soil behaviour

under such conditions. The load-deformation characteristics of the wall-soil system has been assumed as elastoplastic with different values on tension and compression sides. Wall displacements have been worked out for sinusoidal ground motions considering properties of the system and the ground motions in the ranges of general interest. The mass of soil participating in vibration alongwith the wall has been evaluated with a test set-up.

A review of all pertinent publications in the field of dynamic earth pressures has also been made. Thus a major part of the work is to sort out the draw backs in the current design procedures by carefully conducted model tests. The analytical work for computing slip of rigid retaining walls during ground motions reported here opens a new path in the proper dynamic evaluation of the problem.

The main conclusions from these studies are:

- a) The dynamic earth pressures has a better correlation with the peak velocities of the ground motion rather than the peak acceleration. Further tests on walls backfilled with different sands are however necessary to establish an exact correlation between these parameters.
- b) Mononobe-Okabe formula besides having the limitation that it can be used only for rigid walls is having a further draw back that it is valid only for a narrow range of ground motion periods.

c) The dynamic earth pressure distribution on retaining walls is affected by its flexibility.

d) When the ground acceleration is large enough to overcome the base resistance, the displacement of a retaining wall in translation is mostly affected by the period of ground motion.

CHAPTER 2
REVIEW OF LITERATURE

Ever since Coulomb published his classical earth pressure theory in 1773, numerous theories have been proposed by research workers around the world. However, as far as active earth pressures are concerned, only Rankine's (1857) theory has attained the qualification "classical". The above two theories have been popular because of their simplicity. The performance of countless walls built using either of the two theories, have stood in the way of recognition of more sophisticated and perhaps theoretically sounder theories of the last few decades.

A modified version of the Coulomb's theory has been the accepted method of computing the earth pressures on retaining walls during earthquakes for quite some time now. Other forms of theories proposed are yet to make significant head way.

In this Chapter the principles of Coulomb's and Rankine's classical earth pressure theories have been briefly described. Then all theoretical work reported so far on dynamic earth pressures exerted by dry back fill on a retaining walls have been reviewed which is followed by a review of experimental work. Since the present investigation does not encompass the case of saturated backfills, dynamic water pressure on walls has not been considered.

CLASSICAL EARTH PRESSURE THEORIES

Coulomb's (1773) theory belongs to the group known as extreme methods. This method makes use of one condition of equilibrium only but it is supplemented by the necessary number of extreme conditions. A rupture surface is assumed and equation of equilibrium of the wedge is written taking care to see that the unknown stresses on the rupture surface do not enter the equations. These equations for pressures on the wall are then either maximised (active pressure) or minimised (passive pressure). Though Coulomb realised the rupture surface could be curved, he used only a plane surface. The limit equilibrium of the wedge bounded by the back of the wall, the backfill surface and the rupture surface is considered to determine the pressures on the wall. The maximum value of the pressure is then determined by using differential calculus. Coulomb however did not suggest any distribution pattern of the earth pressures. The form of the equation suggests a triangular pressure distribution and as such this has been associated with Coulomb's theory.

Rankine's (1857) theory is based on the theory of plasticity. He considered the state of limiting equilibrium at any point in a soil mass bounded by a plane surface. Using the principle of conjugate stresses, he determined the stresses on vertical planes at incipient failure. By assuming that the introduction of a wall does not affect the

state of stress, ie the wall is frictionless, the pressure on the wall would be equal to the stress on the vertical plane at any point. The earthpressure on the wall was thus determined in terms of the strength parameters of the soil c , the cohesion and Φ the angle of internal friction.

DYNAMIC EARTH PRESSURES-ANALYTICAL METHODS

The first theoretical study in this field dates back to 1916 when Sano (1916) introduced the seismic coefficient method for aseismic design of structures. He suggested substitution of Φ the angle of internal friction of the soil with $(\Phi - \tan^{-1} \frac{k_h}{1-k_v})$ in either Rankine's or Coulomb's theory where k_h and k_v are the horizontal and vertical seismic coefficients. These seismic coefficients stand for a horizontal acceleration of $k_h \cdot g$ and a vertical acceleration of $k_v \cdot g$ where g is the acceleration due to gravity. Also, the term $(\Phi - \tan^{-1} \frac{k_h}{1-k_v})$ denotes the angle of repose of the soil under earthquake conditions. Thus the method considers a pseudo decrease in the angle of internal friction of the material to account for the additional forces caused by the inertia of the backfill. The above makes an interesting contrast with the results of dynamic tests on cohesionless materials where the angle of internal friction has been found to have negligible variation under different types of dynamic loadings.

The above fallacy is however absent in the

modifications of the Coulomb's theory due to Okabe (1924) and Mononobe (1929). Okabe considered the equilibrium of the failure wedge as in Coulomb's theory with additional inertia forces due to the horizontal and vertical accelerations and obtained expressions for dynamic earth pressures exerted by cohesionless as well as cohesive backfill. For cohesionless soil it is given below (Hayashi, 1965) for a vertical wall and a horizontal backfill.

$$p_A = (\gamma_e h + W_e) \frac{\sin(\theta + \zeta - \Phi) \cos \zeta}{\sin \zeta \cos(\Phi + \delta + \zeta)} \quad \dots 2.1$$

$$\text{and } \zeta = \frac{\pi}{4} + \frac{\Phi}{2} - \frac{1}{2} \tan^{-1} \frac{B \cdot C + A\sqrt{B^2 - A^2 + C^2}}{B^2 - A^2} \quad \dots 2.2$$

where p_A = dynamic active pressure at any depth h below the surface of the back fill

$$A = \sin(\delta + \theta)$$

$$B = -\sin(\Phi - \theta) \cos \delta - \sin(\Phi + \delta) \cos \theta$$

$$C = \sin(\Phi - \theta) \sin \delta - \sin(\Phi + \delta) \sin \theta$$

$$\gamma_e = \gamma k_n \operatorname{cosec} \theta$$

$$W_e = W \cdot k_h \operatorname{cosec} \theta$$

$$\theta = \tan^{-1} \frac{k_h}{1 - k_v}$$

γ = unit weight of soil

W = uniform surcharge per unit area of the backfill

Φ = angle of internal friction of the soil

ζ = inclination of the rupture surface with horizontal.

Equations 2.1 and 2.2 imply that the component of dynamic earth pressure due to the weight of the backfill is distributed hydrostatically while that due to surcharge is distributed uniformly with the height of the wall. Mononobe (1929) approached the problem from another angle. He recognized that the direction of gravity rotate by an angle θ ($= \tan^{-1} \frac{k_h}{1-k_v}$) due to the seismic force and the weight of the wedge and surcharge W' can be considered to become $W' k_h \operatorname{cosec} \theta$. Thus the dynamic earth pressure can be calculated by rotating the whole cross section by an angle θ so as to make the direction of the weight $W' k_h \operatorname{cosec} \theta$ vertical. The modified Rankine formula for active pressures then becomes

$$P_A = \frac{(\gamma h + W)}{\cos^2 \theta} \frac{\cos \theta - \sqrt{\cos^2 \theta - \cos^2 \Phi}}{\cos \theta + \sqrt{\cos^2 \theta - \cos^2 \Phi}} \quad 2.3$$

Coulomb's theory would be modified as

$$P_A = (\gamma h + W) \frac{\cos^2 (\Phi - \theta)}{\cos(\delta + \theta) \cos \theta} \left[1 + \frac{\sin(\Phi + \theta) \sin(\Phi - \delta)}{\cos(\delta + \theta)} \right]^2 \quad 2.4$$

The eqs. 2.3 and 2.4 give the dynamic earth pressure on a vertical wall with a horizontal backfill surface at any depth h .

When the backfill surface is inclined at an angle i and the wall back is inclined at an angle α with vertical towards the backfill, the modified Coulomb's theory becomes

$$p_A = \frac{1}{2} \gamma H^2 (1-k_v) \cdot \frac{\cos^2 (\Phi - \theta - \alpha)}{\cos \theta \cos^2 \phi \cos(\delta + \alpha + \theta)}$$

$$\times \left[\frac{1}{1 + \frac{\sin(\Phi + \delta) \sin(\Phi - \theta - i)}{\cos(\delta + \alpha + \theta) \cos(i - \alpha)}} \right]^2 \quad 2.5$$

where p_A is the total pressure on the wall.

The equations 2.4 and 2.1 give identical results and so the modification of Coulomb's theory is generally known as the Mononobe - Okabe formula.

Though the equations by both Okabe and Mononobe give hydrostatic distribution of dynamic pressures, the Mononobe - Okabe formula as widely adopted in the rest of the world has been only for the total pressures as in the case of Coulomb's theory itself. There has also been variations regarding the point of application of the dynamic earth pressures. For example, in Indian Standard Code IS 1893-1962, 1966 and 1970, the dynamic increment defined as the difference between the dynamic and static earth pressures is specified to act at $\frac{2}{3}$ times the height of the wall above the base. The static part of the pressures is however considered to act at $\frac{1}{3}$ times the height above the base only. Similar provisions have been made in the design

specifications for Kentucky Project of the Tennessee Valley Authority (1951) for wall batter less than or equal to 1:3 (4:12). For greater batter the dynamic increment is assumed to act at a lower height of 0.58 times the height of the wall above its base.

Matsuo and Ohara (1960) computed the lateral earth pressure in vibration regarding the backfill as an elastic body of two dimensions. The soil was further assumed as homogeneous and isotropic. This theory was mainly developed for use in quay wall design and two separate cases of a rigid wall and a moving wall were solved. Also, the total pressures for design were given as the sum of soil pressures and hydrodynamic pressures. The theory however is yet to gain ground because of the complications. A comparison of the design curves proposed by Matsuo and Ohara with the Mononobe-Okabe theory has been made by Becker (Seed and Whitman 1970) and reasonably good agreement has been reported. Scott (1973) however states that the theory gives pressures and moments much larger than those from Mononobe-Okabe theory..

Ishii, Arai and Tsuchida (1960) also developed a theory for determining dynamic earth pressures on retaining walls or quay walls. These are almost similar to the theory of Matsuo and Ohara. For the case of a fixed wall the soil is assumed as visco-elastic and for the case of

a moving wall the soil is assumed as elastic but the weight of the wall is also considered.

Kapila (1962) gave appropriate modifications for the well known graphical solutions of the Coulomb's theory by Culmann and Melbye to take into account the effect of dynamic forces. Also, working on the same principles as Mononobe, he gave the modified expressions for the dynamic passive pressure.

Arya and Gupta (1966) theoretically obtained non-linear lateral earth pressure distribution by assuming that the horizontal acceleration varies linearly from base to the top of the retaining wall. Since the design seismic coefficient has been taken as the maximum value at the ground surface, its effective value is only $\frac{2}{3}$ times and this discrepancy in this theory can lead to unsafe designs.

Prakash and Saran (1966) have given non-dimensional plots for determining the dynamic pressures exerted by a $c - \phi$ soil on retaining walls. Gravity effects, surcharge effects and cohesive forces are considered one at a time and the principle of superposition has been utilised. A plane rupture surface below the zone of tension cracks has been taken and design charts have been given. It was found that that part of the total pressure due to cohesive forces is the same in earthquake and non-earthquake cases.

Madhav and Rao (1969) presented design curves for

determining the earth pressure coefficients as functions of cohesion, the angle of internal friction, the seismic coefficient, wall friction and the inclination of the wall back and the backfill. They used a pseudo-static analysis but the direction of the resultant inertia force was so optimised that the resulting pressures were a maximum. They contended that for design purposes it is essential to take that combination of vertical and horizontal accelerations which has most detrimental effects.

Prakash and Basavanna (1969) stressed the fundamental deficiency in Coulomb's theory and hence in the Mononobe-Okabe formula that the moments of forces on the rupture wedge about any point do not balance. This causes difficulty in determining the point of application of the pressures. Therefore, considering failure taking place along the face of the wall and on a plane surface in the backfill, they established that the distribution of earth pressures is similar to the distribution of the soil reaction on the rupture surface. With this condition, the distribution of earth pressures on the wall was determined by balancing of the moments on the rupture wedges. For determining the rupture surface the pressures on the wall and the moments were separately maximised and since they did not give identical results the maximum moment was considered for a rotating wall and maximum pressure for a translating wall.

This step however leaves much to be desired. They have given coefficients for determining the point of application of dynamic earth pressures considering different variables. Some singularities in this case however remain to be explained.

Seed and Whitman (1970) have reported an empirical formula for determining the dynamic earth pressure coefficients. They observed that the results from Mononobe-Okabe formula can be approximated by the simple relation

$$K_{AE} = K_A + \frac{3}{4} k_h \quad \dots 2.6$$

where K_{AE} = active earth pressure coefficients under earthquake

K_A = active earth pressure coefficient under static case

k_h = horizontal seismic coefficient

Seed and Whitman have also compiled the code provisions in various countries (reproduced in Table 1) and noted that only five out of seventeen codes specify Mononobe-Okabe analysis for design of retaining walls. A justification for this is attempted and it is concluded that many walls adequately designed for static earth pressures will automatically have the capacity to withstand earthquake ground motions of substantial magnitude and in many cases special

seismic earth pressure provisions may not be required.

TABLE 1.1 - Building Code Requirements for Lateral Pressures During Earthquakes (Seed and Whitman, 1970)

Country	Year	No indication of special requirement	Method of computing Lateral Pressure for earthquake loading
(1)	(2)	(3)	(4)
Canada	1953	x	
France	1955	x	
Greece	1958		Mononobe-Okabe formula with k_h varying from 0.08 to 0.32 depending on seismic zone and foundation conditions
India	1970 ⁺		Mononobe-Okabe formula with consideration of foundation conditions and inertia force of the wall. Point of application of dynamic increment at $2/3 H$ above base.
Italy	1937	x	
Japan	1957		Mononobe-Okabe analysis with k_h varying from about 0.1 to 0.3
Mexico	1957	x	
New Zealand	1955	x	
Philippines	1959	x	

Contd .. p.21

+ Seed and Whitman have referred to the 1966 revision. Data from 1970 revision has been substituted by the author.

USSR

Table 1.1 Contd.

(1)	(2)	(3)	(4)
Portugal	1958		Design must consider seismic forces, for waterfront structures dynamic pressures of water on structures must be considered
Turkey	1953		For design of retaining walls angle of friction reduced by 3° to 6° depending on seismicity of region
Venezuela	1959	x	
U. S. A.			
1. TVA	1939		Mononobe-Okabe analysis with $k_h = 0.18$
2. Uniform BC	1967	x	
3. S. E. A. O. C.	1967	x	
4. Calif. Div. of Highways	1968	x	
5. AASHO	1965	x	

Basavanna (1970) modified the earlier work of Prakash and Basavanna where it was assumed that full friction along the rupture surface is mobilised even when the components of body forces parallel and perpendicular to the ground surface were acting separately. This discrepancy was avoided and another set of coefficients was presented.

Scott (1973) analysed the problem of dynamic earth pressures to conform more closely to the approaches currently

in use in structural analysis, in view of the pressures and moments measured in small scale earth pressure models. The soil was treated as a one-dimensional shear beam attached to the wall by springs representing the soil - wall interaction. Different cases like

- 1) constant values of shear modulus, density and spring constant.

- 2) constant values of density and spring constant and shear modulus increasing parabolically with depth were considered for a fixed wall and for representing flexibility, the wall was treated as a rigid wall hinged at the base. A torsion spring was used to represent rotation stiffness at the base. It was concluded that the pressures and moments are significantly higher than those calculated by Mononobe-Okabe method. The point of application of the earth pressures are in general around $2/3$ times the height of the wall above its base. He maintained that observation of rupture in the soil behind retaining walls during earthquakes is essentially a post-failure phenomenon because the walls move out under larger pressures than those from Mononobe-Okabe formula and this displacement causes development of rupture in the back fill.

Tajimi (1973) has used a two-dimensional wave propagation theory in a homogeneous elastic body to determine dynamic earth pressures on walls displaced in

either translation or rocking. He concluded that the pressures and the phase difference between the ground acceleration and the pressures are qualitatively similar to those observed in one of the medium sized model tests.

Aggour and Brown (1973) have used a finite element model of a wall-backfill system to determine the dynamic pressures on walls of different thicknesses due to a sinusoidal ground motion. Contact between the wall and the soil is assumed throughout the duration of motion. Effect of the flexibility of the wall, soil modulus, length and shape of the backfill on the pressures were studied. It was concluded that on a flexible wall the pressure near the top of the wall is smaller than that on a rigid wall. Also, the dynamic pressures were found to depend very much on the static pressures.

Nandakumaran and Joshi (1973) have proposed a method of determining the point of application of dynamic earth pressures assuming a rupture surface has already developed behind a wall. By further assuming that the rupture surface does not change under earthquake conditions and also that no tension can develop on the rupture surface, the equilibrium of seismic forces has been considered. By superposition of the dynamic increment, on the static forces, the magnitude and point of application of dynamic pressures has been determined. It is found that the point

of application of the dynamic increment is affected by the geometry of the problem and also the design seismic coefficient. Also in general it is below the two third point above the base of the wall.

The above review clearly shows that the work done so far does not consider the problem in its true perspective. Considering the soil as elastic may be useful only if the design requires practically negligible deformation of the structure. Here too the available method needs corroboration by way of more observations in the field and in laboratory. The theories based on a rupture in the backfill however fail to recognize the importance of the natural frequency of the wall in relation to the forcing frequency. In short, this review shows that what is lacking today is a method of determining the displacement of the wall.

EXPERIMENTAL INVESTIGATIONS

Many experimental studies of the problem have been conducted so far mainly to understand the physical behaviour of retaining walls. As is well known, the basic principle of experiments for earth pressure studies is to simulate the strain conditions in the backfill and thus to treat the set up as a small scale prototype. The very same technique has been used by almost all investigators till now. The first of these studies was conducted by

Mononobe and Matsuo. A box was mounted on a horizontal shake table and was filled with dry sand. The box was subjected to different acceleration levels by exciting the table and the maximum pressures exerted on the wall of the box were measured by means of hydraulic gauges. They concluded that the maximum pressure increases with base acceleration and is in good agreement with values computed by the Mononobe-Okabe formula.

Matsuo (1941) also obtained similar results by conducting tests on a shake table, the soil being sand. However in these experiments Matsuo found that the dynamic component of pressure acts at $\frac{2}{3}$ times the height of the wall above the base as against $\frac{1}{3}$ times assumed in Mononobe-Okabe analysis.

From tests on dry sand conducted by Jacobsen (Tennessee Valley Authority, 1951) the same conclusions were arrived at. He performed his tests using a box mounted on a shake table and the pressures were measured using dynamometers restraining the model wall 3ft (91.5 cm) high. His results showed that the measured values reasonably agree with the values computed by Mononobe-Okabe formula. However, the dynamic component of pressures was found to act at the upper third point of the wall. The restraint provided by the dynamometers could have had some effect on the results.

Matsuo and Ohara (1960) conducted tests on a fixed wall and a movable wall backfilled with dry sand to investigate the effect of vibrations on the lateral pressures. The shake table supported by 4 vertical rigid steel strips with free hinged ends is restrained to move only in one direction and the wall was mounted perpendicular to this direction. Two boxes were used one a steel box 100cm x 90cm x 40cm height and the other a wooden box with a glass side 100cm x 50cm x 40cm height. The pressures were measured using piston type pressure cells, straining gauges being used to pick up the strains in the springs supporting the diaphragm. All the tests were done with the period of vibration of 0.3 sec. On fixed walls it was found that the amplitude of pressure change is large at middle height. On movable walls with a hinge at the lower end and vertically supported by a rod resting on an elastic spring plate, it was seen that the maximum amplitude of pressure decreases as the displacement increases so long as the displacement is below a certain value. When the displacements are larger, phase difference occurs between the pressures at different heights.

The authors have also performed tests on 1.5m high concrete walls of thickness 0.90m and length 2.0m erected in a pit. Vibrations were given externally by a 1 h.p. oscillator mounted in a trough sunk in the ground 4.5m away from the wall and also by a 200 watts oscillator

mounted on the top of the wall. Pressures were measured using pressure cells. Larger pressures with increasing ground accelerations and peak pressures at about $\frac{1}{3}$ times the wall height from the top were observed.

Ishii, Arai and Tsuchida (1960) conducted tests using a shake table on which three boxes of lengths 400cm, 202 cm and 80.5cm were fixed rigidly. The thickness of the sand strata in one of them was varied to 70, 50 and 30cm. Tests on fixed as well as movable walls were conducted, vibrating the table in steps of 100 gals for two minutes each from 100 gals to 1000 gals. The period of the table motion was kept around 0.3 sec. Tests were also done on a gravity type model wall. They observed that upto an acceleration of 500 gals the sand vibrates along with the table and there is no marked change in the lateral pressures. But for accelerations between 500 and 800 gals, termed as the critical stage, sand moves in relation to the box, settlement of the sand surface occurs and the lateral pressure increases. For larger accelerations than 800 gals dry liquefaction is observed but settlements become smaller. They observed that the lateral earth pressures consists of two parts, the static pressure including the increase in its value, called the residual pressure and the dynamic pressure or the oscillating pressure. The former was found to be very large compared to the latter. Also, phase difference upto half the period

was observed between the table motion and the pressures in movable walls.

They also concluded that inspite of the complexity of the problem corresponding to various factors in the test set-up and the field conditions like the characteristics of walls, backfills and ground motions, the maximum pressure is equal to or lower than the Mononobe-Okabe pressures. Also, while the dynamic or oscillating pressure distribution is bow shaped, the residual pressure is distributed hydrostatically.

Murphy (1960) conducted some tests on a solid rubber model of a gravity wall to study the qualitative behaviour of the backfill during vibrations. He found that the slip surface developed is much more flatter than the slip surface under static conditions. He pointed out that the slip surface probably developed at Shinizu Harbour in 1930 had almost the same inclination.

Niwa (1960) has conducted tests on probably the largest retaining wall model to be used so far. The model wall of concrete had a base width of 1.5m and a height of 3.0m and was erected in a pit 5.0m long along the length of the wall. The length of the backfill was 4m. The depth of the sand fill was 2.0m. Vibrations were created in the ground using an earthquake generator placed at 4.5m away from the wall. The amplitude of vibration of the wall was

split into translation and rocking components.

M. Ichihara (1965) measured the pressures and moments created by a backfill on a model wall when the whole set up was vibrated. To avoid the inertia effects of the wall itself, dummy walls were connected to the axis of rotation of the active walls. By using a motor, this axis was made to move and thus the effects of wall movement was seen on the pressures and moments. In general, the movement of the wall was found to reduce both the pressures and the moments.

Aliiev, Mamedov and Radgabova (1973) used a different approach from all the above to obtain the seismic pressure of soils. In this, similitude requirements were used and a centrifuge was used to increase the acceleration due to gravity quite as much as the geometrical dimensions of the model are less than these of the prototypes. Seismic pressures during explosions were measured in the model. Also some field tests were conducted on two walls 3m high built side by side, one founded on rock and the other on a sandy cushion. It was concluded that the introduction of a sand cushion below retaining walls considerably reduces the dynamic earth pressures. Also, the pressures measured and the velocities showed better correlation than the accelerations, though definite conclusions were not made.

Thus, from a review of all important investigations

it can be concluded that as at present no attempt has been made to determine the displacement of the walls during earthquakes and that unless such desirable procedures are available the present method of using the pseudostatic analysis need not be replaced. But it appears that while generally the pressures are believed to be given accurately by Mononobe-Okabe analysis, the effect of various characteristics of the wall and the soil on the point of application needs further study.

CHAPTER 3

TESTS ON FLEXIBLE WALLS

INTRODUCTION

Earth Pressures on retaining structures are known for quite sometime now to be dependent among other factors, on the deformation of the structure and the consequent strains in the backfill material. Terzaghi (1936) was the first to give qualitative and quantitative data on this aspect of the problem.

For design of earth retaining structures, the designer needs information on two aspects, the magnitude of the earth thrust and the fashion in which this thrust is distributed on the structure. Properties of the foundation soil are also required. With these data known, analysis of the structure can be performed for safe designs from laws of Mechanics.

Aseismic design of retaining walls is carried out by assuming an increase in the earth pressure due to inertia forces of the soil mass in addition to the inertia force of the wall itself. Table 1.1 (page 20-21) gives the code provisions in different countries and it can be seen that only a few codes specify an increase in earth pressures for design purposes. India is one of them and the code (IS:1893-1970) specifies modified Coulomb theory due to Mononobe-Okabe for computation of increased earth pressures and based on

Jacobsen's findings, recommends the point of application of the dynamic increment at $2/3$ the height of the wall. These provisions however are based on very little experimental evidence. Further, the test conditions affect the results to a great extent and therefore the results may be considered to be valid for only those conditions which can be represented adequately by the model. High retaining walls definitely fall outside the scope of the experiments performed by Jacobsen as the deformation conditions expected in the field were not simulated. Tall walls are generally built as R.C.C. cantilever or counterfort walls and the strains in the backfill will be due to their flexural bending because the foundations will usually be very rigid. If foundations are not rigid, deformations therein will result in the translation or rotation of the wall as a body resulting in very large strains in the soil compared with those due to its bending. The present methods, it can be seen, overlooks the basic differences in the behaviour of the two types of structures. Since the problem of tall concrete walls has not been tackled, a detailed study of the dynamic earth pressure on such 'flexible' walls is called for.

Model tests where similitude requirements are strictly adhered to, could be considered as a possible solution to the problem. However, in soil Mechanics, where laws of similitude are difficult to apply, the earth

pressure problems are not solved by testing models of a prototype but by treating small scale models as prototypes. However, introduction of bending deformations as well as rotation of the wall in a model prototype pose difficulties as they may not represent conditions of the actual site. In other words, only a particular case of wall geometry and material properties can be simulated in this case. Here too, the selection of the 'model' is not easy because of difficulties in procuring materials for the wall and the backfill to satisfy the similitude requirements. To overcome this difficulty, two separate sets of small scale prototype tests can be performed; one in which only bending deformation of the wall takes place and another where only rotation of the wall takes place. Since the walls are designed for active earth pressures, the design can be based on wall movements required to cause active conditions in the backfill material. The results of the two studies can then be judiciously superimposed on one another. Also the method of back filling has to be similar to that usually done in actual construction since along with backfilling, the wall goes on deflecting and this aspect cannot be covered by a case where the same deflections are permitted after the back is filled under "no deflection" condition. The available earth pressure theories belong to the latter category and hence cannot be used for the cases where backfilling is done after the construction of high concrete

walls. There exists a need to investigate the pressure distribution on such walls.

Tests were performed on a mild steel cantilever wall fixed to the platform of a large shaking table and backfilled with sand to study the effect of backfilling on the pressures acting on the wall and also to investigate the increase in these pressures when the shaking table is excited with a pre-determined impact.

In this chapter, the test set-up, instrumentation, method of test, results and discussions together with main findings for the above case have been described.

TEST SET UP

Test bin:

The test bin is 5.2m long, 2.8m wide and 1.2m high and is mounted on a large horizontal shaking table. The sides of the bin consists of rigid M.S. frame work with glass panels for a length of approximately 3.0m in the middle of both longitudinal faces. All other panels are with 6mm thick M.S. sheets. A photograph of the test bin is given in Figure 3.1. The details of the shake table have been given by Krishna and Chandrasekaran (1962).

Test wall:

As discussed earlier flexible walls in practice are designed to resist active earth pressures. Also with

rigid foundations, the strains in the backfill are caused entirely due to bending of the wall. Thus, the design of a small scale prototype wall for testing consists of determining the thickness for a steel wall fixed at the base of the bin so as to have sufficient displacement to cause active plastic equilibrium in the backfill. The design therefore requires quantitative data on the deformation of the wall necessary to bring about the above condition in the backfill. A survey of the literature shows that for rigid walls active conditions are developed if the wall either rotates about the bottom or translates so as to have a deformation of about 0.4 to 0.5 percent of the wall height at its top (Terzaghi 1936, Mackey and Kirk 1967). The quantitative values given above are, however, for rigid walls where the above conditions would cause the requisite strains in the whole deposit. Since there will be non-linear deformation of the wall from its bottom to the top in the case of flexible walls it has been arbitrarily assumed that the strains in the backfill as stipulated by the above condition be made applicable at the mid-height of the wall. In other words, the deflection of the wall at its middle point, that is sufficient to activate lateral thrust from the soil may be assumed equal to 0.25% of the height of the wall. With this condition active equilibrium should develop to sufficient depth from the sand surface, if previous findings are applicable to the present test

conditions.

Design of Test Wall:

The width of the test bin is 2.8m. Thus the maximum length of the wall that can be used is 2.8m. So as to have a fairly large length to height ratio of the wall to minimise side effects, it was concluded that the height of the wall should not exceed 1.0m. Accordingly for the test wall, a length of 2.45m and a height of 1.0m were adopted.

For calculating the thickness of the wall required, the following values were assumed:

- a) density of the backfill, $\gamma = 1.55 \text{ gm/cc}$
- b) angle of internal friction of the backfill
 $\Phi = 40^\circ$
- c) angle of wall friction $\delta = 0^\circ$
- d) point of application of lateral earth thrust
= lower third point of the wall.

For a cantilever beam of length 'h' loaded with a triangular load $= \frac{wh}{2}$, the deflection at the middle point is given by $\frac{49}{3840} \frac{wh^4}{EI}$.

In the present case, w is given by $\gamma \cdot h \cdot k$ where k is the coefficient of earth pressure, given by $\frac{1 - \sin 40^\circ}{1 + \sin 40^\circ}$

$$= \frac{.356}{1.644} = 0.216$$

Considering the Young's modulus E as 2109×10^6 g per cm^2 , and unit length of the wall

$$\text{deflection at the middle point} = \frac{49}{3840} \frac{1.55 \times 100 \times 0.216 \times 100^4}{2109 \times 10^6 \times l}$$

If this is to be equal to 0.25% of 100 cm; i.e. 0.25 cm,

$$I = \frac{49 \times 1.55 \times 100 \times 0.216 \times 100^4}{3840 \times 2109 \times 10^6 \times 0.25} \text{ cm}^4$$

$$= 0.81 \text{ cm}^4$$

$$\text{thickness of the wall required} = 4 \sqrt{\frac{0.81 \times 12}{1}}$$

$$= 0.991 \text{ cm}$$

The nearest standard thickness available, i.e. 1.0 cm was therefore adopted.

Instrumentation

Eight pressure cells were specially designed and fabricated (Nandakumaran and Dhiman, 1970). The cells are essentially diaphragm type, the diaphragm consisting of a spring strip clamped at its ends. The size of the diaphragm is 3.0 cm span (clear) x 1.2 cm wide, the overall size of the cell is 5.0 cm long 3.0 cm wide and 1.0 cm thick. The cell can be used for a maximum pressure of 0.3 kg/cm^2 with a least count of 0.003 kg/cm^2 . The diaphragm has a bonded wire resistance strain gauge⁺ pasted on its bottom and the cell is calibrated in a special calibration chamber. The

⁺ type SA 10, make Rohit's, Roorkee, Resistance 120 ohms, gauge factor 2.05

strains in the gauges are measured at known applied pressures. The diaphragm has a natural frequency of 1878 Hz.

The cell is shown in Fig. 3.2 and the calibration curve for two of the cells in Fig. 3.3. Eight such pressure cells were housed in rectangular holes 5cm x 3cm cut in the steel wall in three rows, one row in the centre of the wall and the other two rows at 20 cm away from this row, and on either side. The vertical spacing of the cells was 10 cm so that in any single row the spacing of the holes was 30 cm centre to centre. The top cell was placed at 15 cm and the bottom most 85 cm from the top of the wall.

To check the pressures measured using the pressure cells, the bending moments on the wall were measured. For this, the surface of the outside face of the wall was cleaned and eight wire resistance strain gauges were pasted in a vertical row at a spacing of 10 cm centre to centre at the same elevations as the pressure cells. From the measurements of bending strains the bending moments can be computed knowing the properties of the wall. However, to avoid possible discrepancies in assuming the fixity at the base and the effect of cutting holes for housing the pressure cells, the wall was calibrated in position. The calibration procedure consisted of applying a horizontal force on the top of the wall in the direction in which earth pressures would act. To make this horizontal force fairly well

distributed along the length of the wall, three loops were provided, one in the centre and the other two at quarter points of the wall and a wire rope was connected to the three loops. This rope was made to pass over three frictionless pulleys and carried a known weight on its other end. To eliminate the unknown friction further, a tension proving ring was connected on the rope between the wall and the first pulley thereby registering exact loads applied on the wall. The set-up for calibration is shown in Fig. 3.4. Alongwith the horizontal loads, the strains in all the eight strain gauges were also recorded. Fig. 3.5 shows the recorded strains in all the gauges versus the bending moments at the centre of the gauges, calculated from the knowledge of the concentrated load and the lever arm. It will be seen that a single line can relate the bending moments and the bending strains throughout the height of the wall.

As a further check on the measured pressures, the deflected shape of the wall was ascertained using 5 dial gauges fixed in line along the height of the wall.

Method of backfilling the wall:

The wall is shorter than the width of the bin by 35.0 cm. The wall was fixed to the base of the bin using two M.S. angles 75x75x12 mm on either side of the wall and bolted to the wall as well as the base. One end of

the wall was almost in contact with the glass side of the bin with just sufficient clearance to avoid friction. On the other end a temporary wooden support was provided to retain the soil and to fill the gap between the end of the wall and the side of the bin.

After fixing the wall it was backfilled in layers of 10 cm thickness. Dry sand (properties are described later in this chapter) was poured in the bin in weighed quantities and each layer of 10 cm thickness was compacted by placing a wooden plank 30 cm wide and 1.2 m long on the sand surface and by imparting 6 blows of a wooden mallet so as to cover the whole area. After compacting the layer a line of the same sand stained with black ink and dried, was made near the glass side of the bin. These lines were used to monitor any rupture taking place in the backfill. Then the subsequent layers were placed in an identical manner till the backfilling was completed.

During backfilling, five calibrated tins were placed above the previous layer, sand poured and compacted. The tins were then extracted and weighed to determine the density achieved. More than 60% of the samples gave values between 1.560 and 1.570 g per cc. Extreme values observed were 1.540 and 1.582 g per cc and average value was 1.565 g per cc.

Soil Properties:

As discussed earlier, laboratory studies of the

problem of retaining walls are done with small sized prototypes rather than by models. In other words, the studies are used to verify existing theories or to determine the earth pressure coefficients for the given wall geometry, deformation, and backfill properties. Therefore for dynamic conditions also a similar procedure has been followed in the past. In this light, sand as the backfill material has definite advantages. Some of them are i) ideal plastic equilibrium conditions occur in dry uniform sand, ii) reproduction of fill conditions from test to test is much easier in sands than in cohesive soils iii) effects of time rate of loading is negligible in sands.

Therefore, air dried clean Ranipur Sand was used for backfilling the wall. This sand has less than 5% particles passing through I.S:74 μ sieve and exhibits no cohesion in the dry state. Other salient properties of this sand are as given below.

- a. Soil Type SP (Poorly graded sands, little or no fines, according to IS classification).
- b. Effective size D_{10} 0.13 mm
- c. Uniformity Coefficient $C_u = 2.10$
- d. Specific gravity of solids $S_s = 2.66$
- e. Minimum Void ratio = 0.575 (determined under horizontal vibrations and the sand in a submerged state)

- f. Maximum void ratio = 0.86 (determined by dropping small quantities in water kept in a measuring jar.
- g. Void ratio at the test condition = 0.70
- h. Angle of internal friction at the test condition = 40°
- i. Relative density at the test condition $D_R = 56\%$

Grain size distribution curve of this sand is shown in Fig. 3.6.

The shear strength of the soil was determined using direct shear tests for the following reasons:

- i) As the sides of the shear box permits no lateral displacement, the conditions of the test might be thought of as representing plain strain (Harr, 1966).
- ii) In triaxial test which is an indirect test, the tangential and radial stresses are equated and this though convenient, may not be correct (Harr, 1966).
- iii) The angle of wall friction is determined by direct shear test where a steel plate is kept in the lower half and sand in the upper. Therefore it is advantageous to evaluate the value of the angle of internal friction of the soil also by the same test.

The angle of friction between the sand and steel was measured as 23° .

TEST PROCEDURE

Static Tests:

To start with, the leads of all the eight pressure cells and eight strain gauges are connected to the terminals of a selection switch so that the initial readings of each could be read out on a BLH make 'strain indicator'. The selection switch can be operated in such a way that only one of the gauges would be connected with the active gauge terminals of the strain indicator at a time. After recording the initial readings of all the pressure cells and the strain gauges, five dial gauges are fixed such that its spindle is in contact with the outside face of the wall, and at 5 different elevations (Dial gauges were used only in two test series, however). The initial readings of the dial gauges are then taken.

After this stage, the wall is backfilled in layers as already described. As the backfilling proceeds the wall moves out gradually due to bending caused by the lateral thrust. When backfilling is completed, the final readings of the pressure cells, strain gauges and the dial gauges are taken. The difference between the initial and the final readings gives the strains in the cells and strain gauges, corresponding to which earth pressures and bending

moments can be read out from the respective calibration charts. These values give the distribution of earth pressures and bending moments along the height of the wall. The differences between the dial gauge readings before and after backfilling give the deflected shape of the wall due to the lateral earth pressures.

Dynamic tests:

In the dynamic test the shake table on which the whole test set-up is mounted, is excited by the impact of a loaded pendulum. The pendulum is pulled back and kept at a predetermined angle with the vertical and is released using a mechanical clutch. The table vibrates with an initial velocity due to the impact and thereby additional forces on the wall as well as on the backfill material are caused.

During the shock loading as discussed above, it was desired to record the accelerations of the table, and the top of the wall in addition to the increase in the earth pressures at various elevations. Because of the difficulty in procuring sufficient number of recording equipment for recording all these data simultaneously, the procedure followed was as given below.

- i) The dial gauges were removed as they are not suitable for dynamic measurements.

ii) Two accelerometers, one on the shake table and the other on the top of the wall, were fixed and their leads were connected to the input of the recording system.

iii) The leads of any one of the pressure cells were connected to the input of the recording system.

iv) After balancing the recording systems, the pendulum was pulled back to the desired angle and released so that the resulting motion of the table and the wall and the pressure in one pressure cell were simultaneously recorded.

v) The same procedure was repeated till earth pressure records in all the pressure cells were obtained with the same energy input in all the cases.

The reproducibility of results were checked by repeating the blows at least twice for all the pressure cells and in some cases by employing the pressure cells again after the pressures at all the cells have been recorded once.

TEST RESULTS

In all, four series of tests were conducted with peak acceleration of the table as a variable as listed in Table 3.1. Including repeat tests and pilot tests, 8 tests were performed.

TABLE 3.1
Details of Tests Performed

Test Series No.	Peak Table acceleration
1	2
1	4.22 g
2	3.32 g
3	3.34 g
4	4.55 g

From the initial and final readings of the pressure cells, the strains on the diaphragm of the cell was known and from the respective calibration curves the pressure at various elevations was calculated. Fig. 3.7 shows the static earth pressures observed at various elevations caused by the backfilling in all the tests and the Table 3.2 gives the total earth pressures and earth pressure coefficients observed.

TABLE 3.2
Static Earth Pressure

Test Series	Static earth pressure g per cm length of wall	e.p. coefficient
1	2	3
1	2627.0	0.3342
2	2752.0	0.3520
3	2600.0	0.3322
4	2697.0	0.3392

Note : Such large values had to be employed because of the low periods of table motion and this aspect has been discussed in detail on pages 51 and 52

The point of application of the static pressure in the four test series were worked out from the pressure distribution diagram and are given in Table 3.3.

TABLE 3.3

Point of Application of Static Earth Pressures

Test Series	Point of application above base as % of wall height
1	37.6
2	36.0
3	34.25
4	36.0

Fig. 3.8a shows the distribution of static earth pressure in Test series 1. From this, the distribution of bending moments along the height of the wall was computed and is shown as dotted line in Fig. 3.8b. This figure also shows the bending moments actually observed with the help of the strain gauges. Similar data for test series 2,3 and 4 are given in Figs. 3.9a, 3.9b, 3.10a, 3.10b and 3.11a, 3.11b. Figs. 3.10c shows the deflection of the wall computed from the pressure distribution in 3.10a as a dotted line and actually observed deflection of the wall using dial gauges as a thick line. Shown also in this curve is the deflection required (Terzaghi 1936) to bring about active plastic equilibrium conditions in the backfill as a dash-dot line

Fig. 3.11c gives similar data for test series 4.

Fig. 3.12 shows a typical record of the acceleration of the table, acceleration of the wall top and pressure in one of the pressure cells. The record of the pressure is analysed from the calibration of the Wheatstone bridge and also from the calibration of the cells. The former converts the distance in mm into microstrains and the latter the strains into pressures. Since the Wheatstone bridge containing the cell is balanced at the static pressures, the record pertain to additional pressures caused by the shock. These values are superimposed therefore on the static pressures in the Fig. 3.8a, 3.9a, 3.10a and 3.11a to obtain the distribution of dynamic pressures in Test series 1, 2, 3 and 4 respectively and are designated as such in the figures. The total dynamic increment in pressures obtained by integration of the dynamic increment distribution are tabulated in column 2 and ratio of this to the total static pressure (column 2 Table 2) are given in column 3 of Table 3.4.

TABLE 3.4

Dynamic Increment Due to Shocks

Test Series	Dynamic increment in g per cm of wall	Dynamic increment Static pressure
1	2	3
1	1916.0	0.75
2	1659.5	0.604
3	1680.0	0.646
4	2177.0	0.807

DISCUSSION OF RESULTS

General:

The results reported herein pertain to a fairly large sized wall. The larger the size of test bin and the wall, smaller is the possibility of errors which cannot be accounted for. In the height and width of the wall this study had one of the largest dimensions reported so far in the literature (A still larger wall was tested as a part of this study as described in chapter 5). Moreover, this particular model is the first ever where the dynamic earth pressure on a flexible wall has been investigated. This study therefore yields useful and new data on the effect of bending deformation of the wall on earth pressures, both its magnitude and distribution.

Testing Procedure:

The points worth discussing in the testing procedure are a) design of the wall b) mode of backfilling c) instrumentation and d) the mode of applying dynamic load.

In the design of the wall the deflection of the wall has been considered as the prime criterion. The philosophy of retaining wall designs to resist active pressures instead of the larger at rest pressures is well known. Here it is implicit that since the design pressures are smaller than the at-rest pressures, the wall will deform or be displaced so as to lower the earth pressures to

active value. Therefore if a small scale prototype is to be designed, wherein the strains in the backfill are to be simulated and the wall is essentially different from the one in the field, the deformation of the wall to bring about active condition is of paramount importance. Deformation of the order assumed in the design is universally accepted as sufficient on the basis of earlier studies. However, no such criterion is available for flexible walls.

It may be mentioned here that if a wall has a very rigid foundation and hence deforms only by bending, sufficient strains in the backfill to bring about plastic equilibrium conditions in the backfill can never be brought about at the support which has essentially to be treated as fixed. This is irrespective of the wall deformation at its top. Therefore the aim was to cause suitable strains in the backfill to sufficiently large depth from the ground level and hence a deformation of $h/200$ at mid-height was adopted for design. Moreover, it may be seen from Fig. 10c and 11c that actual deflections of the wall are sufficiently larger than the deflection considered necessary in the design, namely, 3.1 and 3.2 mm in test series 3 and 4 respectively as against a minimum desirable value of 2.5 mm.

The mode of backfilling adopted is in some ways opposed to the idealised conditions assumed in almost all earth pressure theories. In these theories, it is

107793

generally assumed that a state of elastic equilibrium exists behind the wall and deformation of the wall brings about a state of plastic equilibrium and lower the pressures to active values. In the present test condition however, deformation of the wall starts at the moment backfilling is started and goes on increasing till the backfilling is finished. After this, there is no further deformation of the wall. The procedure adopted here is more akin to the actual practice in the field and hence the discrepancy with the theoretical investigation is due to the inaccuracies of the latter and not the method adopted here.

As regards instrumentation, a triple check has been employed on the pressure measured using the pressure cells. Fig. 8b, 9b, 10b and 11b show how closely the bending moments computed from the pressure diagrams match those actually measured. Further, Fig. 3.10c and 3.11c show how closely the computed deflections of the wall agree with the ones observed. With these checks one can place sufficient confidence in the performance of the pressure cells. Consequently only the pressure cells have been utilized to measure the dynamic increment during shock loading.

It has already been mentioned that the dynamic loading of the system of wall and backfill is achieved by giving an impact to the shake table on which the wall is mounted. The resulting accelerogram is essentially

different from the ones generally associated with earthquakes notably because of some peaks of extremely large acceleration values and remarkably small durations. The shock loading is much more expedient than steady state forced vibrations and if judiciously employed, can serve the purpose admirably in the laboratory. For example, the response of the wall back-fill system is undoubtedly dependent on the energy input rather than some peaks in the accelerogram and as such, if the energy input is suitably selected the results should be reliable. This point is further discussed in this and the next two chapters.

Static Earth Pressures

The static earth pressure diagrams for the various test series are given in Figs. 3.8a, 3.9a, 3.10a and 3.11a. It is seen that the pressure distribution is not hydrostatic but is curved with a maximum value of pressure at the base. In all the above figures K_a (Coulomb's active earth pressure coefficient) and K_0 (Jaky's, at-rest earth pressure coefficient, Jaky, 1948) lines are also shown. It is seen that the pressures observed are more or less close to the Jaky's at rest pressures. This is so in spite of the fact that the deformation of the wall is more than those stipulated by Terzaghi for more than 60% of the height of the wall. The apparent discrepancy between pressures measured in these tests and the Coulomb's active earth pressures is partly due

to the reasons listed above for the method of backfilling adopted. To emphasise this important aspect this point is discussed further here.

i) Terzaghi had visualised the existence of a wall along with backfill without any deformations of the wall corresponding to 'at-rest' condition. Now, if the wall and backfill are deformed simultaneously the deformations postulated by him should be sufficient to develop "active" conditions resulting in subsequent reduction in pressures on the wall.

In practice, however, the above condition of 'at-rest' pressures and a subsequent reduction to active pressure cannot exist behind walls, especially flexible walls on rigid foundations. Backfilling is started after the wall is constructed and this results in deformations of the wall both above and below the level of the backfill. Thus the deformation of the backfill at any level does not equal the total deformation of the wall at that level.

This aspect is discussed on the basis of probable values of deflections of the wall, elongation of the backfill and strains in the soil. Consider the wall backfilled in 10 layers. The top layer is not strained at all as the wall deformations take place alongwith filling of the layer. The strains in the second layer from the top is caused due to the filling of the top layer alone and in the third layer

due to the filling of the top two layers. Thus in each layer, the strains are caused only due to the filling of the layers above it. If we assume the deflections of the wall as shown in Fig. 3.13 with filling of different layers we can estimate qualitatively the stretching of the backfill as well as the strains caused as plotted in the same figure. This discrepancy therefore between the actual stretching and the one taken on the basis of wall deflection is maximum at the top of the backfill and minimum at its bottom. It is thus obvious that actual deformations in the backfill is not enough to bring down the pressures from at rest to active values.

ii) Field evidence for the above is provided by a recent study by Siedek (1969). In his study of the reasons of damage of abutments of a bridge Siedek made actual measurements of pressures on the abutments and concluded that earth pressures at rest actually occurs with retaining walls on rock. Such walls can be considered flexible because strains in the backfill will only be due to the bending of the walls.

iii) The special significance of 'flexible' walls on rigid foundations would be further apparent when the results of tests on rigid walls with the same backfill conditions are considered. This is given in Chapter 4.

Thus, based on logic, results from a small scale prototype study and a study of actual measurements of earth pressures on bridge abutments it becomes clear that the case of flexible walls on rigid foundations require special considerations. The most significant finding is that the pressures actually existing behind walls under those conditions is given by K_0 and not active pressures as being accepted with the present day knowledge (1973). The point of application of static pressures is slightly above lower third point and this indeed is a point worth considering in rational design of retaining walls.

Rupture Surfaces

As already mentioned on page 40, coloured sand lines were incorporated in the backfill to observe development of rupture surfaces. It was observed that during backfilling these lines remained as such and no sign of breaks was seen. This was because of the insufficiency of stretching of the backfill as explained on page 54. It may be mentioned here that the development of a rupture surface and the condition of active plastic equilibrium are inter-related. Once a rupture surface has developed the pressures on the wall should be active pressures. Thus the observation of the non-development of a rupture surface is a further pointer to the backfill soil remaining in pre-active conditions.

During the dynamic loading it was observed that inspite of further wall movement to a small extent, development of rupture was not in evidence. This could be either due to insufficient amount of wall yielding or due to readjustment of particles throughout the backfill. The latter point is highly probable because the local state of plastic equilibrium as conceived under static conditions may not result when the whole of the backfill is subjected to the dynamic stresses. In other words, the wall displacement is likely to cause a stretching throughout the backfill rather than a wedge in the vicinity of the wall itself.

The above observations indicate that the theories based on the development of rupture in the backfill (Coulomb's, Rankine's, Terzaghi's and many others) may not be applicable for walls which only deform due to bending. This is true for both static and dynamic cases.

Dynamic Earth Pressures

Figures 3.8a, 3.9a, 3.10a and 3.11a also show the dynamic earth pressure. These are obtained, as already discussed, by superimposing the dynamic increment on the static pressures. It will be seen that the dynamic increment is having a value of zero at the top, increases in magnitude with depth upto about the mid height and then decreases again. The total dynamic increment in the different series of tests is already given in Table 3.4. Their

points of application were calculated and are as listed in Table 3.5.

TABLE 3.5

Point of application of Dynamic increment

Test Series	Dynamic increment acts at
1	2
1	54.65% of the height
2	50.30 " " "
3	50.05 " " "
4	48.30 " " "

From this table it is noticed that the height at which the dynamic increment acts is not affected by the peak table acceleration. In Fig. 3-14a, the dynamic increment in earth pressures have been plotted against the peak table accelerations. A definite dependence of the pressures on the table acceleration shown by the curve is explained in terms of larger energy input with larger peak accelerations and hence larger dynamic pressures. Fig. 3-14b gives the relationship between the peak table acceleration and the point of application of the pressures. It is seen that the centroid of pressures is almost independent of the peak accelerations. To explain this aspect further, the dynamic increments per unit of acceleration were worked out at different elevations in all the test series as shown in Fig. 3-15. The shape of the curve suggests that the dynamic

increment per acceleration due to gravity is a unique function of the depth resulting in the centroid of pressures being of the same height from the base. This may be explained as follows:

a) Since there are no vertical stresses at the ground surface the lateral dynamic pressure must necessarily be zero there.

b) Since there is smaller relative acceleration of the backfill with respect to the wall near the base of the wall smaller pressures result irrespective of the table motion characteristics.

In Fig. 3-14 is also shown the dynamic increments as worked out from the Mononobe-Okabe formula upto a seismic coefficients of 0.3, against the ground accelerations. It is worth mentioning here that the Mononobe-Okabe formula gives compatible results only for much smaller seismic coefficients than those corresponding to the peak accelerations used in these tests. Therefore, a direct comparison has been made only with the extrapolated data from the tests upto accelerations of 0.3 g and the Mononobe - Okabe values upto a seismic coefficient of 0.3. It will be noticed that the Mononobe-Okabe values are many times larger than the extrapolated values. This huge difference calls for some rethinking of the mechanism involved.

From the table motion records, the peak table

velocities were worked out and the coefficients of dynamic increments have been plotted against these peak velocities in Fig. 3-16. For a comparison of these results with Mononobe - Okabe values, the ground motion in the latter case was assumed as sinusoidal (as was the condition in most of the previous experimental studies) and three different periods of motion namely 0.25 sec, 0.3 sec and 0.35 sec were considered. With the above, the peak velocities were calculated for different seismic coefficients (ratio of amplitude of ground acceleration and acceleration due to gravity). The curves 1, 2, and 3 were thus obtained between the velocities and coefficients of dynamic increment as seen in Fig 3-16. It will be noticed that the curve corresponding to a period of 0.3 sec represents the observed values to a very great extent. It is interesting to note that most of the Japanese investigators (Matuo and Ohara, 1960, Ishii et al 1960, Ichihara 1965) have used a table motion period of about 0.3 sec. Therefore it is not surprising that the Mononobe - Okabe values were reported to represent the actual dynamic pressures in these investigations. In this light it can be concluded that Mononobe-Okabe formula will hold good only when the period of ground motion is around 0.3 sec and for other periods of motion suitable modifications would be necessary. These modifications can be now made because the dependence of the dynamic pressures on the velocities has been indicated.

This aspect has further been studied in the later part of the work and is discussed in Chapters 4 and 5.

Reproducibility of Results:

To check the reproducibility of the pressures during the shock, two records of the same event were obtained in succession giving two identical shocks to the table. The results of the first and second observations at all the pressure cells in Tests Nos 3 and 4 are listed below in Table 3.6.

To see the effect of the small changes of the values in successive shocks, the data for test No. 4 have been plotted in Fig. 3.17. The variation has been found to have only very small effects on the pressure diagram.

Since eight different sets of observations were used to get data on the pressure distribution, it was desired to study the effect of the sequence of observations on the pressures, if any. In Test No. 3 after complete observation of 17 shocks (as seen in Table 3.6) had been made, four of the pressure cells at 35, 45, 55 and 65 cm depth were reconnected and eight more shocks were given. The average values of pressures in these cells in the first set of observation and in the second set are given in Table 3.7.

TABLE 3.6

Pressures at Various Pressure Cells
During Successive Shocks

Depth of cell cm	Pressure g/cm^2		Remarks
	Shock 1	Schock 2	
15	14.76	-	Test No. 4
25	29.3	29.3	"
35	42.7	44.0	"
45	31.05	31.0	"
35	11.85	10.71	"
65	26.1	24.25	"
75	8.75	13.13	"
85	18.95	12.5	"
15	20.35	13.74	Test No. 3
25	27.7	33.8	"
35	33.42	39.42	"
45	21.6	27.3	"
55	12.4	13.0	"
65	33.55	36.4	"
75	22.2	19.6	18.6 g/cm^2 in 3rd shock
85	8.62	4.4	"

TABLE 3.7

Pressure Observed at the Same Pressure Cell
at Different Times

Depth cm	Pressure g/cm^2		Remarks
	First set	Second set	
35	36.42	27.45	Test No. 3
45	24.45	20.48	"
55	12.70	17.25	"
65	34.97	34.0	"

These values are plotted together with the average values in the first set of observation against the depth in Fig. 3.18 . Though there is some difference, they are inconsequential as far as the pressure distribution is concerned, as seen in this figure.

Further evidence of reproducibility of data is available from i) density measurements (page 40) and ii) the static earth pressures in all the tests, Fig. 3.7.

SUMMARY

i) For flexible walls on rigid foundations the design pressures should be at-rest earth pressures.

ii) The point of application of the dynamic increment in flexible walls is independent of the ground motion characteristics and is at about the mid height of the wall.

iii) The dynamic increment in earth pressures is better correlated with the peak ground velocity and hence the energy input, rather than the peak accelerations.

CHAPTER 4

TESTS ON RIGID WALLS

INTRODUCTION

In the previous chapter, tests conducted on a flexible wall mounted on a horizontal shake table were described. As already discussed, this condition pertains to high cantilever walls with very rigid foundations where the strains in the backfill are entirely caused by bending deformation of the wall. It had also been mentioned that the work pertains only to one part of the problem and the effect of foundation movements whereby the wall can move as a body must be studied for a more clear understanding of the field conditions.

While planning for a rigid wall test the following points need be looked into: i) Foundation conditions ii) Modes of wall deformation and iii) possible behaviour of the wall during dynamic loading. The first two points are somewhat inter-related, in the sense that the foundation conditions do determine the nature of wall deformation. If a well designed key is provided, the wall is likely to have only rotations about the toe; if the friction between the wall base and the soil is likely to mobilize only at large deformations, translation will be the most marked phenomenon. Generally speaking, unequal soil reaction below the retaining wall base leads to predominantly rotation of the

wall. However, the amount of rotation or translation suffered by a wall during different stages of backfilling depends on the properties of the foundation soil and simulation of this is not generally attempted. There is a justification for such sort of studies, especially if the lateral earth pressures are to be investigated. When a wall is designed for lateral earth thrust equal to active earth pressures, under larger at-rest pressures existing (assuming the wall does not deform at all) the wall moves out and the consequent stretching of the backfill causes the lateral earth pressures to drop down to the design pressures (active condition). This is irrespective of the displacements during the backfilling and, the stable position of the system occurs when active earth pressure conditions exist. Therefore, general cases can be studied in the laboratory by creating active plastic equilibrium conditions in the backfill by rotation or translation of the wall by the desired amount. In other words, though it is extremely difficult to achieve the exact simulation of the foundation conditions, its effect on lateral earth pressures can be correctly assessed. For this study therefore the wall is not permitted to displace during the backfilling and is later given rotation or translatory motion to cause active equilibrium conditions in the backfill.

In the present set up only rotation of the wall

has been studied. This is sufficient as after some displacement of the wall the pressure conditions in the two cases of wall displacement are identical. This displacement corresponds to active case and is generally very small. Moreover, while uniform strains exist in the backfill of a wall which rotates about its base the strains are unequal when the wall moves out parallel to itself thereby causing arching active conditions before the fully active conditions are developed. Since, in the field we are only interested in the active conditions and the theory of arching has not as yet been fully analysed, for a study of dynamic earth pressures, the case of rotation is more appropriate.

Tests were performed on a rigid wall made as a composite section of steel and brick work and back filled with sand to study the effect of shock loading on the earth pressures. During the shocks the effect of wall movement was also studied.

Details of the test set-up, test procedure and results are discussed in this chapter.

TEST SET-UP

Test bin: The same bin as described in Chapter 3 was used.

Test wall: The size of the wall was kept as the same as in the case of flexible walls, ~~i.e.~~, the wall was 1.0 m high and 2.4 m long. For making the wall rigid either a R.C.C.

wall or a brick wall was considered necessary. But since it was proposed to rotate the wall in a controlled fashion, both the above materials had some drawbacks. A composite section of steel and brick work provides many advantages like ease in fixing of knife edges below the heel of the wall, screw jacks near the outer end (toe) of the wall and housing of pressure cells on the plane of contact between the wall and the soil etc.

A cross-section of the wall used in this investigation is shown in Fig. 4.1. The back and the base of the wall were formed of 1.0 cm thick M.S. sheet and the filling was done in brick masonry in cement mortar. The wall just rested on the base of the test bin (which was mounted on the shake table described in Chapter 3), on three knife edges each 10.0 cm long at the heel of the wall and two screw supports 20.0 cm away from these knife edges. One of the knife edges was placed at the centre of the wall along its length and the other two at 1.0 m away and on either side. The two screw supports were placed 0.70 m away on either side of the centre of the wall and had holed heads for rotating them slowly whereby the wall could be rotated about the knife edges. Suitable arrests fixed to the bin were provided to keep the wall in position during backfilling and also during shock loading when no movement was desired. Fig 4.2 is a photograph of the set-up

showing a general view.

Instrumentation:

Eight pressure cells as briefly described in the previous chapter were used for measurement of static and dynamic earth pressures. The static pressures were measured using a B.L.H. strain indicator and the dynamic pressures were recorded on Brush self writing ink oscillograph after amplification of the signals by a Brush Universal Amplifier. During the Dynamic Test, along with the pressures, the table accelerations were measured using Miller accelerometers.

Method of Backfilling the Wall:

Here too, as in the case of the steel cantilever wall, the wall was placed with one of its ends near the glass side of the bin. A temporary support was used in the gap between the other end of the wall and the side of the bin.

The wall was first made vertical by suitably rotating it using the screw supports. The vertically was checked with a plumb bob. Then the wall was arrested at the top and the base using suitable M.S. pieces bolted to the bin. Then the backfilling was done in layers of 10.0 cm thickness. The soil used was clean air dried Ranipur sand, the properties of which have already been described in Chapter 3. The density conditions were also indentical in the two types of tests as ascertained from measurements using calibrated tins.

Here too the reproducibility of density was excellent. More than 65% of the samples gave values of $1.565 \pm .005$ g per cc. Extreme values observed were 1.554 and 1.58 g per cc.

During the backfilling, after each layer of sand had been poured and compacted, a line of dyed Ranipur sand was incorporated near the glass side of the bin. This was to visually examine development of any rupture in the backfill during the rotation of the wall and also during shock loading.

Soil Properties:

The soil used was clean air dried Ranipur Sand with less than 5% particles passing through I:S 74 μ sieve and exhibits no cohesion in the dry state. The soil is classified as SP according to I:S classification. The other properties of the sand are

$$D_{10} = 0.13 \text{ mm}$$

$$C_u = 2.10$$

$$S_s = 2.66$$

$$e_{\min} = 0.575$$

$$e_{\max} = 0.86$$

$$e \text{ at the test condition} = 0.70$$

$$D_R \text{ at the test condition} = 56\%$$

$$\Phi \text{ at the test condition} = 40^\circ$$

$$\text{angle of wall friction} = 23^\circ$$

TEST PROCEDURE

The initial reading of all the eight pressure cells were taken after the wall was made vertical and clamped. All the leads of the cells were connected to the active terminals of a strain indicator through a selection switch. All the cells had a common dummy gauge kept at the same conditions as the active gauges. Then the backfilling was done as described earlier. After this, the readings of the pressure cells were taken again, the difference between these strain readings furnishing the data for computing the "at-rest" pressures. Two dial gauges were fixed on rigid poles fixed to the base of the bin such that the rods of the dial gauges abutted against the wall at its top level and at a distance of 50.0 cm on either side of the centre. The arrests at the top were removed but not the ones at the base, since the latter were so arranged as to permit rotation of the wall but not horizontal displacements. The pressure cell at 85.0 cm depth was connected to the active terminals of the strain indicator and a rotation of the wall was given by gently turning the heads of the two screw supports simultaneously. The readings of the dial gauges were noted and care was taken not to have any twist in the wall about the vertical axis. The reading of the pressure cell was also taken. In this way data on reduction of lateral pressures due to yielding of the wall was obtained.

A very slow rate of wall displacement was maintained till the pressures at the depth of 85.0 cm became constant. By this time a rupture surface was also found to develop in the backfill. All the pressure cell readings were again taken and data for computing active earth pressures on the wall was obtained.

The dynamic tests were done after active plastic equilibrium conditions had been brought about in the backfill. The dial gauges were removed and the wall and the soil were subjected to a shock loading of a pre-determined intensity by the impact of a loaded pendulum on the shake table. Simultaneous records of the table acceleration, and increase in earth pressures at any one of the pressure cell locations were obtained during any particular shock. This procedure was repeated a number of times to get data at all pressure cell locations, to check reproducibility, to study the effect of the sequence in which readings were made (i. e. to study the effect of previous shock loadings on the pressures at any elevation) etc. After the shock loading all the pressure cells were read again to see the effect of shocks on the 'static' earth pressures. In three of the tests the wall was clamped during shock loading while in the remaining the wall was allowed free movement. This was done to study the effect of wall movement on the dynamic pressures.

Table 4.1.

TESTS PERFORMED

Six series of tests (including pilot tests and repeat tests, a total of 8 tests) were performed with three acceleration levels and two conditions of wall displacements. In Table 4.1, are listed, table motion and deformation conditions at the top of the wall during dynamic tests.

TABLE 4.1
Details of Tests

Test Series No.	Peak Table Acceleration	Remarks
1	2	3
1.	4.21 g	Wall was clamped
2.	3.71 g	during shock
3.	3.31 g	loading
4.	4.21 g	Wall free to
5.	3.71 g	move during shock
6.	3.31 g	loading

Because of the low period of vibration of the table, larger acceleration levels had to be used for all the tests to get results comparable with usual force and damage potential associated with actual earthquakes as explained further in this chapter.

TEST RESULTS

The strains in the diaphragm of all the pressure

cells due to the thrust exerted by the soil, were obtained by taking the differences between the initial readings and the readings after backfilling was completed. From these strains and appropriate calibration curves the at-rest pressures were calculated, Fig. 4.3. The horizontal lines show the range of pressures observed in different series of tests. This scatter can be considered to be within experimental errors and average values can be taken with confidence. In this figure is also shown the pressure distribution corresponding to Jaky's postulation (Jaky 1948). By and large, the observed pressures are close to the line corresponding to Jaky's postulation, i. e. $K_0 = (1 - \sin\Phi)$ where K_0 is the coefficient of earth pressure at-rest and Φ the angle of internal friction.

When the wall yielded by rotation, the pressures dropped as shown in Fig. 4.4. This figure shows the pressures at a depth of 85.0 cm at various amount of yielding in all the tests. It will be seen that there is a sharp fall in pressures in the initial stages but then the pressures tend to become constant. This value pertains to active conditions. The wall displacement at its top which corresponds to the active conditions is around 0.4% and compares favourably with the value of 0.5% postulated by Terzaghi (1936).

The active earth pressure distribution obtained

by first determining the strains and then the pressures after the wall was made to yield sufficiently, are plotted in Fig. 4.5 for all the tests. In this figure is also shown a line corresponding to an earth pressure coefficient equal to $\frac{1-\sin\phi}{1+\sin\phi}$. The observed values of active earth-pressure coefficients are larger than those from either Rankine's or Coulomb's theories. While $\frac{1-\sin\phi}{1+\sin\phi}$ equals 0.216 for $\phi = 40^\circ$ and $\delta = 23^\circ$ Coulomb's theory yields a coefficient of 0.2, the minimum and maximum values observed in these tests are 0.234 and 0.286 respectively with an average value of 0.257. The centre of pressures obtained from the pressure distribution diagram ranges between 0.354 to 0.38 times the height of the wall.

The black lines incorporated in the backfill showed breaks after the active conditions were brought about. The distances to the rupture surfaces from the original position of the face of the wall were carefully measured and the rupture surfaces in all the tests fall within the shaded area in Fig. 4.6. In this figure is also shown the rupture surface corresponding to Rankine's theory, that is, inclined at an angle $(45 + \phi/2)$ with the horizontal.

The method of determining the dynamic increment in earth pressures from the records has been described in Chapter 3. Following an identical procedure, the distribution

of dynamic increment with depth was worked out for all the tests. Figs. 4.7 through 4.9 show the dynamic increment diagram in all the tests. From these diagrams, the total pressures as well as the points of application were calculated and these are listed in Table 4.2 below.

TABLE 4.2
Results of Dynamic Tests

Test Series	Dynamic increment g per cm	Point of application in % height above base	Remarks
1	2	3	4
I	2647.0	41.5	
II	2469.5	36.4	Wall clamped
III	1732.5	40.6	
IV	2394.0	44.3	
V	2377.6	37.4	Wall free to move
VI	1486.5	41.2	

DISCUSSION OF RESULTS

General:

As already discussed these studies are complimentary to the studies reported in Chapter 3, as far as high retaining walls are concerned. This is however an independent study as far as gravity type retaining walls, where bending does not occur, are concerned. By the use of the special

facilities, at-rest and active earth pressures, dynamic increment in earth pressures and the pattern of the distribution of the above have been obtained.

Testing Procedures:

These tests essentially differ from the work reported earlier in the literature in two aspects, a) the size of the model is comparatively larger and b) the size and weight of the wall are sufficient so as to stand safely under the lateral thrust from the backfill, without additional support.

The wall, on which dynamic tests are reported in this chapter is the largest wall ever tested on a shake table in the laboratory. The advantages of a larger test set-up cannot be overemphasised. The effects of friction between the soil and the side of the bin, and the slight changes in the density condition etc. become comparatively negligible in this case. Also, larger number of pressure-measurement points are available for obtaining a more dependable pressure distribution diagram.

In some of the earlier studies, (T.V.A., 1951, Matsuo and Ohara, 1960, Ishii et al 1960) a steel plate formed the wall and this was supported externally and back-filled. It was thought that if the wall would be stable against the earth pressures by its weight alone, its behaviour

under the dynamic loading would be better simulated. In this case, the external supports do not hamper the response of the wall during the table motion and hence a more realistic pressure pattern would emerge. To illustrate this point further, let us imagine the wall is restrained by an elastic spring. The strains in the spring would necessarily be dependent on the response of the wall which in turn depends on the stiffness of the spring, the mass of the vibrating system, the properties of the soil and the table motion characteristics. Thus there is a likelihood of the spring getting strained more than that under the actual dynamic earth pressures. These strains cause the wall to be pressed against the soil thereby causing partial passive conditions and hence results of questionable nature. This undesirable and unrealistic feature as far as actual walls are concerned is completely avoided in the present set-up.

The method of dynamic loading adopted here was similar to the one described in Chapter 3. The shake table housing the wall and the backfill was set in motion with the impact of a loaded pendulum. This results in a motion characterised by a few peaks of extremely high acceleration levels, low time periods and short duration. In this, it is possible to have a direct comparison with the data obtained regarding dynamic pressures on flexible walls where such a type of table motion was used. It may

be recalled here that the tests reported in this chapter were partly meant to be complimentary to the tests reported in chapter 3.

In addition to the above, it is necessary to employ high acceleration peaks when the period of the load pulses is low and the whole loading is of short duration. This is because the forces and the duration are both equally important in the response of the wall which in turn will affect the earth pressure acting on the wall.

Static earth pressures:

A study of Fig. 4.3 would show that the at-rest pressures increase linearly with depth and that the variation from test to test is of small order. Also, the observed values are in general close to the values given by Jaky's equation $K_0 = (1 - \sin\phi)$ though slightly on the higher side. It is well known that tamping of the soil would result in larger "at-rest" earth pressures.

As already mentioned, on yielding of the wall by rotation, the pressures dropped from the at-rest values. The reduction takes place only for a small amount of yielding, (about 0.4% of the wall height) after which the pressures remain constant. This constant value pertains to active case. The amount of yielding causing active plastic equilibrium conditions in the backfill generally agree well with the values obtained by previous investigators

(Terzaghi, 1936 , Mackey and Kirk, 1967).

Active earth pressures obtained in this study is seen to be more than the values given by either Rankine's of Coulomb's theories. The average earth pressure coefficient in all the tests is 29 % more than that given by Coulomb's theory for $\Phi = 40^\circ$ and $\delta_s = 23^\circ$. An explanation for the higher pressures and higher point of application of the pressures can be made in terms of a possibility that the wedge formed is looser than the rest of the backfill. That is, on yielding of the wall, instead of a rigid wedge being formed, the backfill may become loose in the vicinity of the wall. This loosening leads to decrease in the angle of internal friction and hence in increased earth pressures. Also, the higher point of application of the pressures than the conventional 0.33 times the height of the wall above its base, is an indication of larger degree of 'loosening' towards the top of the wall. These aspects need be investigated in greater detail and more laboratory tests are called for in soils with high values of Φ . Since this study was intended to investigate the dynamic earth pressures, the static earth pressures were treated only as the initial boundary conditions and no detailed investigation of the static earth pressure was undertaken.

Rupture Surfaces:

An examination of Fig. 4.6 shows that the rupture

wedges in all the tests are smaller than the Rankine wedge. However, for some depth from the sand surface, the inclination of the rupture surface is roughly equal to $45 - \frac{\Phi}{2}$ degrees, which corresponds to Rankine's theory. The smaller wedge is essentially caused by the curvature of the rupture surface near the base of the wall. An identical observation was made in a smaller model (Narain, Saran and Nandakumaran, 1971) for almost similar test conditions. This could be because of the system employed for visual examination of the rupture surface.

It was observed during the dynamic tests that the rupture surface developed during the rotation of the wall to bring about active conditions in the backfill, continued to develop further if the wall was permitted to move under the shock.

Dynamic Earth Pressures:

Figs. 4.7, 4.8 and 4.9 show the variation of dynamic increment with wall height in all the tests. Each figure gives two cases of wall restraint and has been drawn for the same peak acceleration of the table. It will be seen that the dynamic increment increases gradually with the depth upto some distance wherefrom there is a tendency for decrease in the pressure intensity. A similar trend was observed in tests on flexible walls also. But the peak values in rigid walls occur at a greater depth from

the top compared to the flexible walls. This tendency may be because a rupture surface has already been formed behind the rigid wall and no such surface was formed behind the flexible wall. When a rupture surface is formed, the soil mass which causes increased pressures could be limited to the rupture wedge. In the case of flexible wall, the bending of the wall and hence larger deflections near the top could cause larger soil mass to be effective in this region and hence larger pressures might occur close to the top of the wall.

An examination of Table 4.2 shows that in general the clamped wall experiences larger earth pressures than the moving wall. The movement of the wall during shock loading was however different from the movement given to it for developing active pressures. While the latter caused a rotation of the wall about its heel, the shock loading caused a rotation of the wall about its toe (the screw jack supports to be exact). This has changed conditions slightly. But qualitatively this gives data on the effect of the movement of the wall on the dynamic pressures. Though the direction of frictional force on the wall is reversed, since the horizontal pressures alone are measured, no change in this is foreseen. Larger earth pressures on the clamped walls, as compared to an unclamped wall, may be attributed to the energy absorbed in the moving wall. When the wall

is clamped, there is hardly any work done and hence no absorption of energy. Therefore, with the same energy input larger pressures are caused on clamped walls. Also, this is in general agreement with the findings of Aliev, Mamedov and Radgabova (1973) who conducted laboratory model tests and field observations on two walls identical except in the foundation conditions. One of the walls was built on firm base while a sand cushion separated the wall and the foundation in the other. Shock type of dynamic load was applied with an explosion. It was found that the wall on rocky or firm foundations experiences larger pressures. In a field test conducted by them a wall founded on rock collapsed while its counterpart built by its side but with a cushion below the wall did not suffer any damage.

A comparison of the pressure values with those obtained from Mononobe-Okabe formula is made in Fig. 4.10a. The dash-dot line gives the value from Mononobe-Okabe formula. It was seen as in the case of flexible walls (Chapter -3) that the observed values are much smaller when peak acceleration is used for comparison.

To assess the reasons for this behaviour the dynamic increment in earth pressures has been plotted against the peak table velocity in Fig. 4.11. Also, as done in the case of flexible walls the base accelerations were assumed to be sinusoidal motion with periods of motion

as 0.25, 0.3 and 0.35 sec. The amplitude of acceleration was taken as $k_h \times g$ and for the velocities computed from the accelerations and periods the velocities were calculated. Also, the dynamic increments were worked ^{out} for seismic coefficients k_h . The curves between peak velocities and dynamic increment was obtained in this fashion and are plotted in Fig. 4.11. A very close agreement between the computed values for a period of 0.3 sec and observed values is seen. Thus it can be concluded that the dependence of dynamic pressures on peak velocities indicated in Chapter 3 holds for rigid walls also.

Fig. 4.10b gives the point of application of the dynamic increment as a function of the peak table acceleration and no definite conclusion is possible in the absence of tests at low acceleration levels, which were performed later on another wall 2 m high. However, the centroid of pressures in moving walls falls above that for clamped walls. This is believed to be because of larger soil mass moving along with the wall in its upper reaches. The tests reported in Chapter 5 on a 2 m high rigid wall were performed at lower acceleration levels. The point of application of the dynamic increment are also studied there.

SUMMARY

i. The dynamic pressures are dependent on the peak velocities of the base motion rather than the peak accelerations.

ii. The point of application of the dynamic increment is independent of the acceleration level in the ranges tested.

iii. No change in the rupture surface takes place during shock loading if a rupture surface has already developed.

CHAPTER 5

TESTS ON A LARGER RIGID WALL MODEL

INTRODUCTION,

The tests performed on the shake table and described in Chapters 3 and 4 indicated dependence of dynamic increment on the table velocities. However, the above tests were performed in a very narrow range of table accelerations and velocities. The acceleration levels employed (peak values) were much larger than would be considered of interest in general engineering applications. Moreover, the dynamic increment values were compared with those from Mononobe-Okabe formula only after extrapolation. This had to be done because the peak accelerations were used for comparison and at large accelerations as employed in the tests the above formula is not compatible. Therefore, it was decided to study the cases with much smaller peak accelerations also. Another aim of the study was to obtain more information on dynamic pressures at velocities farther away from the ones employed in the previous tests. The effect of steady state vibration was also desired to be studied. The set-up on the shake table did cause some difficulties in this regard because of extremely small pressure values resulting. With all the above objectives, the test facility had necessarily to be larger to cause measurable pressures under smaller shocks. A larger shake table was not available and

therefore it was decided to erect the model wall in a pit dug in the ground and then backfilled. Because of continuity of the ground and the backfill, shock-type vibrations could be induced by dropping a heavy weight on the ground and away from the test pit. By causing steady state vibrations in the ground, it was also possible to transmit sufficient waves to the wall and the backfill for causing dynamic earth pressures. Once it was decided to carry out the tests in this fashion, it also presented an excellent opportunity to study one of the aspects which needed to be gone into. This was the inertia force of the wall itself. Indian Standard Code (1893-1970) specifies the inertia force of the wall as the seismic coefficient times the weight of the wall while for the Kentucky Project (TVA, 1951) half this value was recommended. These recommendations are however not based on any study and are therefore of an arbitrary nature. Therefore it was decided to make a hollow retaining wall which could be filled so as to obtain different weights and thus to study the inertial effects.

To summarise, the aim of this test series was:

- i) To study the effect of impulse-type shocks of smaller acceleration levels on the dynamic increment in the pressures.
- ii) To investigate the validity of the dependence of the dynamic increment on the ground velocities

as found in the earlier tests.

- iii) To study the difference in the nature of dynamic loading, namely, impulse type and steady state type, on the dynamic earth pressure and
- iv) To investigate the problem of inertia forces of the wall during ground motions.

TEST SET-UP

Fig. 5.1 shows the plan and section of the test set up used in this investigation. The set up consists of a wall (marked (1)), supported on a knife edge (2) at the heel of the wall and a system of screw jack and proving ring supports (3) below the toe, both resting on a well-built R.C.C. trough (4) a pit in which the wall is erected and later backfilled (5) a small wall around the pit (6), steps to approach the front of the wall (7) and a heavy weight (8) which is dropped at 4.0 m away from the pit so as to cause shock waves in the backfill. Fig. 5.2 shows the wall ready to be backfilled.

The wall:

The test wall is 2.0 m high and 2.4 m long. The top width is 0.40 m and base width 1.0 m. The wall is made up of M.S. trapezoidal frames connected at top and bottom with M.S. flats at the corners. 6 frames with made-up

I-sections were used. After connecting the frames at the top and the bottom, the longitudinal sides were covered with 6 mm thick M.S. Sheets as were the ends and the bottom. The top was left uncovered to facilitate filling with any material to increase the weight of the wall. A continuous strip of angle iron with the two flanges inclined at 45° was welded to the bottom of the wall so that the right angled edge of the section could serve as a knife edge. The knife edge rested on a steel plate kept on the vertical wall of the trough below and was prevented from sliding by a second piece of angle iron welded to the steel plate. Rotation of the wall was however possible. Three screw jacks each of capacity 5T were fixed in a row 90.0 cm away from and parallel to the back of the wall. To facilitate proper support, a rigid connection between the frames of the wall was made along this line. The screw jacks rested on three proving rings; a 5T proving ring in the middle and two 2T rings on either side of it which in turn were placed on a channel kept on its web over the base of the R.C.C. trough. In this fashion the overturning moment at the knife edge support could be measured and also, with careful adjustment of the screw jacks, rotation of the wall could be effected.

The Trough:

The trough consists of a base slab 2.45m x 1.9m x 0.15m

thick and two vertical walls A and B, all of R.C.C. and was intended to provide a rigid support to the test wall. Wall A is 30.0 cm wide and supports the heel of the test wall. The toe of the wall rests on the load measuring unit resting on the base slab. Wall B is 15.0 cm wide and is at a clear distance of 1.0 m from wall A.

The Pit:

The pit behind the wall is 2.43 x 2.05 m in plan and has a maximum depth of 1.5m below ground level near the R.C.C. trough. This depth is only for a distance of 0.75 m from the outer face of wall A of the trough wherefrom steps were cut so as to provide sufficient stability. The dimensions of the pit were arrived at from considerations of the rupture wedge which was to be confined to the pit alone with additional backfill space of at least 30. cm at the ground surface. To have a backfill depth of 2.0 m, 0.5 m high brick walls were erected on three sides of the pit, its fourth side being covered by the test wall.

Facilities for Producing Dynamic Forces:

Two separate systems were used, one for creating impact type motion and the other for sinusoidal motions. In both cases disturbance of the desired type was generated on the ground (about 4m away from the wall in the first case and about 3m in the second) wherefrom seismic waves

travelled through the backfill to cause seismic pressures on the wall.

Impact Type Motion:

A heavy box 50 x 60 x 60 cm in size made as a mild steel box, filled with plain concrete was lifted up and dropped on the ground to cause impact type shocks. To guide the box weighing 700 kg during its fall and also to ascertain the height of fall, a guide rod was provided. This moved in a hole running through the concrete for its total height. The guide rod was welded to a mild steel base plate on which the box was made to fall.

Sinusoidal Motions:

By mounting a mechanical oscillator driven with a d.c. motor, on a block cast in the ground sinusoidal vibrations were generated in the test set up. The block was 50 x 50 x 100 cm deep and was cast along the centre line of the pit 3.0 m away from the wall. The top of the block was kept at the ground surface

INSTRUMENTATION

Pressure Cells:

The pressure cells used in the earlier studies and described briefly in Chapter 3 were modified slightly by pasting two strain gauges each on the diaphragm of the

cell. Smaller strain gauges of grid length 5.0 mm made by Mahavir (India) were used. By pasting one gauge on the tension zone along the middle of the diaphragm and the other on the compression zone near the fixed end the sensitivity was slightly improved and the temperature compensation was effected more satisfactorily. 10 such gauges were fixed in rectangular holes 5x3 cm cut along a vertical line at the centre of the wall (in plan) at 20 cm spacing. The topmost cell was kept at 8cm and the bottom-most at 188 cm from the sand surface of the backfill.

Proving Rings:

As already mentioned earlier, three proving rings were used to measure the overturning moments on the wall. For measuring the dynamic loads on the proving rings they were converted into dynamometers by pasting 4 strain gauges each at the mid-height of the ring, two on the outer and two on the inner sides. In this fashion a complete wheatstone bridge was obtained and hence a high sensitivity. All the rings were then calibrated on a load frame. For static load measurement the dial gauges were used. During dynamic tests the dial gauges were made inoperative by pulling back its rod so as to avoid any damage and only the strain gauges were used for all measurements.

Other Measurements:

For obtaining the accelerations Miller acceleration pick ups were used and as in the previous tests, Brush amplifiers and ink-writing oscillographs were utilised for recording the signals from the pressure cells, proving rings and the accelerometers.

BACKFILLING

Because of the large quantity of sand involved in one filling operation and since sufficiently uniform densities can be obtained in dry sands more readily, only shovelling in of the sand with frequent measurement of densities was used. To start with, the wall was made vertical by operating the screw jacks supporting it near the toe. Air dried Ranipur sand (properties of this sand have already been described in Chapter 3) was shovelled in so as to have a free fall of at least 60.0 cm and taking care to have a level sand surface as far as practicable during all the stages of backfilling. A standard proctor mould and also a modified AASHO mould with the cutting edges were placed on the sand surface during the operation of further backfilling and were retrieved to calculate the density achieved; this was done for every 30 cm thickness of the backfill. It was observed that uniform densities of 1.575 g per cc were obtained in the whole deposit. The extreme values observed were 1.56 and 1.58 g per cc.

Wall Filling:

In order to study the inertia forces of the wall three wall weights were employed in these studies, viz. wall in empty state, wall filled with saw dust and also wall filled with Badampur sand. Wide ranges of wall weights were thus obtained. In the cases of filling, weighed quantities of the material were poured in the wall and compacted before the backfilling stage. Three different weights namely 895.35 kg (wall alone), 1587.35 kg (with saw dust) and 5237.35 kg (with Badampur sand) were thus obtained.

TESTS CONDUCTED

The details of the tests conducted are listed in Table 5.1.

TABLE 5.1 Details of Tests Conducted

Test No.	Wall filling	Backfill condition before dyn. test	Accelerations, g
1	Empty	at-rest	0.248, 0.221, 0.197, 0.161
2	Saw dust	at-rest	0.23, 0.216, 0.187, 0.313
3	Saw dust	active	0.237, 0.220, 0.175, 0.147
4	Empty	at-rest	0.283, 0.232, 0.206, 0.19
5	Badampur Sand	at-rest	0.268, 0.244, 0.218, 0.159
6	Badampur Sand	active	0.27a, 0.257, 0.225, 0.172
7	Empty	at-rest	0.30, 0.272, 0.258, 0.23
8	Empty	active	0.252, 0.242, 0.220, 0.180
9	Empty	active	Steady State Vibration

TEST PROCEDURE

Accelerations in the Pit:

Before conducting any of the actual tests it was desired to study the nature of the acceleration pulses generated in the backfill due to the falling weight. For this, three accelerometers were buried at three locations in the backfill and the weight dropped. The magnitude of the peak acceleration pulse at different locations in the plan area and with depth were obtained by separate series of observations.

Static Tests:

The wall was kept vertical initially and the initial readings of the three proving rings using the dial gauges and the ten pressure cells using a strain measuring bridge were made. After this the wall was filled with either saw dust or Badampur sand or left empty. In the case of filling, the readings of the proving rings were taken again to ascertain the moment caused by the filler material. Then the wall was carefully backfilled as already described. The proving ring readings and the pressure cell readings were taken again, the differences between these readings and the initial readings providing the data for computation of the at-rest earth pressure on the wall and the overturning moment about the heel.

For obtaining active plastic equilibrium conditions in the backfill, the wall was rotated about the knife edges. Wall displacements at its top were measured with two dial gauges. After active conditions were caused, all the pressure cells and the proving rings were read to get the active earth pressures and the overturning moments.

Dynamic Tests:

The increase in earth pressures due to the falling weight and the resulting seismic waves were investigated with two separate initial conditions. These were i) at-rest earth pressures on the wall and ii) active earth pressures on the wall.

Three channels of recorders were employed in these tests. One channel was connected to an accelerometer buried in the sand behind the wall, a second to one of the proving ring dynamometers and the third to one of the pressure cells and they were balanced. After balancing the circuit the weight was lifted to a desired height and released. The resulting records of accelerations, increase in reaction on the given proving ring and the increase in pressure on the pressure cell were recorded on the paper of the oscillographs. With the same transducers connected to the recording system, the height of fall of the weight was changed to three other values and the records were

obtained. Invariably, two records at the same conditions of fall were made to check reproducibility of data. After this, the pressure cell was changed and the procedure repeated. After measuring the pressure increment at three pressure cells the proving ring was also changed. Thus, repeating the procedure 10 times the complete data were obtained regarding dynamic increment determination and the overturning moments at four different acceleration levels.

Tests Under Steady State Vibrations:

Steady state vibrations were caused in the backfill by a mechanical oscillator fixed rigidly to a block cast 1.1m from the pit. A d.c. motor was used to drive the oscillator and various frequencies were thus achieved. However, large accelerations were not achieved at low frequencies and hence the pressure cells did not give readable output. Therefore only the overturning moments were measured using the proving rings.

Only one series of tests was conducted with the largest eccentricity setting. Two channels of the recording system were connected to two of the proving rings and one to an accelerometer. The d.c. motor was started from the lowest frequency and was run step by step to the largest frequency using a speed control unit. The records of the accelerations and the increased loads on the proving rings

were taken during each step. The test was repeated to get the record of the third proving ring also.

TEST RESULTS AND DISCUSSIONS

Accelerations in the Pit:

Fig 5.3a shows the peak accelerations recorded at a depth of 20.0 cm and at different locations in the plan of the pit. In Fig. 5.3b are plotted peak acceleration values with depth at one location during impact loading at 4.0m away from the wall. The accelerations are found to be uniform throughout the deposit. The small variations are well within the experimental errors.

Static Tests:

Fig 5.4 shows the at-rest pressures measured. As already mentioned, two different methods, one directly by the pressure cells and the other indirectly from the overturning moment measured by the proving ring supports were used. The full line gives the at-rest pressure distribution computed from the overturning moments assuming a hydrostatic distribution of pressures. The hatched area gives the results from the earth pressure cells during 5 tests (Table 5.1) and the dash-line represents the at-rest earth pressure distribution according to Jaky's value, $K_0 = (1 - \sin\Phi)$.

On yielding of the wall, the pressures and the

overturning moments reduced and attained constant values at wall displacements of 4 to 8 mm at the top. This value compares favourable with the value of 0.5 percent of wall height (which works out as 10 mm) given by Terzaghi.

In the Fig. 5.5 are shown the active pressure distribution curves obtained from the proving ring readings (line a), from Coulomb's theory for $\Phi = 40^\circ$, $\delta = 23^\circ$ (line b) from Rankine's theory for $\Phi = 40^\circ$ (line c) and from the earth pressure cells (hatched area).

Dynamic Tests:

To interpret all the data on the dynamic pressures obtained using the pressure cells, the pressures are plotted against the corresponding peak accelerations separately for all the pressure cells in Fig. 5.6. Here, it was noticed that the initial conditions, namely the active and at-rest pressures did not alter the dynamic pressures measured during the shocks. Since one of the pressure cells (at a depth of 148.0 cm) did not function properly, only nine curves are shown. From these curves the distribution of dynamic increment on the wall at five different accelerations were worked out and are plotted in Fig. 5.7.

From Fig. 5.7, the overturning moments were worked

out about the point of rotation and are given in Fig. 5.8 as a function of peak acceleration (curve a). Curves b and c correspond to the overturning moments from Seed and Whitman's (1970) simplification, and Mononobe-Okabe formula respectively. For the former, the point of application has been taken as $2/3$ times the wall height above base and for the latter at mid height.

The overturning moments obtained using the proving rings are plotted in Fig 5.9. Curve a is for the wall filled with saw dust and c for the sand filled walls. These moments are due to the dynamic increment in earth pressures as well as inertia force of the wall. Since the curves b, c and d refer to overturning moments due to the earth pressure as well as the inertia force of the wall, Fig. 5.10 was plotted between the peak accelerations and the additional overturning moments above those in the empty wall. From the two curves (lower for the case of the wall filled with saw dust and the upper, for the case of sand filling) the inertia force of the wall itself was computed and curve d in Fig. 5.9 has been plotted as the overturning moment caused by the dynamic increment alone.

Fig. 5.11 is a plot between the amplitude of acceleration and the overturning moment measured in the case of steady state vibration tests with an empty wall. In this figure the quantity given in brackets indicate the

frequency at which the measurements were made. Also the dotted line gives the overturning moment calculated on the basis of Mononobe-Okabe formula and the point of application at 60% of the height above the base.

Because of the poor correlation between the observed and calculated (from Mononobe-Okabe formula) pressures at different acceleration levels, it was thought that the velocity of the table and thus the energy input has an important part to play. Therefore, the peak velocities of the table in different tests were calculated by integrating the acceleration record and are tabulated in the table 5.2 along with the corresponding dynamic increment coefficients. The point of application of the pressures are also listed here.

Table 5 Peak Ground Velocities and Coefficient of Dynamic Increment

Peak Table Velocities cm/sec	Coefficient of Dynamic Increment	Point of application of Dynamic increment as % height above the base	Remarks
0.56	0.00322	59.4	2m high wall. Tests described in this chapter. Based on Pressure cell readings
0.84	0.00623	61.0	
1.12	0.01052	57.3	
1.4	0.01710	53.6	
1.68	0.02622	51.4	
12.98	0.2181	40.6	1m high rigid wall. Tests described in chapter 4
14.54	0.3142	36.4	
16.52	0.3370	41.5	

The above values have been plotted in Fig. 5.12a.

In the same figure is also plotted a curve obtained using Mononobe-Okabe theory with a table motion considered as sinusoidal with a period of 0.3 sec. This table motion has been considered on the basis of the findings described in Chapters 3 and 4 where it was established that a sinusoidal motion with a period of 0.3 seconds would give earth pressures corresponding to the Mononobe-Okabe theory. This was done on the basis of comparison of the velocities and the earth pressure coefficients with the ones actually observed in the tests reported in chapters 3 and 4. Also, a review of the work by Japanese investigators show that they have used a period of 0.3 seconds in their investigations. For these accelerations, the table velocities were calculated by dividing the values by the circular frequency. Thus the coefficients of dynamic increment have been plotted against the velocities as a firm line in Fig. 5.12a.

In Fig. 5.12b the point of application of the dynamic increment above the base as % of the wall height in the rigid wall tests (the present series and the one described in Chapter 4) has been plotted as a function of the peak velocities.

DISCUSSION OF RESULTS

General. Two large size walls have been tested for determining dynamic earth pressures and have been briefly reported in English language (Matsuo and Ohara, 1960 and

Niwa, 1960). In both the cases the wall was erected in a pit and vibrations were created by large rotating-mass machines kept at some distance from the wall. However in the tests, only sinusoidal vibrations were caused and the measurements were made using pressure cells. No attempt has been made to study the effect of the energy in-put or the ground velocities as all the results reported pertain to comparatively long time periods. Moreover, there had been no attempt to determine the inertia force of the wall in either of these studies. By employing comparatively short period motions of the ground and using a measurement system where the pressure distribution as well as overturning moments were obtained, data has been obtained in this investigation on two very important aspects, the energy input and the inertia force of the wall.

Method of testing. As already described earlier in this chapter, mainly impulse type loads were used for a direct comparison with the results obtained in the earlier studies made on the shake table. Those studies had indicated a dependence of the pressures on the peak velocities rather than the peak accelerations. Later, as it was found that the impulse type loads led to much smaller pressures than those given by Mononobe-Okabe formula for the peak accelerations employed, it was desired to study if any fundamental difference existed between impulse type and

steady-state type (favoured by all investigators till today) exciting forces. The oscillator used however could not produce sufficiently large acceleration levels at low frequencies, but it did create up to 0.16g at larger frequencies. Also different acceleration levels were obtained at frequencies above 15 cps to about 25 cps. These were sufficient to study if any difference in response characteristics of the system exists under the two types of ground motions.

Accelerations in the Pit:

The Fig. 5.3 shows that the peak accelerations in the pit remain practically the same throughout the deposit under identical impact (of the falling weight and the ground) conditions. This shows that the distance of the falling weight from the wall is sufficient. Also by causing the waves to travel through the ground, the conditions in the field is simulated to a great extent.

Static Earth Pressures:

Fig 5.4 gives the at-rest pressures acting on the wall and measured by the pressure cells and the proving rings in 5 of the tests. For the latter, a hydrostatic pressure distribution was assumed to calculate the pressures from the overturning moments. The at-rest pressures measured by the pressure cells are almost equal to the calculated values from $K_0 = (1 - \sin\phi)$. This can be expected

because there was no tamping of the deposit behind the wall. Fig. 5.5 gives the active pressures measured. These pressures are slightly higher than the pressures from both Rankine's ($\Phi = 40$) and Coulomb's ($\Phi=40, \delta = 23^\circ$) theories. This difference may be considered as a permissible experimental error. The pressures computed from the overturning moments measured using the proving ring supports are smaller than those from the pressure cell measurements. In the case of at-rest pressures it is only about 66 % of pressures from the pressure cells while in active conditions, the reduction is still larger and the value is only just more than 60 %. This points towards a possibility of arching with the side wall contributing significantly by friction. Also, since the difference exists under at-rest conditions, it is evident that extremely small displacements are sufficient to bring about arching as the deflections of the wall are no more than those caused by the elastic compression of the proving rings.

Dynamic Earth Pressures :

The dynamic earth pressures as described here denote the instantaneous increase in earth pressures recorded as the output of the pressure cells at various elevations. No attempt were made here to measure the phase difference between the peak accelerations and the peak pressures.

Fig 5.7 has been plotted to show the nature of the distribution of dynamic increment on the wall. From these curves, the overturning moments were computed at 5 acceleration levels and this is shown in Fig. 5.8. A comparison of the dynamic increment from the pressure cells (curve a) and that from the measurement of overturning moments (curve d, Fig 5.9) show that the latter is only about 45 to 50 % of the former. No other explanation except that the response of the proving rings could be slow because of the ball support seems to be valid because it is highly improbable that arching would develop under the loading conditions used here. However, no improvement of the support system was considered possible because the static tests described here need the ball support for transferring the load centrally and to facilitate rotation of the wall. (A clue to the possibility of slow response of the proving ring assembly was available during steady state vibration tests where the actually measured pressures with the proving ring, followed the general pattern of the relationship between the dynamic increment from the pressure cells and the peak ground velocity. Fig. 5.12).

In both Fig 5.8 and Fig 5.11 it is apparent that the Mononobe-Okabe theory overestimates the pressures if the shock is of high frequency type. Thus, the pseudo-static approach suggested by the codes of practice in many

countries is not valid for all types of ground motions and a need exists to take into account the nature of the ground motion. In an attempt to consider the frequency of the motion the peak velocities were used for comparison as in Fig. 5.12. The velocities corresponding to various acceleration levels and a period of 0.3 sec was used for a comparison of the dynamic increment in these investigations and the pseudo-static approach in vogue. It will be seen that a fairly good prediction is possible if the velocities are used for comparison instead of accelerations. This can be expected because the energy of the ground motion is an important factor determining the response of the system. Aliev, Mamedov and Radgabova (1973) have also reported a better relation between the velocities the of the ground and the dynamic pressures than between the pressures and accelerations, but no detailed data is available there. It is felt that this important factor went unnoticed because of the fact that most of the previous investigators used a period of vibration of the table on which the set up was mounted, close to 0.3 sec. and at this period there happens to be a correlation between the pressures and accelerations as given by the Mononobe-Okabe theory.

Since three different types of ground motions

- i) Impulse type with very large magnitude of accelerations
- ii) Impulse type and iii) Steady state with magnitude of

accelerations of the same order as are usually associated with earthquake shocks, have been used here and a unique relationship between the peak velocities and the dynamic increment in earth pressure has been obtained.

Point of Application of the Dynamic Increment:

From Fig. 5.11 it is seen that the point of application of the dynamic increment is higher at smaller velocities and the data from the tests described in chapter 4 have been used to get the trend at higher velocities. It appears that the point of application remains at a constant height at higher velocities. This may be associated with possibilities of movement because at smaller velocities the movement of soil particles may be limited to the top portion while at larger values of ground velocities sufficient movement takes place at lower elevations also. Moreover, the values obtained have no practical significance at low velocities as they are extremely small from earthquake considerations.

Inertia Force of the Wall:

The overturning moments on the wall during shock loading were measured with identical backfill conditions but three different wall weights. These were empty wall, wall filled with saw dust and wall filled with a sand. These overturning moments are plotted against the corresponding

peak accelerations in Fig. 5.9. The contribution of the increased earth pressure alone has also been worked out and is shown in the same figure (curve d). As already described, the values recorded are small, but even after making the necessary corrections, it appears that the inertia force of the wall is extremely small. However, these values in relation to the overturning moments of the earth pressures themselves are not negligible and so there is a possibility that the inertia force of the wall is also a function of the energy input. Therefore it was desired to study the relation between the inertia forces and the dynamic increment in earth pressures.

The centre of gravity of the wall is at about 45% of the wall height above its base in these tests. The dynamic increment however acts at about 40% of the wall height. Therefore if it ^{is} assumed that they act at the same height and if the ratio of the overturning moments due to the inertia forces and the earth pressures are taken to be equal to the ratio of inertia forces and the earth pressures themselves, the estimation of the inertia forces would be conservative. Fig 5.13 has been plotted between the ratio of inertia forces of the wall and the dynamic increment against the ratio of the weight of the wall and the static earth pressure. It is found that for all the acceleration levels considered, the relationship between the two ratios would

be confined to a narrow band. The value of inertia forces are larger for larger wall weights and for reasonable ratios of wall weight and the static earth pressures, the ratio of inertia forces and the dynamic increment would not exceed 0.5. The ratio is much smaller for lighter walls.

Thus if the dynamic increments are calculated on the basis of the ground velocities, the inertia forces can be obtained by multiplying it with a ratio which however depends on the ratio of the wall weight and the static earth pressures.

SUMMARY

i. The dynamic increment in earth pressure exerted by sands is having a unique relation with the peak velocities irrespective of the type of ground motion. Mononobe-Okabe theory however gives the same results if the ground motion is characterised by an acceleration amplitude of $k_h g$ but a definite time period of 0.3 sec.

ii. The point of application of the dynamic increment on rigid walls may be taken at 40% of the height of the wall above its base.

iii. Tentative relationship between the inertia force of the wall and the dynamic increment in earth pressures has been established considering the weight of the wall.

INTRODUCTION

A review of the past work and design practices shows that the designs of retaining walls are prepared on the basis of calculated lateral thrust. However, a number of factors lead to a condition that the actual lateral earth pressures (both static and dynamic) on the wall are unknown to the designer. These factors may include

- a. The properties of foundation soil in the actual state of strain.
- b. Real behaviour of wall. Rigid walls rotate only due to the deformation of soil below the foundation and flexible walls (cantilever and counter-fort walls included) deform and rotate due to bending of the wall and the strains in the foundation soil respectively. Perhaps in practice a wall acts partly as rigid and partly as "flexible".
- c. The nature of ground motion in relation to the natural frequencies of the retaining wall.

Thus, in the absence of adequate information on the lateral earth pressure, both in magnitude and distribution, the design becomes rather empirical and only leads to a satisfaction of some precautions having been incorporated.

The factor of safety incorporated in the design assures a provision of greater resistance than the known forces require. In other words, all earthquakes may not cause failure of a wall depending upon the dynamic forces generated and the factors of safety used. The dynamic force which may reduce the Factor of Safety of the wall to unity can conveniently be represented as an acceleration called 'yield Acceleration'.

Assuming a rigid plastic behaviour of the foundation soil, it can be said that if the earthquake accelerations are smaller than the yield acceleration no displacement of the wall would result. On the other hand, if the accelerations exceed the threshold value, displacements occur depending upon the time for which these conditions prevail. The present design procedures however do not take into account the 'damage causing potential' of ground motions as also the reversal of forces and the resulting displacements, which may be small. Most walls can safely be permitted to undergo small displacements during earthquake likely to be experienced only a couple of times during the life time of the structure. However, in structures such as bridge abutments, wing walls where only small displacements can be permitted or none at all, the present design procedure is totally inadequate as no estimate of displacements is made. Also, a larger factor of safety under dynamic conditions with

the present design procedure for such structures does not necessarily ensure small or no displacements. It is due to the fact that the displacements depend very much on "damage potential" or the energy of the expected ground motion and not the force levels only. It is well known that shocks of even smaller acceleration amplitudes can cause heavier damage compared with larger acceleration pulses if the former acts for much larger duration. In short a need exists to assess the earthquake induced displacements of retaining walls for more realistic designs.

MATHEMATICAL MODEL

For devising a mathematical model of the retaining wall-foundation soil-backfill system, the physical behaviour of the system needs be examined in detail.

To start with, the deformation of the wall under various types of forces may be looked into. A rigid wall either moves parallel to itself (translation) or rotates at the foundation level about the toe of the wall depending on the foundation conditions. However, both the forms of movements can also occur simultaneously.

Considering a high concrete wall, possibility of a well designed foundation rules out translation or rotation as the major movements and flexural bending of the wall itself and its base may be dominant. In short, a true mathematical model should be one where all the three

modes of movements (plus vertical movements to be more exact) are considered. This becomes rather involved because of the non-linear behaviour of the soil behind and below the wall. Hence to begin with, simpler cases may be considered. Assumption of a rigid wall considerably reduces the number of degrees of freedom and disregarding vertical motions which would be insignificant, only a two degrees of freedom system - translation and rotation about the toe, would result. These assumptions are valid to a great extent since i) deformations in the soil resulting in translation or rotation of wall will be much more prominent than those of the wall and ii) the vertical ground motions in majority of cases may not be that important. In the present work however only one degree of freedom is considered, that of translation, which should be sufficient in majority of cases of walls in alluvial deposits and at the water front. Here the 'wall displacement' has been used as the total displacement from the original position of the wall and the deformation of the soil and the relative displacement between the wall and the soil have not been considered separately.

A one degree of freedom system can be represented as a spring-mass-dashpot system. The mass includes the mass of the retaining wall and that of some portion of the back-fill which vibrates along with the wall. The latter has been called variously as "apparent soil mass" (Barkan 1962)

and "virtual" mass. The spring characteristics take into account the resistance to displacement of the soil below and behind the wall. This means that by assuming the wall as rigid it has been considered to have only inertial properties and no elastic properties. A dash pot is included to take into account the energy absorption characteristics of the system. Thus with the assumptions made the system can be mathematically described after evaluating the mass, the spring characteristics and damping. The apparent soil mass and the damping cannot be assessed with the already available information. But reliable information on the spring characteristics can be obtained by a careful interpretation of the past work.

Evaluation of Spring Forces:

The resisting forces in the case being considered result from the soil both below and behind the wall. Therefore the net resistance can be considered as the sum of the forces from the backfill and the foundation soil, the two being considered separately from well established theories. For example, the reaction from the backfill as a function of wall displacement is shown in Fig. 6.1(a). At zero displacement or when there is no strain in the backfill, the lateral pressure on the wall is equal to 'at-rest' pressure A. This value increases fairly linearly with displacement till failure of the backfill occurs at a pressure B. This is

known as the state of passive plastic equilibrium. On the other hand the displacement of the wall away from the backfill causes reduction in lateral pressures to the active pressures C .

The base resistance or the frictional force at the foundation level could be achieved by the embedment of the wall or just by friction between the wall and the soil. Whatever be the fashion in which the resistance to sliding is achieved, some amount of displacement is essential for its mobilization. So it is reasonable to assume a resistance function as shown in Fig. 6.1(b) for the base resistance. Thus the net force as a function of wall displacement is obtained by summation of the two as shown in Fig. 6.1c. For maintaining equilibrium the wall has to displace to the position XX under static conditions. Therefore, for dynamic analysis of the system the skeleton curve will be as given in Fig. 6.1(c). A simplified version of this is given in Fig. 6.1(d), where the displacement-force relationship on both sides has been taken as elasto-plastic though on the compression (of the backfill) side both the stiffness and the yield level of the forces are larger than those on the tension side. The yield level on the compression side is approximately equal to 30 to 35 times the active pressure (based on realistic values of K_p , the coefficient of passive pressures) while that on the tension side is approximately 0.5 times

the active pressure as the factor of safety against sliding is generally taken as 1.5. Thus for all practical purposes the system does not go to plastic state on the compression side. With the above assumptions the mathematical model proposed for the system is as shown in Fig. 6.2.

The mass of soil participating in vibration can be determined only from a carefully planned experiment in the absence of mathematical procedures or published work on this aspect. A new type of experimental set up was devised and has been described later in this chapter.

The effects of various parameters have been studied by analysing the response of the system using a numerical technique.

Analysis:

An exact solution of the model in Fig 6.2 a subjected to ground motion is not available. Also, because of unequal spring stiffnesses on the tension and compression sides and much smaller yield force on the tension side the closed form solution, even if developed will be highly involved. Hence a numerical technique was used.

Linear acceleration method (Biggs 1963) was selected for numerical integration of the equation of motion which can be written in the form

$$m \ddot{x} + c (\dot{x} - \dot{y}) + R(x-y) = 0 \quad \dots 6.1$$

$$\text{or } m \ddot{z} + c \dot{z} + R(z) = -m \ddot{y} \quad \dots 6.2a$$

$$\ddot{z} + 2p \zeta \dot{z} + p^2 R(z)/k = -\ddot{y} \quad \dots 6.2b$$

where $z = (x-y)$,

$p^2 = k/m$ where k has been defined as the stiffness on the tension side.

In the linear acceleration method, the three equations given below need be satisfied at each instant of time or at the end of each time interval selected

$$z_{n+1} = z_n + \dot{z}_n \Delta t + \frac{\Delta t^2}{6} (\ddot{z}_{n+1} + 2\ddot{z}_n) \quad \dots 6.3$$

$$\dot{z}_{n+1} = \dot{z}_n + \frac{\Delta t}{2} (\ddot{z}_{n+1} + \ddot{z}_n) \quad \dots 6.4$$

$$\ddot{z}_{n+1} = -\ddot{y} - 2p \zeta \dot{z}_{n+1} - \frac{p^2}{k} R(z_{n+1}) \quad \dots 6.5$$

where z_{n+1} , \dot{z}_{n+1} and \ddot{z}_{n+1} are the displacement, velocity and acceleration (all relative to the ground) at instant t_{n+1} and z_n , \dot{z}_n and \ddot{z}_n are their values at instant t_n , Δt is the time interval between t_n and t_{n+1} and ζ is the fraction of critical damping.

For ease in computations all the three equations (Eq. 6.3 to 6.5) can be divided by Z_y the relative displacement on the tension side at which the resistance becomes constant (yield displacement) to obtain the following relations

$$\psi_{n+1} = \psi + \dot{\psi}_n \Delta t + \frac{\Delta t^2}{6} (\ddot{\psi}_{n+1} + 2\ddot{\psi}_n) \quad \dots 6.6$$

$$\dot{\psi}_{n+1} = \dot{\psi}_n + \frac{\Delta t}{2} (\ddot{\psi}_{n+1} + \ddot{\psi}_n) \quad \dots 6.7$$

$$\ddot{\psi}_{n+1} = -\ddot{y} - 2p \zeta \dot{\psi}_{n+1} - p^2 Q (\psi_{n+1}) \quad \dots 6.8$$

$$\begin{aligned} \text{where } \psi &= \frac{Z}{Z_y} \\ \dot{\psi} &= \frac{\dot{Z}}{Z_y} \\ \ddot{\psi} &= \frac{\ddot{Z}}{Z_y} \\ Q &= \frac{R}{R_y} \end{aligned}$$

$$R_y = \text{yield force} = k_z Z_y$$

Now if the force-displacement relationship is redrawn between ψ and Q as shown in Fig. 6.2 c, it will be seen that a non-dimensional plot results, with stiffness and yield force values on the tension side as unity and the stiffness value on the compression side equal to $\eta = k'/k$. With this relationship between Q and ψ , the analysis is performed to satisfy Eq. 6.6 to 6.8 for the ground accelerations.

Ground Motion:

Earthquake motions are erratic and no two accelerograms are similar. Therefore, unless the response of a system due to a given accelerogram is desired, it is

advantageous to make some sort of a parametric study. The two main parameters of any ground motion are the amplitude of accelerations and the number of zero crossings in unit time. A very simple and convenient form of ground motion for studying the above parameters is a sinusoidal motion. Moreover, while proposing a method for analysing the liquefaction potential of sand deposits, Seed and Idriss (1970) contended that any given accelerogram can be considered equivalent to some definite number of cycles of loading of equal magnitude. Such idealisations have the advantage that after studying the effect of the two parameters either analytically or in the laboratory the effect of a probable earthquake motion at any site, can be analysed. Because of the above advantages sinusoidal ground motions were utilised in the present study.

VARIABLES CONSIDERED

Yield Displacement:

The retaining walls will suffer permanent or irrecoverable displacement only if the system goes into the 'plastic' stage during ground motions. Here the behaviour of the system has been defined as elasto-plastic on the tension side and elastic on the compression side. So, permanent displacements can be considered by specifying the displacement of the wall corresponding to the transition

from elastic to the plastic range.

Various cases of retaining walls can be studied by taking a few values of the yield displacements in the computations. A low value of yield displacement generally is associated with a low value of force required to bring the system into plastic state for identical stiffness values. This means that a low value of yield displacement and a large exciting force level would cause large plastic displacements of the wall, termed as 'slip' in this study. On the other hand, a large value of yield displacement and a low value of exciting force (the two are relative, of course) would ensure small slips and even elastic conditions. The latter occurs when the exciting force level is smaller than the force level required to bring about plastic conditions.

Behaviour of the backfill to investigate the possible values of yield displacements in actual walls, it is necessary to consider the cases of active and passive pressures as well as the displacement of the wall required for mobilisation of these pressures and the base friction. A review of the relevant literature shows that there is fair agreement in the values of wall movements considered necessary for development of active earth pressures (Terzaghi, 1936, Mackey and Kirk, 1967, Tests in the present work, Chapter 4). This value may be taken as 0.5% of the

height of the wall. For passive pressures very few test reports are available, however. (Rowe and Peaker, 1965, Narain, Saran and Nandakumaran, 1969). For the case of translation, passive earth resistance has been found to mobilize at a displacement of 5 to 10 percent of the wall height. However to account for the steeper initial slope, for active case a displacement of 0.25% and for passive, 2.5% wall height have been taken. These findings, together with the pressure values can be used to find out the slopes of the curve in Fig. 6.1a.

Behaviour of the Foundation Soil:

There is very little published data to determine the curve in Fig. 6.1b. Some reasonable assumptions have therefore been made based on qualitative data available.

1. An elastic wedge is formed in the soil below the wall, bounded by the base of the wall and two sides inclined at Φ , (the angle of internal friction of the soil) with the base.

2. On application of a lateral force to the wall, the resistance offered by the soil is equal to the passive resistance on the altitude of the triangle formed.

By making the above assumptions which are reasonable, both the magnitude of the base friction and the wall displacement necessary for its mobilisation can be conveniently

determined to study the feasibility of making use of the above concept, some computations were made. The coefficient of base friction was calculated from the values of pressure obtained as above. Cases of gravity walls with vertical face was considered, Φ and δ the angle of internal friction and wall friction respectively were taken as 36° and 24° . The results are tabulated in Table 6.1

The values of coefficient of base friction (column 7) as computed are very near the value 0.5, commonly used in designs. In these computations the base width has been taken as 0.5 times the wall height. Had the soil been weaker or the angle Φ been smaller, larger base width to height ratio would have been used. This would lead to larger values of h (column 3) but smaller values of $k_p \cos \delta$ (column 4). The base friction would increase but not at the same rate as the increase in the weight of the wall and thus the coefficient of base friction would decrease which is quite compatible for weaker soils.

From the column 3 in Table 6.1, it will be noticed that 'h' is approximately 0.2 times the wall height and therefore the displacement required for mobilisation of base friction is equal to $2.5/100 \times 0.2H = 0.5\%$ of the wall height. However, for development of active pressure behind the wall a wall displacement of 0.25% of wall height is required.

TABLE 6.1

Calculation of the Coefficient of Base Friction from the Suggested Method.

Wall height H m	Base width B m	Altitude of elastic wedge $h = \frac{B}{2 \tan \phi}$ cm	$k_p \cos \delta$ (Coulomb's theory)	Base friction $= \frac{1}{2} \gamma h^2 k_p \cos \delta$ tons	Weight of wall Tons	Coeff. of base friction $\frac{5}{7}$	Remarks
1	2	3	4	5	6	7	8
2.0	1.0	36.3	11.0	1.16	2.6	0.446	
4.0	2.0	72.6	11.0	4.64	9.2	0.504	
8.0	4.0	145.2	11.0	18.56	34.4	0.54	

Note : Actual values in column 7 shall be slightly smaller than the ones computal because the vertical component of earth pressure has not been considered in these computations

For equilibrium of the wall, the base resistance and the active pressures should be equal and therefore for the mobilization of requisite base resistance the wall movement must be $(1/1.5) \times 0.5\%$ of wall height where 1.5 is the factor of safety against sliding. Thus the yield displacement is equal to $0.5\% (1 - \frac{1}{1.5})$ or 0.166% of the wall height. Considering wall heights of 2.0 m to 20.0 m, the yield displacements would be 0.33 to 3.3 cm.

In the computations five different values, 0.1, 0.2, 0.3, 0.5 and 1.0 cm have been used. In parametric study yield displacements larger than 1 cm were found to result in elastic displacements of

Wall in most cases.

The relationship between the wall height and the displacements for mobilisation of base resistance has been approximated only for the purpose of obtaining reasonable values in the parametric study. Actual solutions would require proper evaluation of the above as shown later in this chapter.

Natural Period of the Walls

The natural period is defined here as $2\pi\sqrt{m/k}$, where m is the mass of the system and k the stiffness of the system on the tension side. The stiffness k is more significant because once the yield displacement is given, the yield force level is obtained as the product of k and the yield displacement. Also, the stiffness on the tension side would be decisive in the response of the mass on this side and hence in the irrecoverable displacements.

In the absence of practically any procedure to determine the natural period of retaining walls, it was decided to consider four different values arbitrarily. These values are 1.0, 0.5, 0.3 and 0.2 sec. In a parametric study these values would give most useful results because of their similarity with the periods of ground motion generally associated with earthquake shocks.

Ground Acceleration Amplitudes: _s

Since a sinusoidal ground motion has been used for this study, the amplitude of ground acceleration can be somewhat smaller than the peak accelerations in recorded ground motions during past earthquakes. Accordingly, a maximum value of 300 gals was taken. It will be noticed here that higher acceleration levels are present in the accelerograms of past earthquakes but only for one or two cycles. The 'average' value of accelerations will be of the order of 300 gals or less. By considering two other acceleration values, it has been possible to extrapolate the results at even higher acceleration levels. The values considered are 300, 200 and 100 gals.

Period of Ground Motion:

The period of ground motion is influenced by the type of the soil cover at any site. Short periods are associated with stiff soil (or say rock) and long periods with loose soils. From the available records of past earthquakes obtained on a variety of ground conditions at site, it can be concluded that the predominant frequencies of earthquakes range from about 2 to about 10 Hz. Accordingly, four values of ground motion periods namely 0.5, 0.3, 0.2 and 0.1 sec have been considered here.

Ratio of Stiffnesses on the Compression and Tension Sides:

In general the stiffness of the system on the tension side would be influenced by the base resistance characteristics or in other words the mobilisation characteristics of passive pressures. The stiffness on the compression side is likely to be twice this value because the latter is influenced by the passive pressures behind the wall as well as the base resistance. Hence η , the ratio k'/k has been given a value of 2.0. However to study the effect of variation in this value on the slips, a few computations were made with η equal to 3.0.

Damping as Fraction of Critical Damping:

In soils it is customary to consider values of damping such as 15% or 20% critical in view of larger energy absorption compared to other engineering structural materials. In the present study however, energy absorption in the form of plastic displacement of the wall has been considered. Therefore smaller damping values would be appropriate. To study the effect of damping, three values, namely 5%, 10% and 15% of critical damping have been considered.

All the variables considered are listed in Table 6.2

TABLE 6.2

Variables Considered in Computations

Yield Displacement (Z_Y)	0.1, 0.2, 0.3, 0.5 and 1.0 cm
Natural period (T_n)	1.0, 0.5, 0.3, and 0.2 sec
Ground acceleration amplitude (A)	100, 200 and 300 gals
Period of ground motion (T)	0.5, 0.3, 0.2 and 0.1 sec
Ratio of Stiffnesses (η)	2.0 and 3.0
Damping as fraction of (ζ)	5, 10 and 15 % critical damping

RESULTS OF COMPUTATIONS AND DISCUSSIONS

Checks for the Computer Programme:

Time interval : Biggs (1963) has suggested that while using linear acceleration methods, a time interval of one tenth of the natural period is sufficient for accurate computations. Two smaller time intervals, namely $1/22$ and $1/32$ of the smaller of the natural period and the ground motion period were therefore considered. The difference between the slips in the two cases were only slightly different with the smaller time interval giving 2 % less values. In view of this and the computation time, the former time interval was selected.

Analysis of an Elastic System:

The variables in the programme can be so chosen that the

system becomes a spring-mass-dashpot system with linear spring characteristics. For this the ratio η was taken as unity and the yield displacement as 20.0 cm. The response of this system with a natural period of 0.3 sec and damping of 10% to a ground motion of acceleration amplitude 300 gals and period of 0.3 sec was studied, Fig. 6.4. In the same figure, the amplitude of motion (after steady state has been achieved) of the system from the closed form solution has also been given for comparison. It is seen that 1) Steady state conditions are reached in about 6 cycles of ground motion and 2) The amplitude of motion obtained from the numerical technique is in close agreement with that from the exact solution. The values from the numerical method and the closed form solution are 3.30 and 3.375 mm respectively, a difference of only 2.2 percent. For most engineering purposes, this accuracy can be considered adequate.

Study of Response Characteristics of the System:

To study the response characteristics of the system, two cases were considered; one in which plastic deformation does not take place and the other in which it does. The system is characterised by a natural period of 0.3 sec, $\eta = 2.0$ and damping of 10% critical. The yield displacements were however different at 20.0 and 1.0 cm, the latter for a yielding case. The ground motion is described by a ground motion amplitude of 300 gals and a period of 0.3 sec.

Fig 6.5 shows the response of the 'elastic' system. It will be noticed that steady state conditions are attained in about 6 cycles and also that the displacements on the tension side are larger than those on the compression side. Also, when compared with Fig. 6.4 where the response of the system where all variables except η are the same as in this case but η is equal to 1.0, it will be seen that the amplitude of motion is decreased with this increase in η . This is because the system in Fig. 6.5 has different natural frequencies on the tension and compression sides and hence resonance does not take place.

The response of the system wherein slips take place have been plotted in two ways in Figs 6.6 and 6.7. Fig. 6.6 shows the time-wise displacement of the system and it will be seen to move gradually towards the tension side with time. Fig. 6.7 is plotted between the displacement function (ψ) and the resistance function (Q). This shows how the system behaves during the ground motion and that even when plastic deformations take place, a sort of steady state is achieved in the sense that the slip per cycle becomes a constant after about 6 cycles.

Slip per Cycle:

The response calculations here have been made on the basis of the system starting from 'rest'. However, it is felt that identical conditions would not prevail in retaining

walls in the field. Here, by the time damaging pulses arrive at its base, the wall is likely to be in motion already because of the small waves preceding. Therefore, if the ground motion is to be simplified as an equivalent sinusoidal motion, the slips at steady state conditions would be more appropriate. It was indicated in Fig. 6.7 that the slip per cycle remains a constant after a few cycles of ground motion. To study the aspect further, the slip was plotted against the number of cycles for various cases of system and ground motion properties, Fig 6.8. It will be observed that in these curves after 4 to 5 cycles the slip per cycle becomes constant.

Effect of Damping :

Fig 6.9 shows the effect of damping on the slip per cycle for a typical structure of natural period = 0.5 sec and yield displacement = 0.1 cm due to 5 different ground motions. It will be noticed that when the natural period is not equal to the forcing period, the effect of damping is small. In the case of large acceleration levels and natural period equal to the forcing period, the difference between 5% and 15% damping is upto 1.6 cm. However the effect of damping between the extreme values considered is only 9% different from the mean value for all the curves. Therefore it is reasonable to consider a damping of 10% critical as against 15 or 20% critical because plastic deformations

have been considered.

Effect of Ground Acceleration Amplitude :

Fig 6.10 presents the effect of the ground acceleration amplitude on the slip per cycle for systems of different natural period and damping of 10 % critical. All curves except 2, are for a yield displacement of 0.1 cm and curve 2 for a yield displacement of 0.2 cm. In all the cases, the slip per cycle has been found to have a linear relationship with the ground acceleration amplitude. A comparison of curves 1, 4 and 5 (drawn for $T = T_n = 0.5, 0.3$ and 0.2 respectively) shows that at 'resonance' condition, longer ground motion period causes not only larger slips but the rate of increase with acceleration is also larger. Comparison of curves 1, 3 and 6 ($T = 0.5$ sec, $T_n = 0.5, 1.0$ and 0.2 respectively) shows that for a given ground motion, the resonance condition causes larger slips and larger rate of increase in slip. By comparing curves 1 and 2, it will be seen that larger yield displacement causes smaller slips, all other variables remaining the same, but there is hardly any change in the rate of increase in slip with acceleration amplitudes. From these curves, it is also possible to extrapolate the results for accelerations larger than 300 gals as well as smaller than 100 gals.

Effect of Natural Period of the System:

Fig. 6.11 has been plotted between the slip per

cycle and the natural period of the system for various ground motions and a yield displacement of 0.1 cm. It will be noticed that for any given acceleration amplitude and period of ground motion larger slips occur when the natural period coincides with the forcing period. Also in general a ground motion with a period of 0.5 sec causes larger slip than all other periods for any given acceleration amplitude. Similar observations can be made for other yield displacements also from Fig. 6.12 to 6.15 where similar curves are plotted for various yield displacements of 0.2, 0.3, 0.5 and 1.0 cm.

Effect of Yield Displacements:

In Fig. 6.16(a) are plotted the slip per cycle for various yield displacements and three acceleration amplitudes. Here the forcing period as well as the natural period of the system are equal to 0.5 sec and damping is equal to 10% critical. Similar curves for 'resonance' conditions are plotted in Fig. 6.16(b) (forcing period and natural period equal to 0.3 sec) and Fig. 6.16c (forcing period and natural period equal to 0.2 sec). From these plots, it will be seen that

1. Increase in yield displacement causes decrease in the slip per cycle, all other variables being unchanged.
2. The above decrease in slip, expressed as a fraction of the slip per cycle for a yield displacement

of 0.1 cm, is smaller for larger periods of ground motion. This is because the forces causing the slip act for longer periods and there is larger damage potential for long period ground motions. The above comparison is made only for the conditions of resonance, but the same trend will be observed for all other cases as is evident from an examination of Figs. 6.11 through 6.15.

Effect of η :

As already described on page 125, two values of η were used. To compare the slips in the two cases, Fig. 6.17 was plotted between the slip and the number of cycles. Curves 1 and 2 are for $\eta = 3.0$ and 2.0 respectively with all the other variables remaining the same. The ground motion is characterised by an acceleration amplitude of 300 gals and period of 0.5 sec and the system by a natural period of 0.5 sec and damping of 10 % critical. The yield displacement was taken as 0.1 cm. A slight increase in slip is observed when η is increased from 2.0 to 3.0. This is because the increased stiffness reduces displacement of the mass on the compression side and increases it on the tension side where plastic displacements take place. The difference is small and even a value of 2.0 may be larger than the ratio in actual problems. A similar observation can be found when curves 3 and 4 are compared.

In these, the natural period of the system is 1.0 sec.

In view of the above, a value of $\eta = 2.0$ is recommended for design purposes.

USE OF THE RESULTS FOR ACTUAL PROBLEMS

With the assumptions made and discussed for the analysis of the retaining walls, one can determine all but one data required to use the curves for displacement computations. The data required are a) Natural frequency of the wall b) Yield displacement c) Damping d) Ground acceleration amplitude and forcing period. Of these, natural frequency of the wall can be determined if the stiffness on the tension side and the mass of the system are known. The former can be determined with the assumptions already discussed but the soil mass vibrating along with the wall poses some difficulties. All other data required can be obtained easily.

Determination of Soil Mass:

Since it is difficult, to determine analytically the soil mass that would participate in vibrations, it was decided to experimentally determine the same. For this the mathematical model was translated to an experimental set up (Figs. 6.18, 6.19) with a model wall 'A' made of 1.80 cm thick M.S. plate 30 cm high and 100 cm long hung from the top of the side walls of a bin in which the wall

is placed. In this position the wall is only able to translate. The wall is however restrained from movement by six plates (B) 6 cm high bearing against sand placed in six separate containers as shown in Fig 6.18. They are kept in two rows at the $\frac{1}{3}$ and $\frac{2}{3}$ rd points of the wall. The middle containers are 11.0 cm wide and all others 6.0 cm wide. The model wall is backfilled, thereby giving the idealisation shown in Fig. 6.1(a). The bearing plates which restrain the wall from movement have sand filled on either side so as to show the characteristics shown in Fig. 6.1(b). The bin is mounted on a horizontal shake table which can be excited by a mechanical oscillator mounted below the table and in its centre. The oscillator is driven by a variable speed d.c. motor. The instrumentation include a Miller accelerometer to measure the table accelerations and a spring type displacement gauge mounted on the top of the wall. The displacement gauge consists of a strain gauge mounted flat spring strip with one of its ends fixed to the wall and the other rigidly to the bin. Any displacement of the wall would cause bending of the strip and measurement of the bending strains in the strain gauges would indicate the wall displacements. A calibration of the gauge showed that for one millimeter displacement of the wall as much as 52 microstrains are produced in the strain gauges.

In an attempt to avoid the side effects from the side walls of the bin the test wall was made in three

segments, the middle one 50.0 cm wide and the end ones 25 cm wide. However, since all the segments were connected to the same rod and bearings on top, this might have resulted only in a minor advantage.

Test Procedure:

Static

The wall was backfilled and the containers in which the plate B which restrain wall movements are placed, are filled and the table excited for compaction. The backfilling is done in three layers of 15 cm each. Then the wall was moved both away from and towards the backfill in two separate fillings. The load required for these movements were measured with a proving ring and small movements were made possible with a screw jack. The resulting load deformation curve is shown in Fig. 6.20. On the tension side the stiffness was found to be 400 kg/cm.

Dynamic

The arrangement for static loading was removed and the wall was restrained only by the rods and plates (B). The plates were backfilled and the wall was restrained from any movement by clamping at the bearing level with G-clamps. The backfilling was done in three layers each time compacting it with exciting the shake table to acceleration levels larger than those used in the tests. After backfilling is

completed, the clamps were removed and the shake table was excited starting from the smallest frequency, a continuous record of the table accelerations and wall displacements being obtained.

From these records, it was observed that the wall vibrates in elastic (for all practical purposes) state till accelerations of the table was very large at high frequencies of motion. The amplitudes of vibrations obtained from the displacement gauge are plotted against the forcing frequencies in Fig. 6.21.

The natural frequency and the stiffness k on the tension side being known, the mass involved can be calculated. It will be noted that the stiffness on the tension side alone has been considered because of the results shown in Figs. 6.11 to 6.15 wherein maximum response has been found to occur when the forcing frequency equals the natural frequency defined on the basis of stiffness on the tension side.

The soil tested had the following characteristics:

density = 1.592 g/cc

Angle of int. friction = 42°

All other properties of the soil are as listed in Chapter 3 under the sub heading, 'Soil Properties'.

The mass of soil participating in vibration can be obtained from the equation

$$w_n = \sqrt{\frac{k}{m + m_s}} \quad \dots 6.9$$

where w_n is the natural frequency in rad/sec.

k is the stiffness on the tension side, 400 kg/cm

m is the mass of the wall and fittings = $\frac{72.5}{981}$ kg sec²/cm

m_s is the soil mass participating in vibrations.

Thus the soil participating in vibrations is found to be weighing 25.5 kg. This corresponds to a triangular wedge of height 30.0 cm (height of the wall) and a top width of = 10.63 cm. If the Rankine wedge is considered, it will have a top width of 13.36 cm. Therefore the soil mass participating in vibrations may be taken as equal to 0.8 times the mass of Rankine's wedge. It was also observed that the rupture wedge developed behind the wall was also smaller, its emergence at the surface being about 0.8 times the value from Rankine's theory, away from the wall.

ILLUSTRATIVE EXAMPLE

Consider a retaining wall as shown in Fig. 6.22. The wall is gravity type and it is assumed that the wall will translate when subjected to an earthquake motion. The properties of the soil below and behind the wall are listed in Fig. 6.22. If it is required to find out the displacement this wall would experience when an earthquake idealised as 15 cycles of sinusoidal motion with a peak acceleration of 250 gals and a period of 0.3 sec occurs, the solution would consist of the following steps.

- a. Determination of of the natural period of the wall.

This involves determination of i) the stiffness on the tension side and ii) the mass of soil and the wall.

- b. Determination of the yield displacement.
- c. Determination of the slip per cycle from Fig. 6.11 to 6.15 corresponding to the yield displacement, the natural period of the wall and the ground motion considered. This might require interpolation also.
- d. Computing the total slip during the ground motion.

These are illustrated below

- a. Determination of the Natural Period

- i) Determination of stiffness on the tension side

As described on page 120, the base resistance is equal to the passive pressure on a height A B (see Fig. 6.22b)

$$\text{Height } AB = h = 0.3 + 0.364 = 0.664 \text{ m}$$

$$\text{Passive Pressure Coeff. } K_p \cos \delta$$

$$(\text{Coulomb's theory for } \Phi = 36^\circ, \delta = 24^\circ) = 11.0$$

$$\text{Base resistance} = \frac{1}{2} \times 1.8 \times (0.664)^2 \times 11.0$$

$$= 4.35 \text{ tons.}$$

$$\begin{aligned} \text{Displacement required for} \\ \text{mobilisation of the base} \\ \text{resistance (} 2 \frac{1}{2} \% \times \text{AB) } &= \frac{2.5}{100} \times 66.4 = 1.567 \text{ cm} \end{aligned}$$

$$\begin{aligned} \text{Active pressure on the wall} \\ (K_a \cos \delta = 0.21 \text{ for } \Phi = 36^\circ, \\ \delta = 24^\circ) &= \frac{1}{2} \times 1.8 \times 3^3 \times 0.21 \\ &= 1.703 \text{ tons} \end{aligned}$$

$$\begin{aligned} \text{Displacement required for} \\ \text{mobilisation of the above} \\ (0.5 \% \times 3.0 \text{ m}) &= \frac{0.5}{100} \times 300 = 1.5 \text{ cm} \end{aligned}$$

$$\begin{aligned} \text{At rest pressure on the wall} \\ (K_o = 1 - \sin \Phi = 0.587) &= \frac{1}{2} \times 1.8 \times 3^3 \times 0.587 \\ &= 4.25 \text{ t} \end{aligned}$$

As already explained on page 114 the wall moves out under the at-rest pressure (say a distance 'a') till the thrust on the wall is equal to the base resistance mobilised at a displacement 'a'. The thrust reduces from 4.25t to 1.703 t when the wall moves out by 1.5 cm

$$4.25 - (4.25 - 1.703) \times \frac{a}{1.5} = 4.35 \times \frac{a}{1.567}$$

$$a = 0.95 \text{ cm}$$

$$\text{Now, yield force} = 4.35 - 1.703$$

$$= 2.647 \text{ tons}$$

$$\text{yield displacement} = 1.567 - 0.95 = 0.617 \text{ cm}$$

$$\text{Stiffness} = \frac{2.647}{0.617} = 4.3 \text{ t/cm}$$

2) Determination of total mass

$$\text{mass of wall} = (0.7 \times 3 \times 2.4) \frac{1}{g} = \left(\frac{5.04}{g} \right)$$

$$\begin{aligned} \text{mass of soil} &= (0.8 \times \frac{1}{2} \times 1.8 \times 3^3 \times \tan 27^\circ) \frac{1}{g} \\ &= \left(\frac{3.296}{g} \right) \end{aligned}$$

$$\text{Total mass} = \frac{8.34}{981} \text{ t sec}^2/\text{cm}$$

$$\begin{aligned} \text{Natural period of wall} &= 2\pi\sqrt{m/k} \\ &= 2\pi\sqrt{\frac{8.34}{981 \times 4.3}} = 0.279 \text{ sec} \end{aligned}$$

b. Yield displacement

This has already been determined as 0.617 cm

c. Slip per cycle.

The curves plotted are for yield displacement values of 0.1, 0.2, 0.3, 0.5 and 1.0 cm. Since in this case the yield displacement is 0.617 cm, it will be necessary to interpolate the results from Figs. 6.14 and 6.15 where the yield displacements are 0.5 and 1.0 cm respectively.

i) Slip per cycle for yield displacement of 0.5 cm

From Fig 6.14, for a natural period of 0.279 sec and a ground motion acceleration of 250 cm/sec and period 0.3 sec, the slip per cycle is 1.625 cm.

ii) Slip per cycle for yield displacement of 1.0 cm

From Fig. 6.15 the value can be read as 0.91 cm

iii) Intepolation for yield displacement of 0.617cm

$$\begin{aligned} \text{Slip per cycle} &= 1.625 - (1.625 - 0.91) \times \frac{0.117}{0.5} \\ &= 1.625 - 0.1674 = 1.4576 \text{ cm} \end{aligned}$$

d. Total slip

$$\begin{aligned} \text{Total slip in 15 cycles} &= 15 \times 1.46 \\ &= 21.90 \text{ cm} \end{aligned}$$

It will be noticed that near resonance condition has caused this displacement which can be considered detrimental for important walls. Also, the base width provided is only 0.33 times the wall height which may be insufficient.

SUMMARY

i) A method has been presented to compute probable displacements of retaining walls under idealised earthquake shocks. The main advantage in using this procedure would be that the function of the structure can be taken into account in terms of permissible displacements.

ii) The use of Mononobe-Okabe theory would result in increased base width of the walls. Using the proposed procedure, the displacement of the wall designed for static conditions can be checked and only if the displacements are more than the permissible values, the dimensions of the wall

need be altered.

iii) The parametric study shows the importance of the natural period of the wall in relation to the predominant period of ground motion. Also it shows the importance of the energy concept in the design of retaining walls. It is found that for same acceleration levels, motions of longer period cause much more slip than those of shorter period. A motion of period 0.1 sec causes only minor displacements even at the 'resonance' conditions.

SUMMARY AND CONCLUSIONS

In the preceding Chapters the following types of investigations have been described.

- a. Tests on a 1.0 m high steel cantilever wall backfilled with a dry sand and subjected to impact type of base motion. This was intended to take into consideration the nature of strains in the soil behind a high cantilever wall with a rigid foundation, and its effects on both the static and dynamic earth pressures.
- b. Tests on a 1.0 m high steel and brick work composite wall backfilled with dry sand and subjected to impact type of base motion. This was done to study the effects the strains in the backfill caused by rotation of the wall at the foundation level. This condition would be required to be studied for understanding the pressures on rigid walls as well as for taking into account the possible foundation rotation of a high wall which also deforms by flexural bending.
- c. Tests on a 2.0 m high rigid wall backfilled with dry sand and subjected to both impact type and steady state vibrations. This was undertaken to study two aspects of the earth pressure problem, namely i) the effect of small peak accelerations of the shock type motion and different velocities of the ground and ii) the inertial effects of the wall.

d. An analytical approach for the determination of displacements retaining wall would suffer when subjected to sinusoidal type base motion.

The parts a, b and c above have been undertaken to understand the limitations of the current design practice and the part d as a beginning of a more rational solution of the problem of retaining wall design in seismic areas.

The conclusions arrived at on the basis of the experimental studies are:

- i) The static pressure on a high retaining wall resting on rigid foundations is best approximated by the Jaky's formula for at-rest pressures rather than the active earth pressure theories currently in use.
- ii) The dynamic increment in earth pressures is better correlated with the velocities of base motion than the accelerations.

It was found that the observed values can be correlated with Mononobe-Okabe formula if the ground motion is considered as a sinusoidal motion of period 0.3 sec and acceleration amplitude of the seismic coefficient times acceleration due to gravity. So as to obtain an experimental correlation between the peak velocities and the earth pressure coefficient for dynamic increment, these values are plotted in Fig 7.1.

In this figure the coefficients for dynamic increment from tests on flexible wall (chapter 3) and rigid walls (chapter 4 and chapter 5) are plotted against the corresponding peak velocities. The maximum value of velocity used in these investigations was 17.65 cm/sec. Only small and medium values of velocities have been used in these studies. Approximate values of peak velocities in some of the past earthquakes are given in Table 7.1 for comparison.

Table 7.1 Peak Velocities During Past Earthquakes

Earthquake motion	Peak velocity cm/sec	References
Taft, 21 July 1952 N 69°W Comp	20	Berg and Housner (1961)
Taft, 21 July 1952 N 21°E Comp	13.75	"
El Centro 30 Dec 1934 N.S. Comp	32	"
E.W. Comp	19	"
El Centro 18 May 1940 N.S. Comp	41	"
E.W. Comp	41	"
Olympia 13 April 1934 N 10°W Comp	18	"
N 8° E Comp	21.5	"
San Fernando 1971	113	Trifunac and Hudson (1971)
Parkfield 1966	70	"
Koyna 27th Dec 1967	23	"

An examination of the Table 7.1 points towards a need to extrapolate the data for high velocities also. Since experimental investigations by earlier workers (Jacobsen, (TVA, 1951), Ishii et al (1960)) show almost linear relationship between the pressures and the seismic coefficients such a relation was considered suitable here also. Accordingly, a straight line passing through the origin was fitted by the method of least square (curve a). Here the relation between ΔK_{AE} , the coefficient of dynamic increment is found to be

$$\Delta K_{AE} = 0.01728 V \quad \dots 7.1$$

where V is the peak velocity in cm/sec.

A curve is drawn based on a sinusoidal base motion of acceleration amplitude $k_h \cdot g$, of a period 0.3 sec, and the empirical relation

$\Delta K_{AE} = \frac{3}{4} k_h$ (Seed and Whitman, 1970), (Curve b, Fig 7.1). It is found that this curve is also sufficiently accurate to predict the pressure coefficients. In this

$$\Delta K_{AE} = 0.016 V \quad \dots 7.2$$

Since this is much more simpler, based on an empirical formula already proposed and fairly accurate the relation (Eq. 7.2) is suggested for the case of a vertical wall, backfilled with dry sand and a horizontal backfill surface.

iii) The point of application of the dynamic increment in the case of flexible walls is at about mid-height.

iv) The point of application of the dynamic increment in the case of rigid walls is at about 40 % height above the base.

The above two conclusions show that the Japanese practice (Mononobe-Okabe formula and triangular distribution of pressures) can lead to unsafe designs while Indian Standard specifies much larger moments.

v) The inertia force of retaining wall is also dependent on the velocity of base motion. Also the force depend on the weight of the wall. If it is considered that the resistance to sliding is caused by the weight of wall alone and also that the coefficient of friction between the base of the wall and soil is 0.5 and the factor of safety against sliding under static conditions is 1.5, the ratio of the weight of the wall and the static earth pressure would be 3.0. Under such cases, the inertia force is about 50 % of the dynamic increment in earth pressures. In most cases the above is true. However for different ratios of weight of the wall and static earth pressure Fig 5.13 may be made use of.

vi) A mathematical model has been proposed to analyse the displacement of gravity type wall in translation. These have been studied for a sinusoidal ground motion.

SUGGESTIONS FOR FURTHER RESEARCH

The study reported here contains only observations using a dry sand at medium density. The effect of saturation of the backfill on the dynamic pressures is an area where very little work has been reported. It will be useful for the designers of quay walls and other water-front structures if this aspect is investigated.

This study shows two aspects regarding static earth pressures, which are contrary to the earlier knowledge. These are concerning a) the static pressure behind a cantilever retaining wall with a rigid foundation and b) the active pressures when the angle of internal friction is fairly large. In the former case, the pressures are not active but nearly equal to Jaky's at-rest pressures. In the latter, it appears that the sand gets loose and thus a reduction in Φ takes place. These aspects need be studied in greater detail. Some field evidence on the larger pressures on cantilever walls is on record however (Casagrande, 1973).

The displacement analysis of the wall has been done only for the case of translation of the wall. It is necessary to undertake similar studies for different modes of vibrations like rotation and simultaneous rotation and translation. Also the displacement analysis needs be carried out for flexible walls.

Further, the effects of the cohesion and, saturation of and the surcharge on backfill, on the displacements need be investigated, taking into account possible liquefaction of sands and reduction in strength of cohesive soils.

Since hardly any case history of damage to retaining walls is available, a large scale model study with simulated ground motions would help in further improving the analytical procedure developed.

REFERENCES

1. Aggour M.S. and Brown G.B. (1973), "Retaining Walls in Seismic Areas" Preprint, Fifth World Conference on Earthquake Engineering, Rome.
2. Aliev, H. Mamedov, H. and Radgabova, T. (1973), "Investigation of the Seismic Pressure of Soils on the Retaining Walls and Interdependence Between Foundation Soils and Constructions", Proc. Symposium on Behaviour of Earth and Earth Structures Subjected to Earthquakes and Other Dynamic Loads, Roorkee.
3. Arya, A.S. and Gupta, Y.P. (1966), "Dynamic Earth pressure on Retaining Walls due to Ground Excitations", Bull. Indian Society of Earthquake Tech., Roorkee, Vol.III, No.2.
4. Barkan, D.D. (1962), "Dynamics of Bases and Foundations", Mc Graw Hill Book Co., Inc, New York.
5. Basavanna, B.M. (1970), "Dynamic Earth pressure Distribution Behind Retaining Walls", Fourth Symposium on Earthquake Engineering, University of Roorkee, Roorkee.
6. Berg, G.V. and Housner, G.W. (1961), "Integrated Velocity and Displacement on Strong Earthquake Ground Motion", Bull. Seism. Soc. of America, Vol. 51, No.2, pp.175-180.
7. Biggs, J.M. (1963), "Introduction to Structural Dynamics", Mc Graw Hill Book Co., Inc, New York.
8. Casagrande, L. (1973), "Comments on Conventional Design of Retaining Structures", Jl. of Soil Mech. and Found. Divn., Proc. ASCE, Vol. 99, No. SM2.
9. Coulomb, C.A. (1773), "Essai Sur une application des regles de maximis et minimis a quelques problems de statique relatifs a l'architecture", Memoire de la Mathematique et de Physique, presentes a Academie Royale des Sciences, par divers savants, et lus dans sis Assemblies, Vol.7, Paris, 1773, De L Imprimerie Royale, 1776.
10. Harr, M.E. (1966), "Foundations of Theoretical Soil Mechanics", Mc Graw Hill Book Co. Inc, New York.

11. Hayashi, S. (1965), "Lateral Earth pressure in Earthquakes", Text book on Soil Mechanics and Foundation Engineering, Port and Harbour Technical Research Institute, Japan.
12. Ichihara, M. (1965), "Dynamic Earth Pressure Measured by a New Testing Apparatus", Proc. Sixth International Conference on Soil Mech. and Found. Engg. Montreal Canada, Vol. II.
13. Indian Standard Institution (1962, 1966, 1970), "Recommendations for Earthquake Resistant Design of Structures", IS: 1893-1962, First Revision 1966, Second Revision, 1970, Indian Standard Institution, New Delhi.
14. Ishii, Y., Arai, H. and Tsuchida, H. (1960), "Lateral Earth pressure in an Earthquake", Proceedings, 2nd World Conference on Earthquake Engineering, Japan, Vol. 1.
15. Jaky, J. (1948), "Pressure in Silos", Proc. Second Int. Conf. on Soil Mech. and Found. Engrg., Vol. 1.
16. Kapila, I.P. (1962), "Earthquake Resistant Design of Retaining Walls", Second Symposium on Earthquake Engineering, University of Roorkee, Roorkee.
17. Krishna, J. and Chandrasekaran, A.R. (1962), "Design of Shock Vibration Table", Proc. Second Symp. on Earthquake Engineering, University of Roorkee, Roorkee.
18. Mackey, R.D. and Kirk, D.P. (1967), "At Rest, Active and Passive Pressures", Proc. South East Asian Regional Conference on Soil Mechanics and Foundation Engineering, Bangkok.
19. Madhav, M.R. and Rao, N.S.K., (1969), "Earth Pressures Under Seismic Conditions", Soils and Foundations, Japan, Vol. IX, No. 4.
20. Matsuo, H. (1941), "Experimental Study on the Distribution of Earth Pressure Acting on a Vertical Wall During Earthquakes", Journal Japanese Society of Civil Engineers, Vol. 27, No. 2.

21. Matsuo, H. and Ohara, S. (1960), "Lateral Earth Pressure and Stability of Quay Walls During Earthquakes", Proceedings, 2nd World Conference on Earthquake Engineering, Japan, Vol.1.
22. Mononobe, N. (1929), "Earthquake Proof Construction of Masonry Dams", Proceedings, World Engineering Congress, Vol. 9, page 275.
23. Murphy, V.A. (1960), "The Effect of Ground Characteristics on the Aseismic Design of Structures", Proc. Second World Conference on Earthquake Engineering, Tokyo, Japan.
24. Nandakumaran, P. and Dhiman, H.C. (1970), "A Miniature Earth Pressure Cell for Dynamic Studies", Jl. Ind. Nat. Soc. of Soil Mechanics and Found. Engrg., Vol.9, No.1.
25. Nandakumaran, P. and Joshi, V.H. (1973), "Static and Dynamic Active Earth Pressures Behind Retaining Walls", To be published in Bulletin, Indian Society of Earthquake Technology, Sept. 1973.
26. Narain, J. Saran, S. and Nandakumaran, P. (1969), "A Model Test for Passive Pressures in Sand", Jl. of Soil Mech. and Found. Divn., Proc. ASCE, Vol. 95, SM4.
27. Narain, J. Saran, S. and Nandakumaran, P. (1971), "A Study of Rupture Surface in Cohesionless Backfill in Rigid Wall", Indian Geotechnical Journal, January 1971, Vol. 10, No.1.
28. Newmark (1965), "Effects of Earthquakes on Dams and Embankments", Geotechnique, Vol. XV, No.2.
29. Niwa, S. (1960), "An Experimental Study of Oscillating Earth Pressures Acting on a Quay Wall", Proc. Second World Conference on Earthquake Engg., Tokyo Japan.
30. Okabe, S. (1924), "General Theory on Earth Pressure and Seismic Stability of Retaining Walls and Dams", Journal of Japan Society of Civil Engineers, Vol. No. 6.

31. Prakash, S. and Saran, S., (1966), "Static and Dynamic Earth Pressure Behind Retaining Walls", Proceedings, Third Symposium on Earthquake Engineering, University of Roorkee, Roorkee, Vol.1.
32. Prakash, S. and Basavanna, B.M. (1969), "Earth Pressure Distribution Behind Retaining Walls During Earthquakes", Fourth World Conference on Earthquake Engineering, Chile.
33. Rankine, W.J.M. (1857), "On the Stability of Loose Earth", Phil. Trans. Royal Soc. Vol.147, London.
34. Rowe, P.W. and Peaker, K. (1965), "Passive Earth Pressure Measurements", Geotechnique, Vol.15, No.1.
35. Sano, R. (1916), "Theory of Aseismic Design of Buildings", Report of Imperial Earthquake Investigation Committee Vol. 83, A.
36. Scott, R.F. (1973), "Earthquake Induced Earth Pressures on Retaining Walls", Preprints, Fifth World Conference on Earthquake Engineering, Rome.
37. Seed, H.B., (1966), "A Method of Earthquake Resistant Design of Earth Dams", Journal, Soil Mech. and Foundations Division, Proc. ASCE, Vol. 92, No. SM1.
38. Seed, H.B. and Idriss, I.M. (1970), "A Simplified Procedure for Evaluating Soil Liquefaction Potential", Report No. EERC 70-9, Earthquake Engineering Research Centre, University of California, Berkeley, California, U.S.A.
39. Seed, H.B. and Whitman, R.V. (1970), "Design of Earth Retaining Structures for Dynamic Loads", 1970 Speciality Conference, Lateral Stresses in The Ground and Design of Earth Retaining Structures, American Society of Civil Engineers.
40. Siedek, P. (1969), "Erddruck auf Brückenwiderlager", Strasse und Autobahn, Bad Godesberg, West Germany, No. 4.

41. Tajimi, H. (1973), "Dynamic Earth Pressures on Basement Wall", Preprint, Fifth World Conference on Earthquake Engineering, Rome.
42. Tennessee Valley Authority (1951), "Design of Kentucky Structures Against Earthquakes", Appendix D, The Kentucky Project, Technical Report No. 13.
43. Terzaghi, K. (1936), "A Fundamental Fallacy in Earth Pressure Computation", Reprinted in Contributions to Soil Mechanics 1925-40, Boston Society of Civil Engineers, Boston, 1940.
44. Trifunac, M.D. and Hudson, D.E. (1971), "Analysis of Pacoima Dam Accelerogram", Bull. Seism. Soc. of America, Vol. 61., No. 5.

FIGURES



FIG. 3.1 PHOTOGRAPH OF TEST BIN

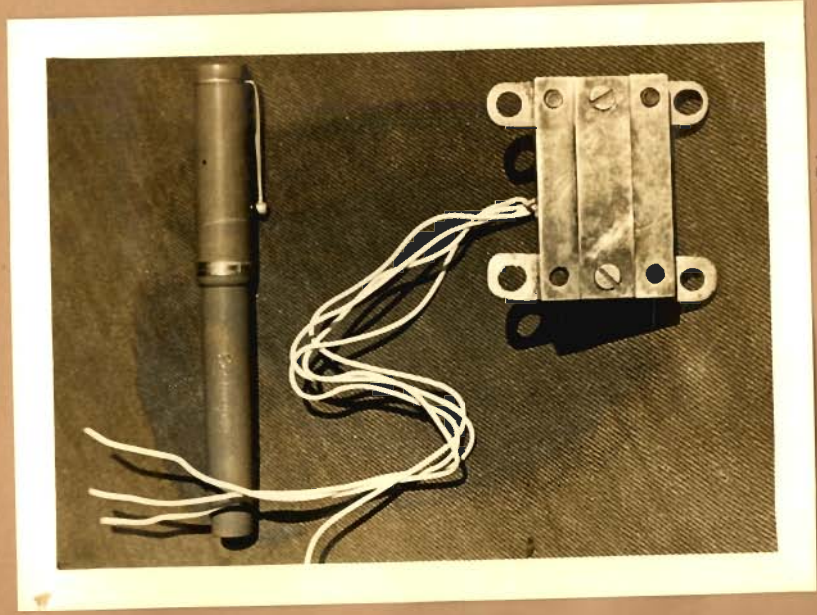
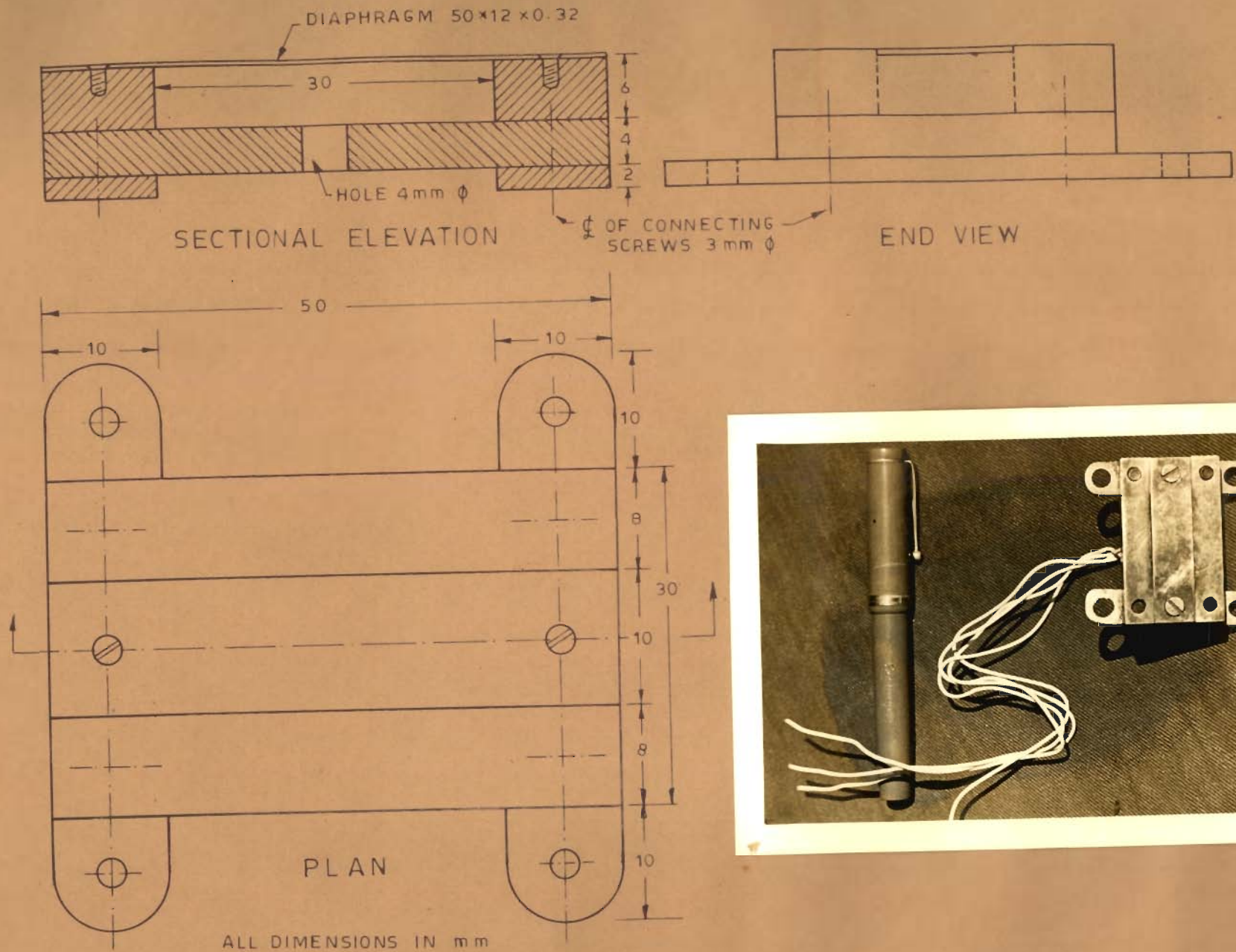


FIG. 3. 2 _ EARTH PRESSURE CELL

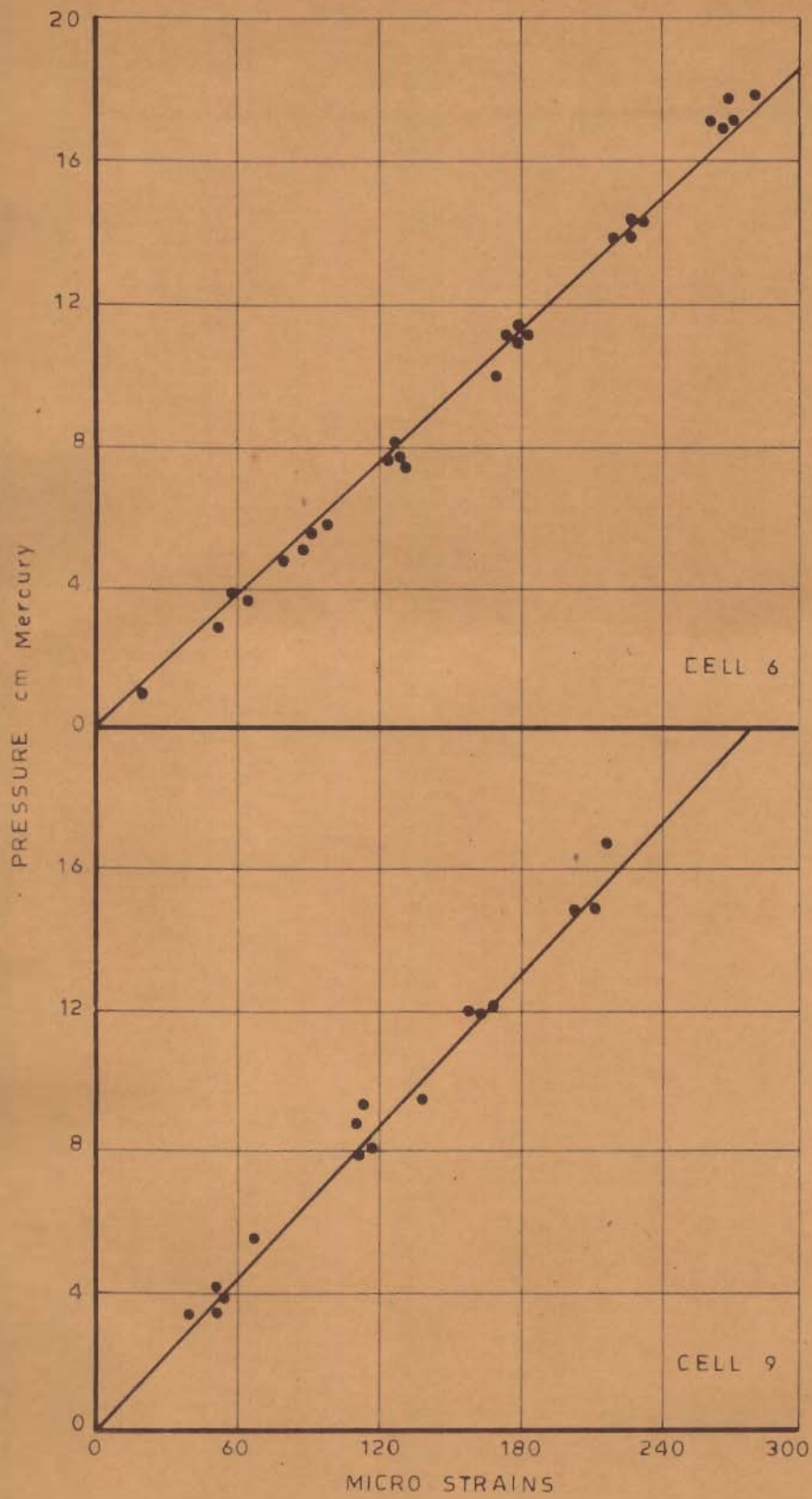


FIG. 3.3 _CALIBRATION CURVES FOR TWO CELLS



FIG. 3.4 SET-UP FOR CALIBRATION
OF WALL

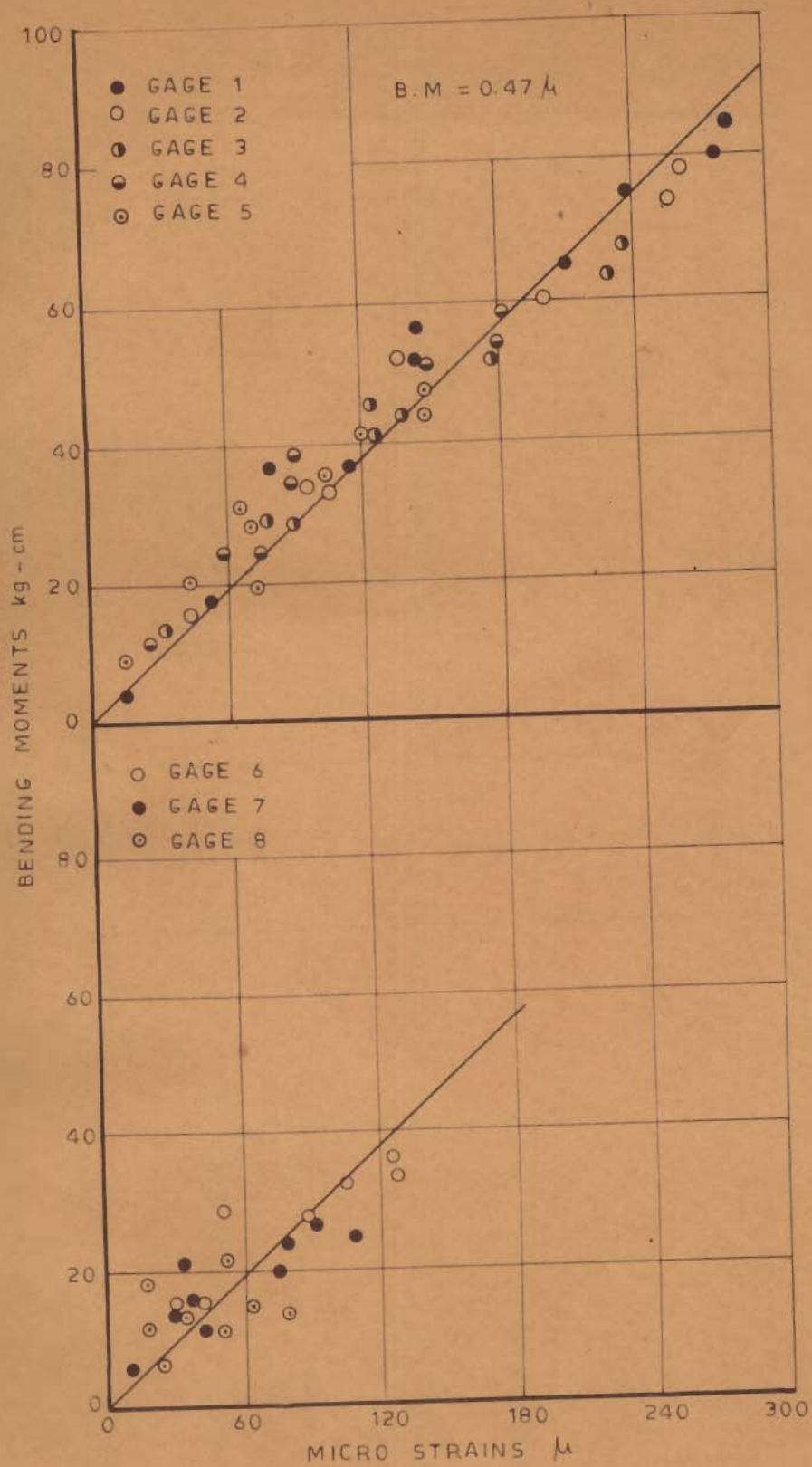


FIG. 3.5-CALIBRATION OF WALL BENDING MOMENTS VS STRAIN

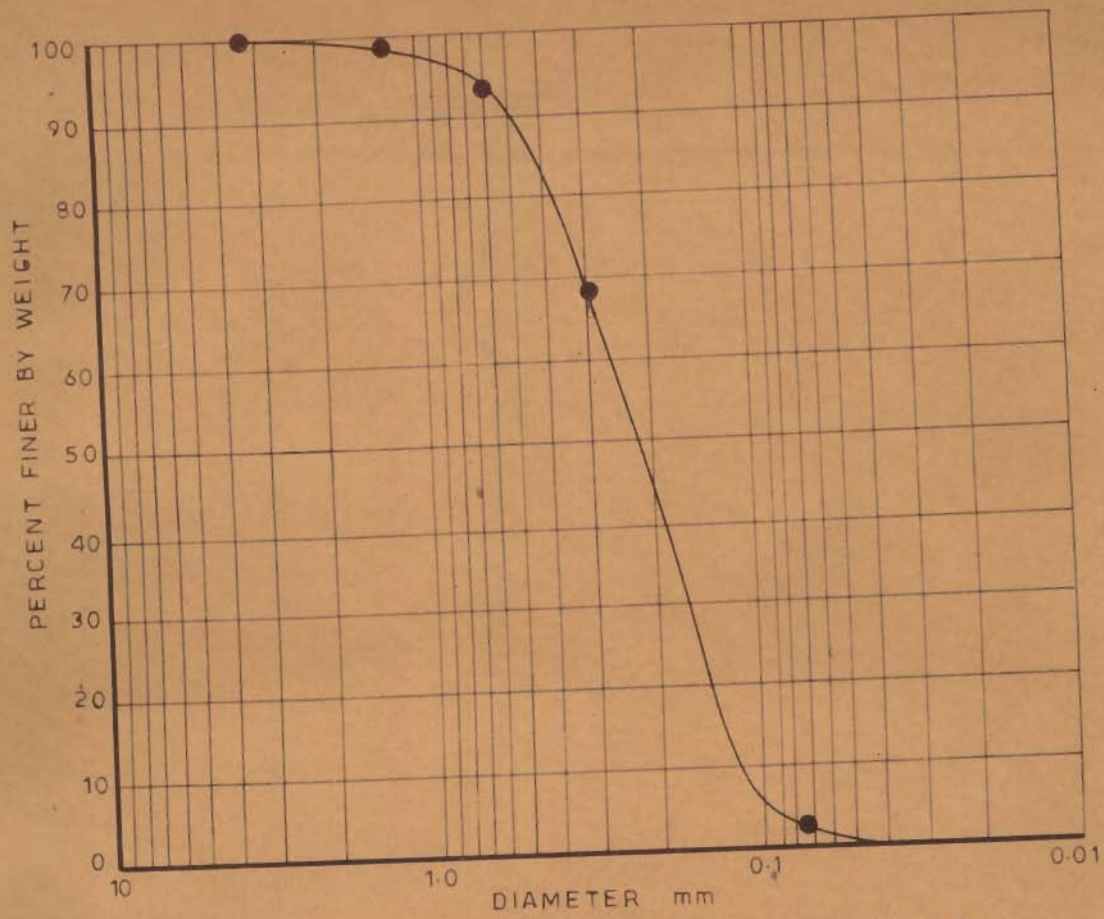


FIG. 3.6 _ GRAIN SIZE DISTRIBUTION CURVE

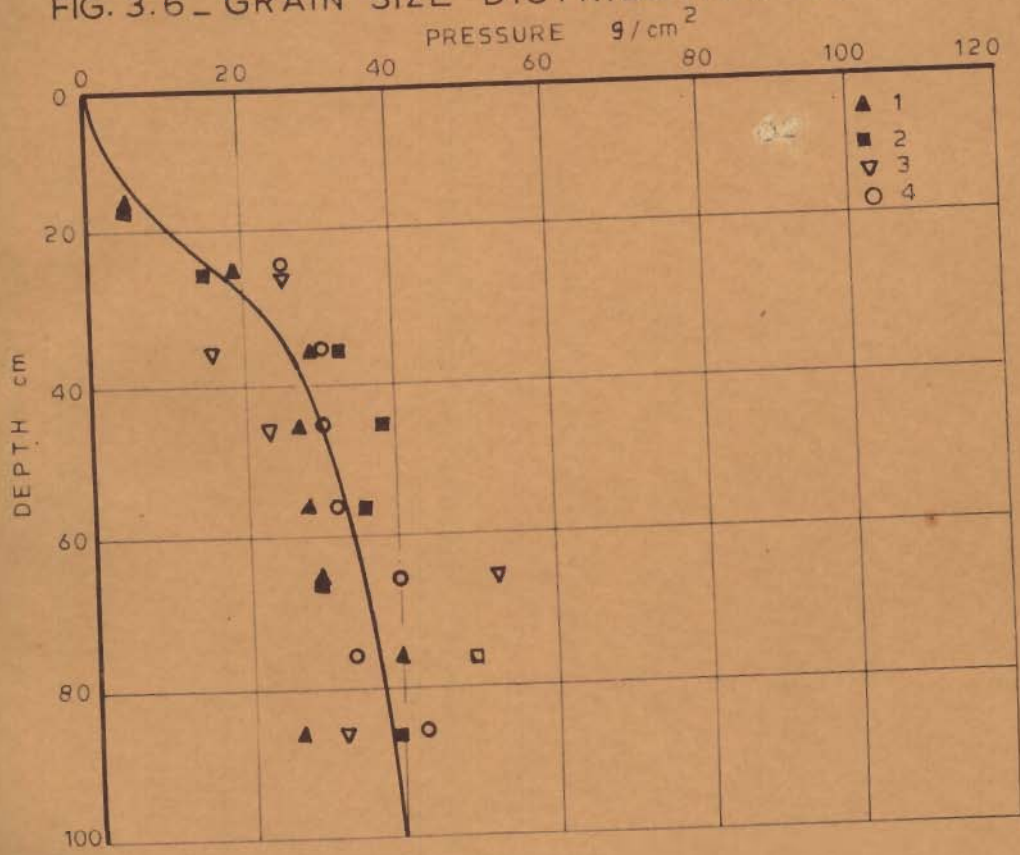


FIG. 3.7 _ STATIC EARTH PRESSURE DISTRIBUTION

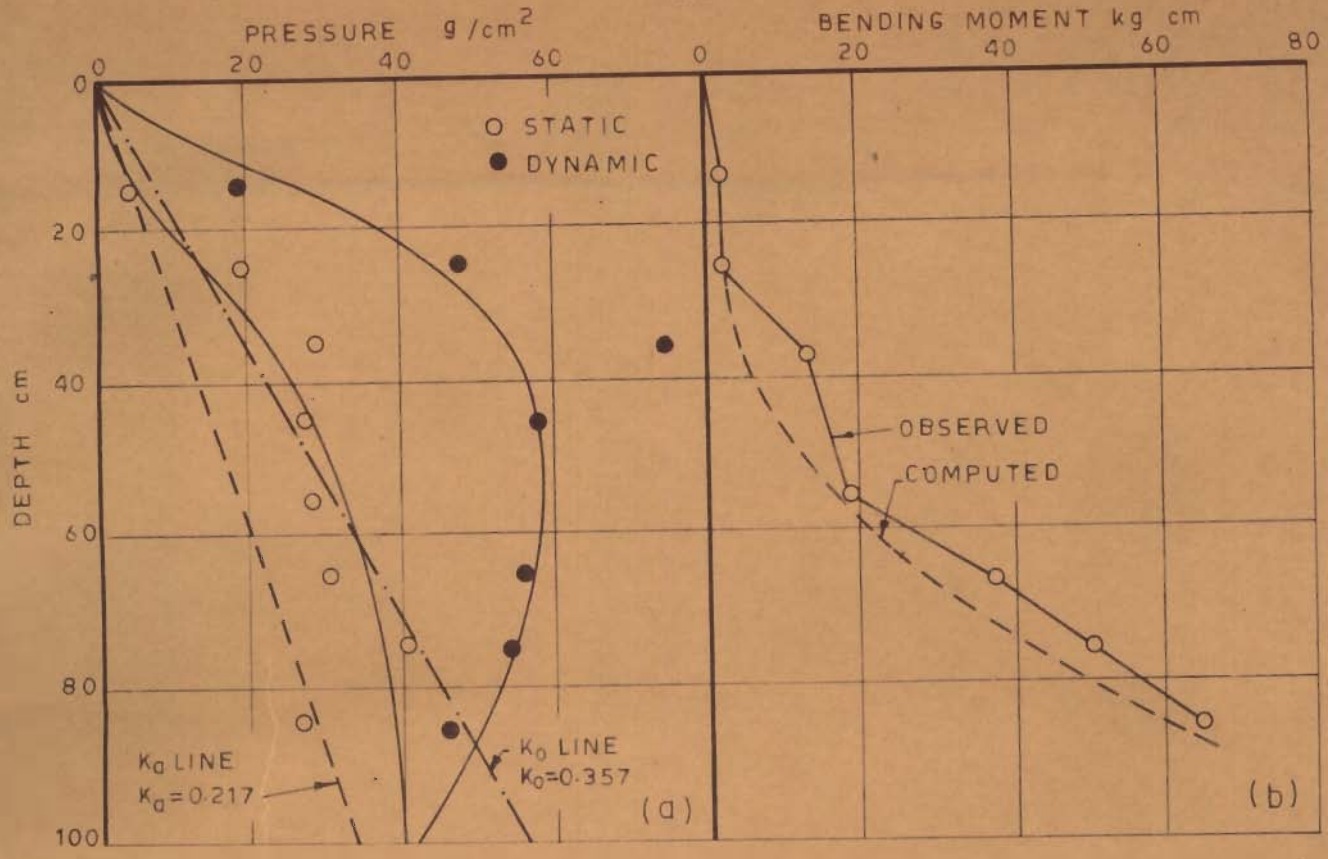


FIG.3.8_PRESSES AND BENDING MOMENTS, TEST 1

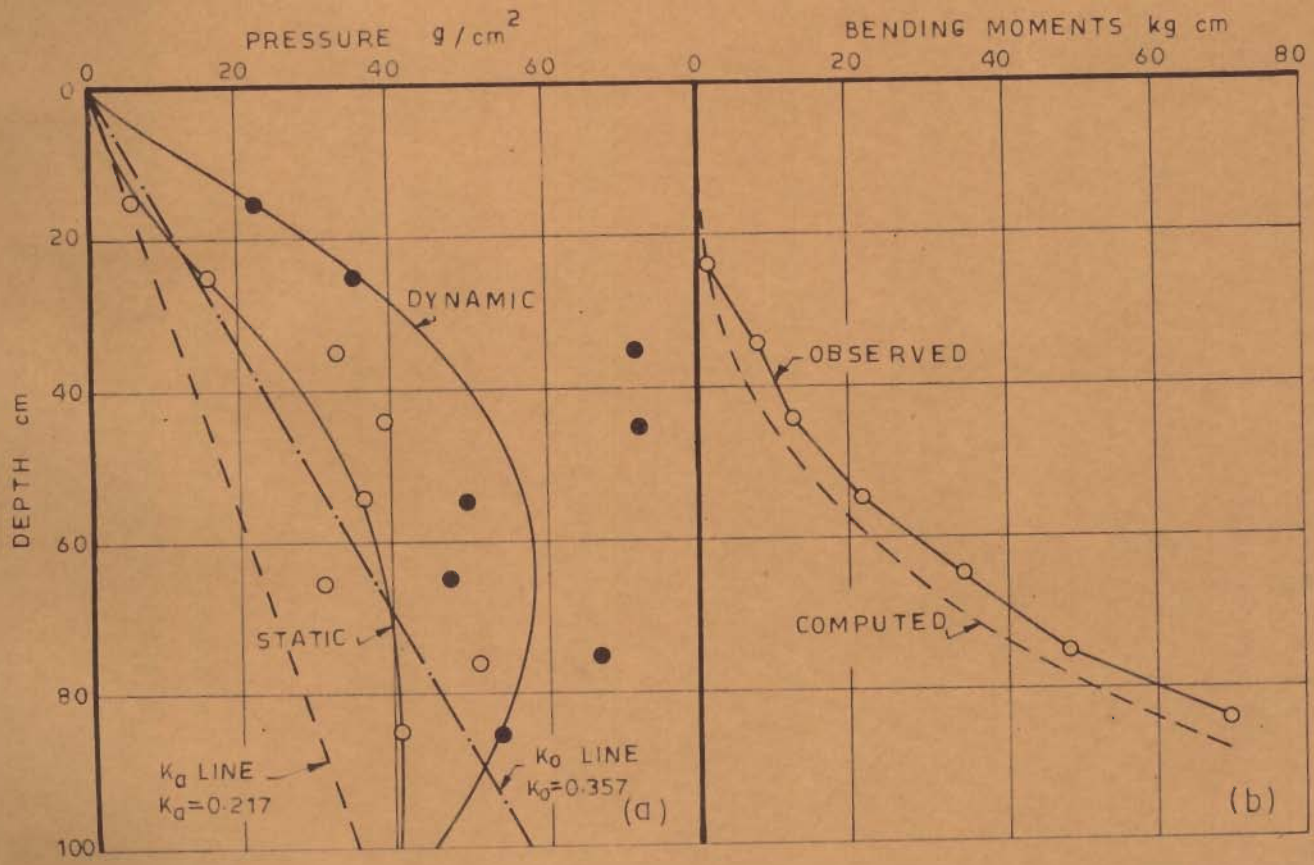


FIG.3.9_PRESSES AND BENDING MOMENTS, TEST 2

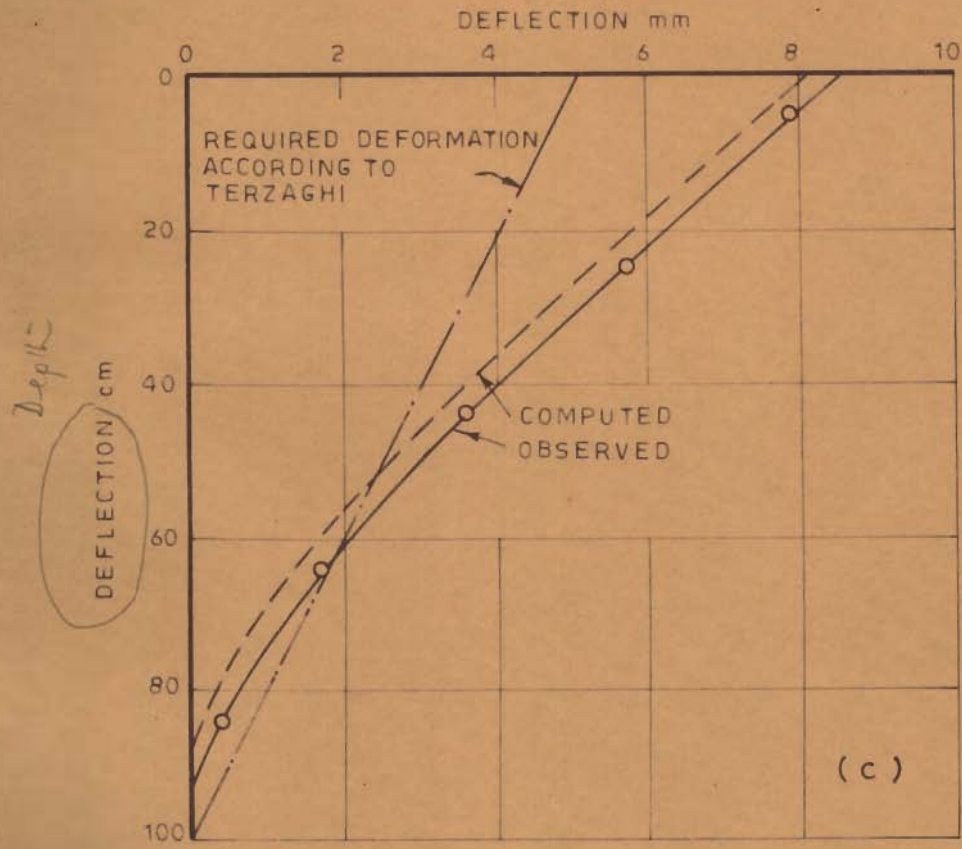
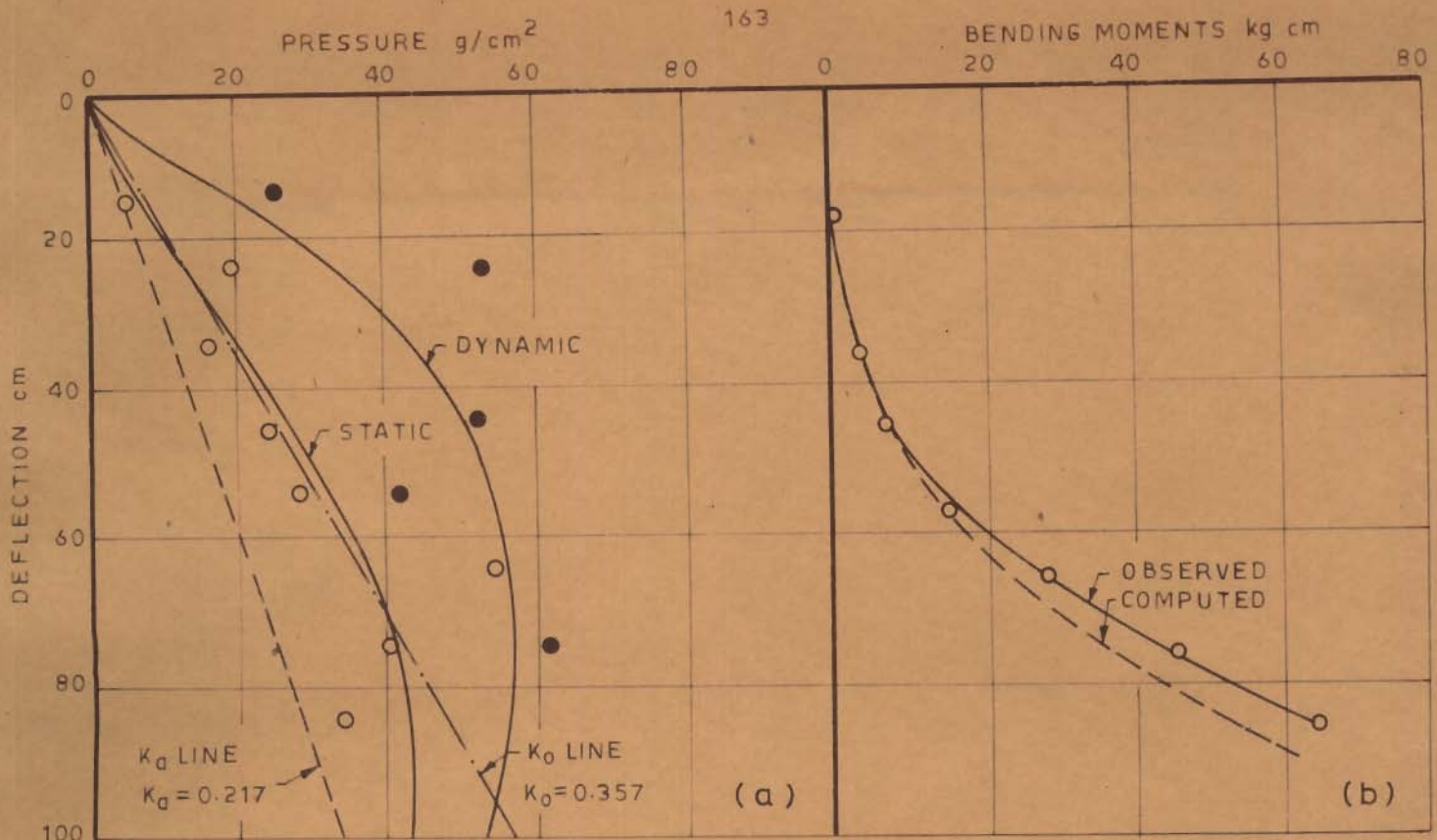


FIG. 3.10- PRESSURES, BENDING MOMENTS AND DEFLECTIONS TEST 3

PRESSURE g/cm^2

BENDING MOMENTS $kg\ cm$

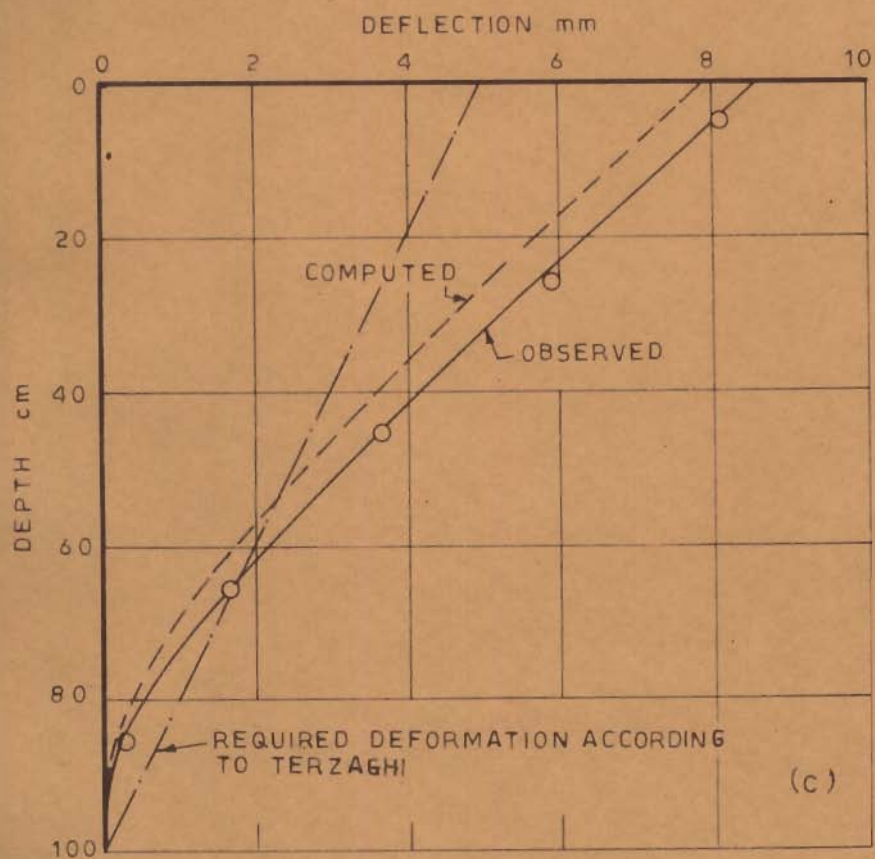
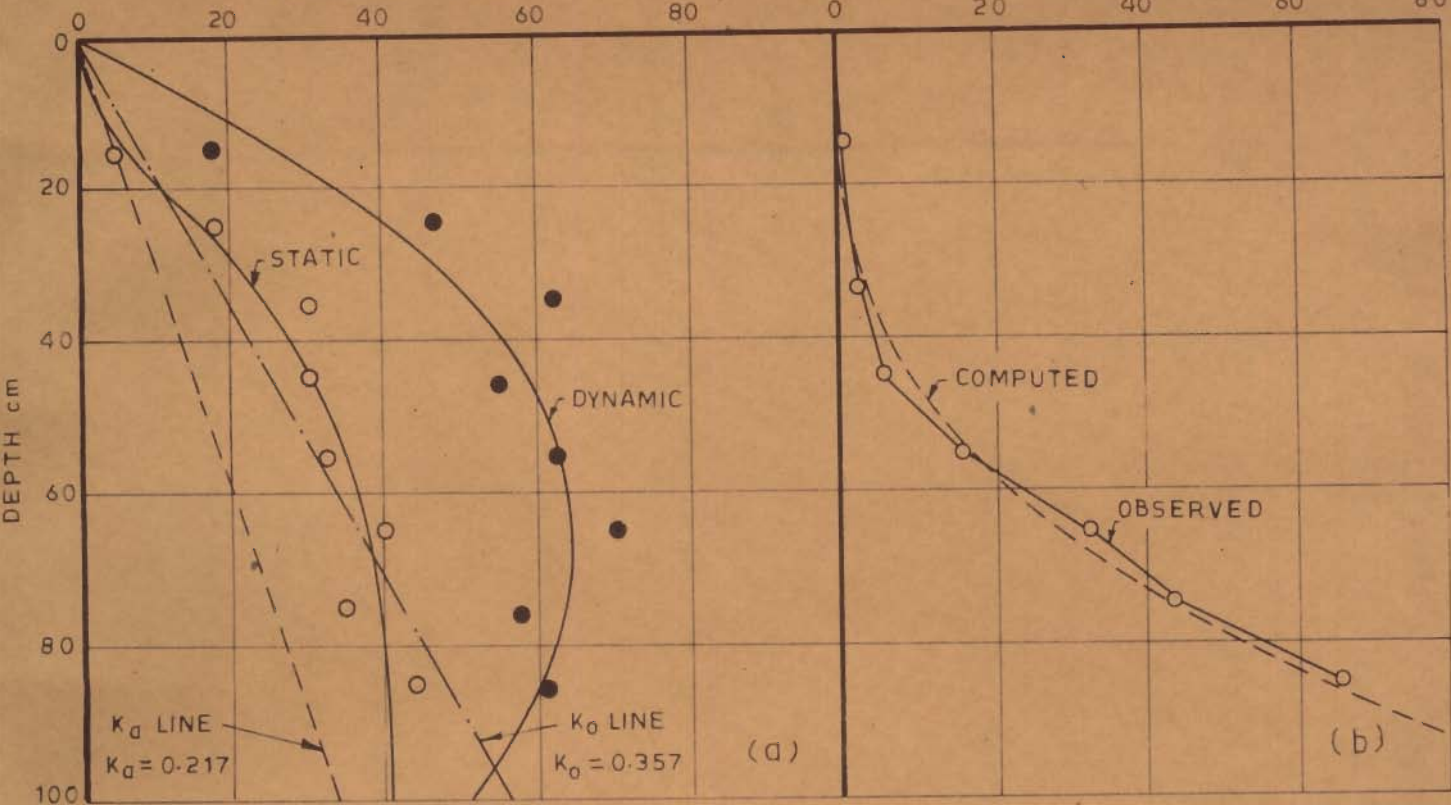


FIG. 3.11- PRESSURES, BENDING MOMENTS AND DEFLECTIONS TEST 4

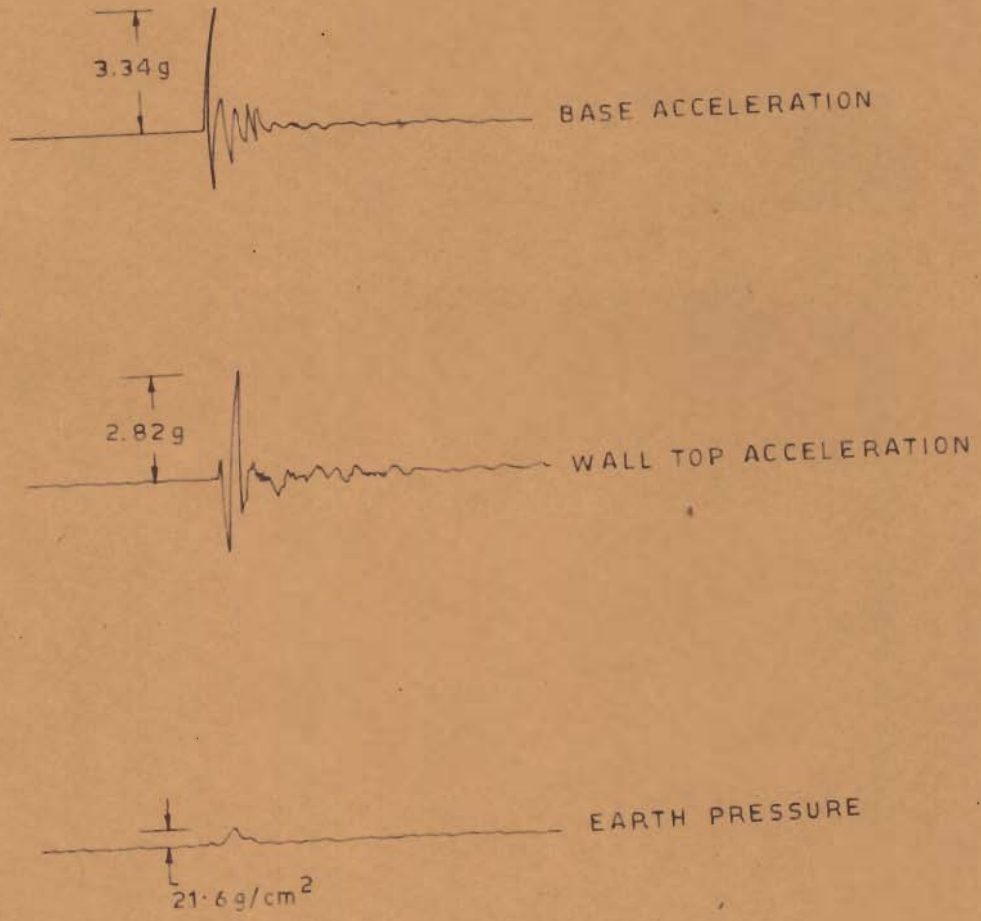


FIG. 3.12 - TYPICAL RECORD OF OBSERVATION
TEST 3

NOT TO SCALE

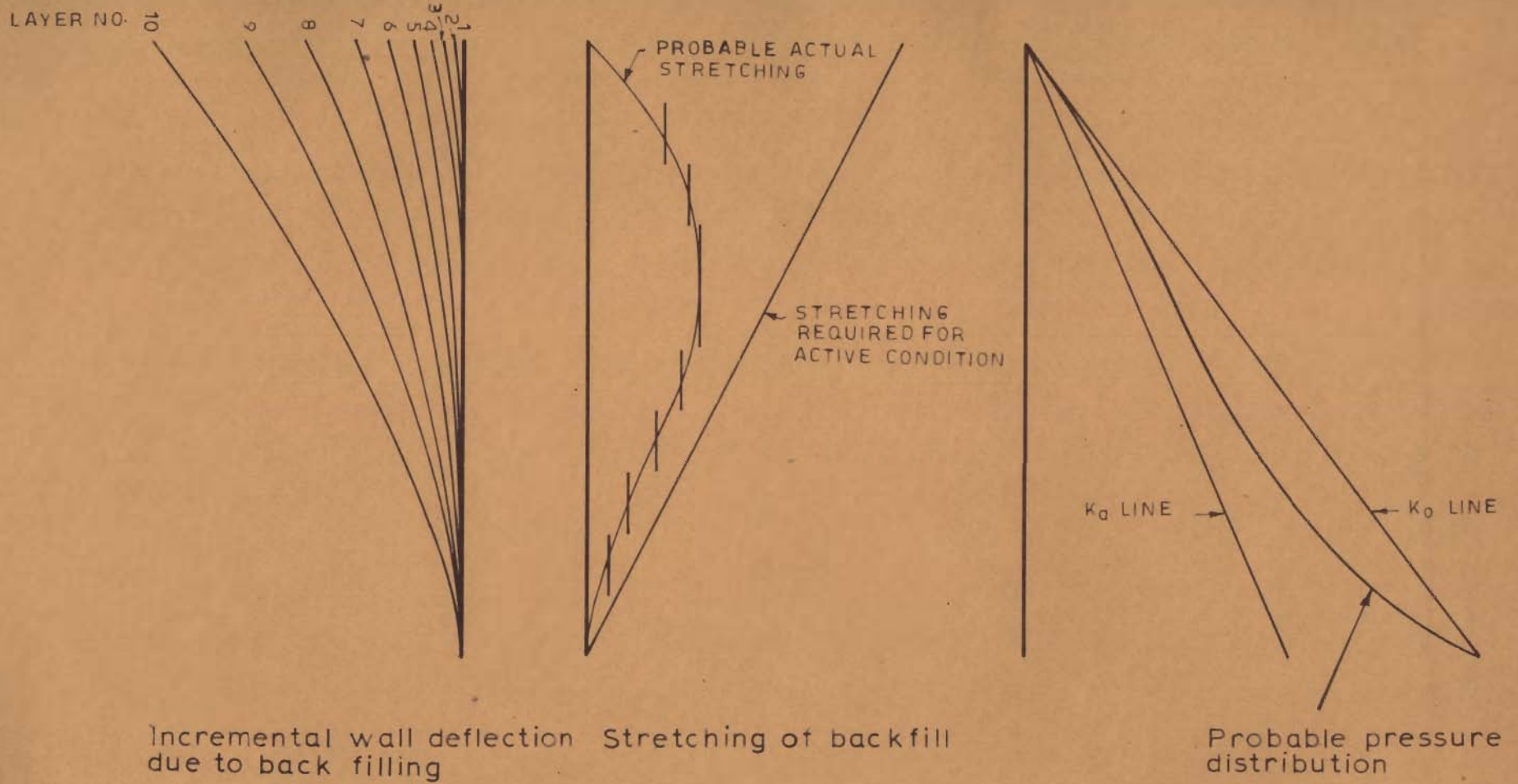


FIG. 3.13_ STATIC EARTH PRESSURE PROBLEM IN FLEXIBLE WALL

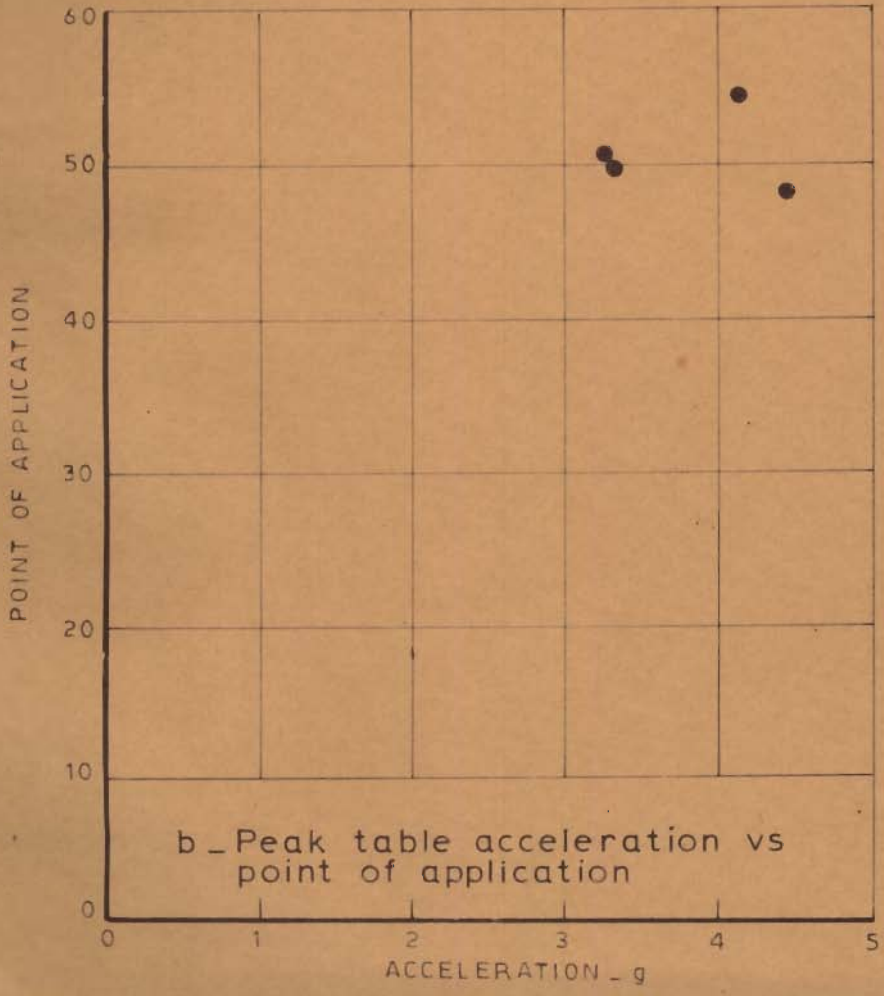
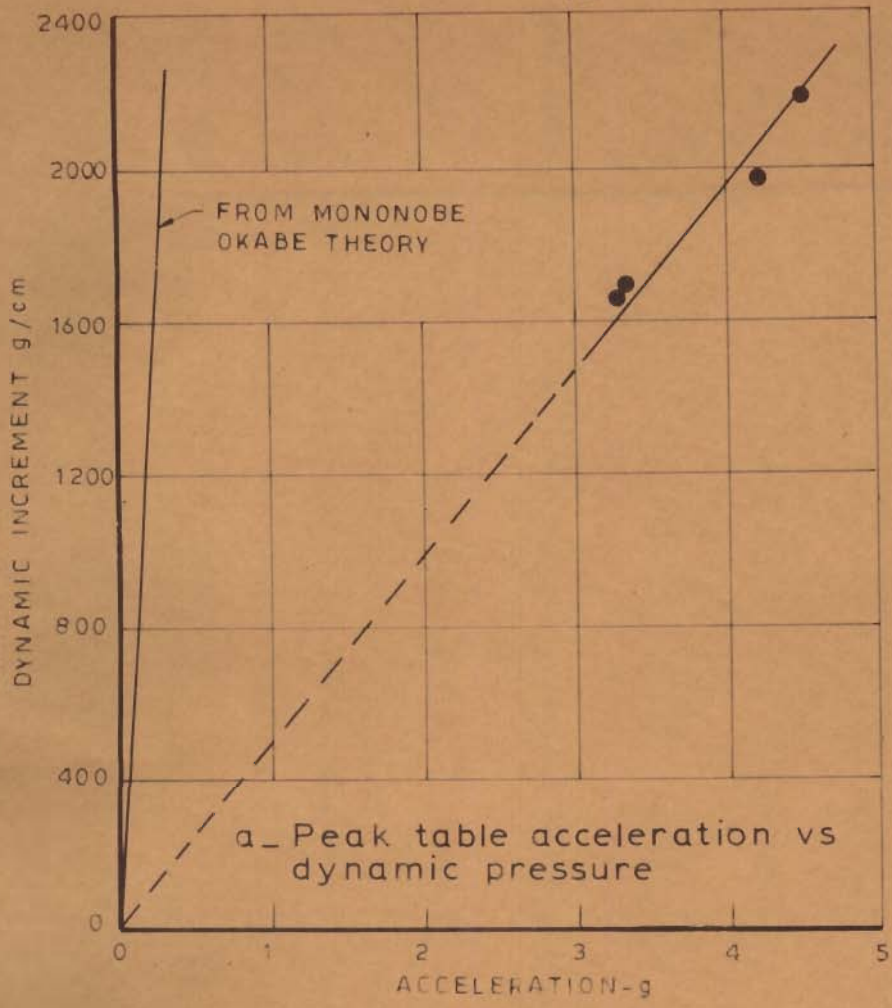


FIG. 3.14_ EFFECT OF ACCELERATION ON DYNAMIC PRESSURES

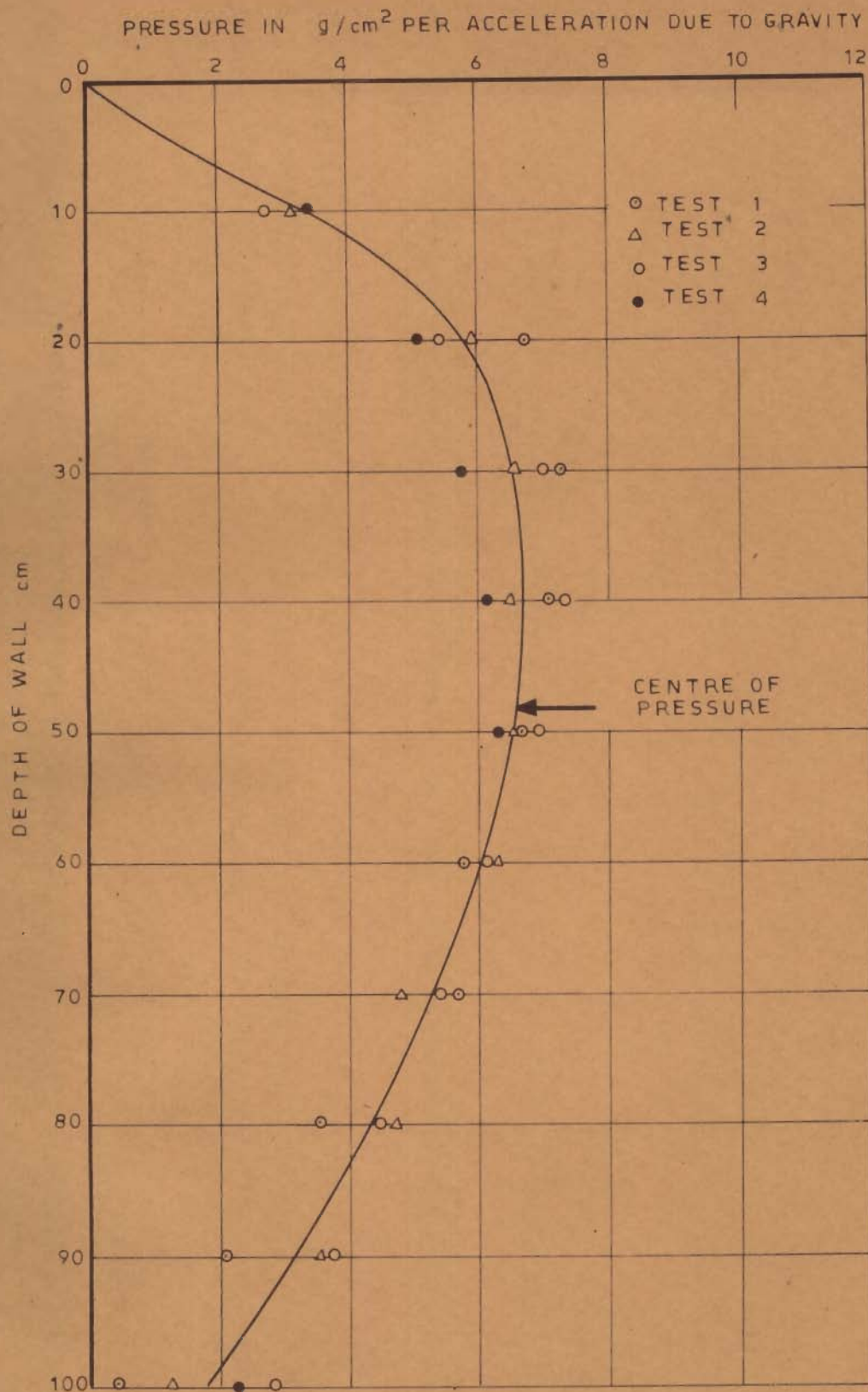


FIG. 3.15 - DISTRIBUTION DIAGRAM OF DYNAMIC INCREMENT PER UNIT OF ACCELERATION DUE TO GRAVITY WITH HEIGHT OF WALL

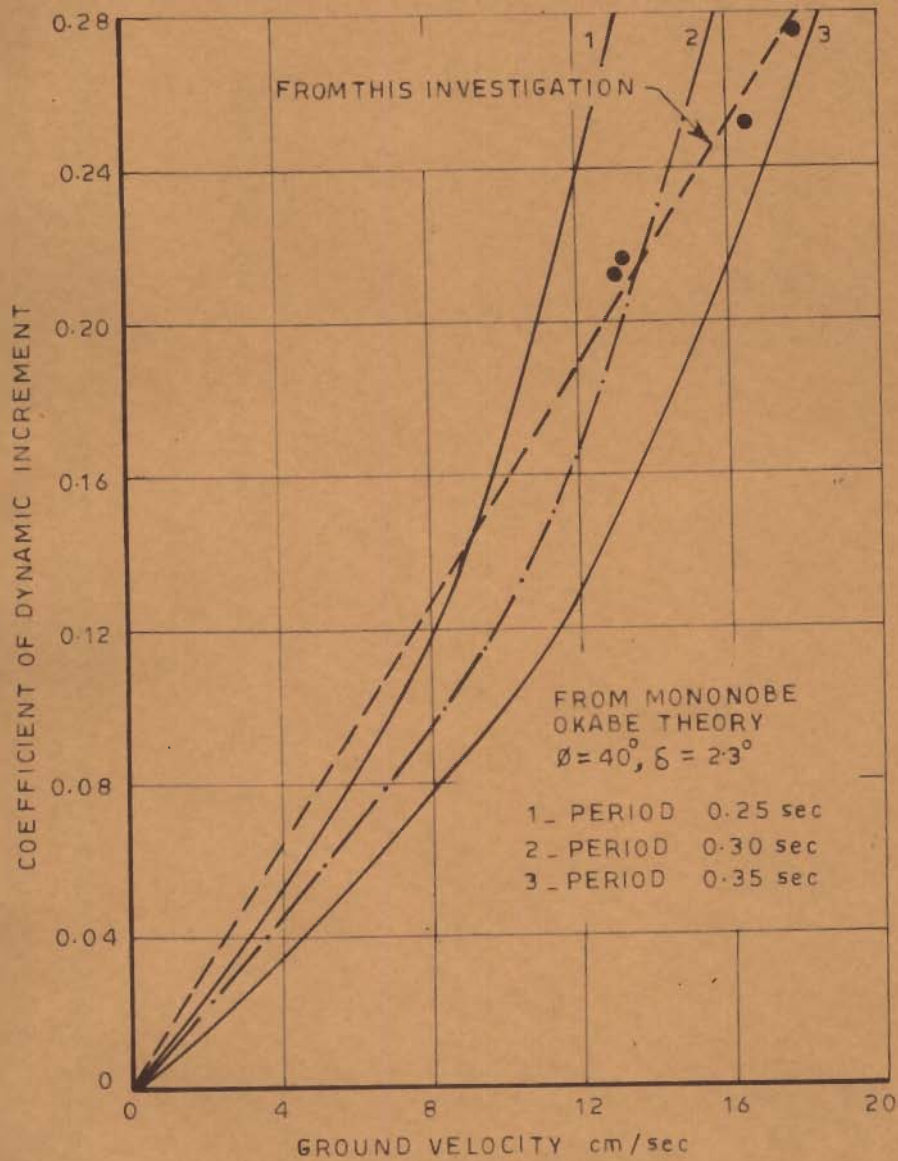


FIG. 3.16 - GROUND VELOCITY VS DYNAMIC INCREMENT COEFFICIENTS

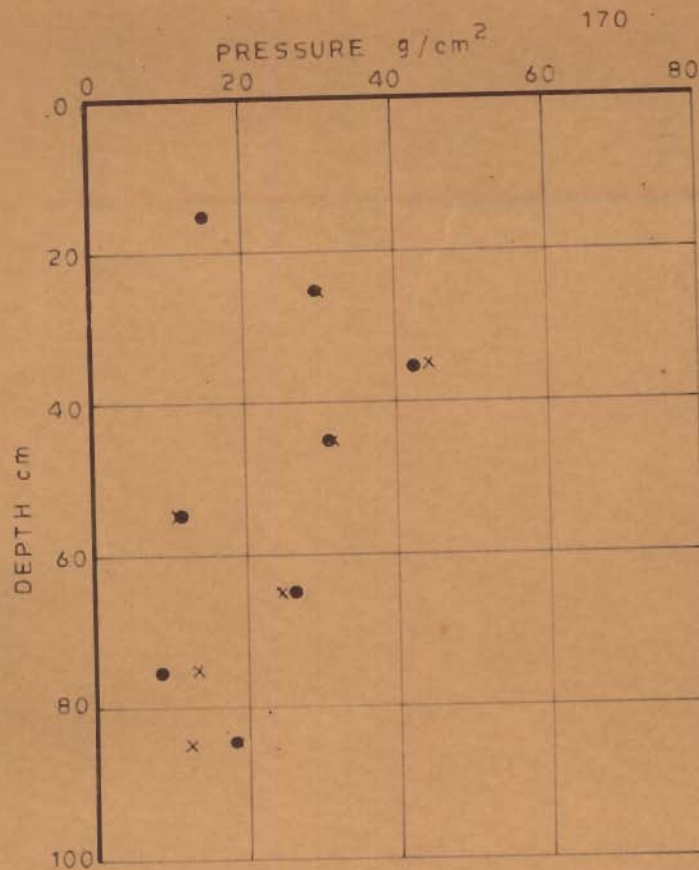


FIG. 3.17 - VALUES OF DYNAMIC INCREMENTS IN THE SUCCESSIVE SHOCKS - TEST 4

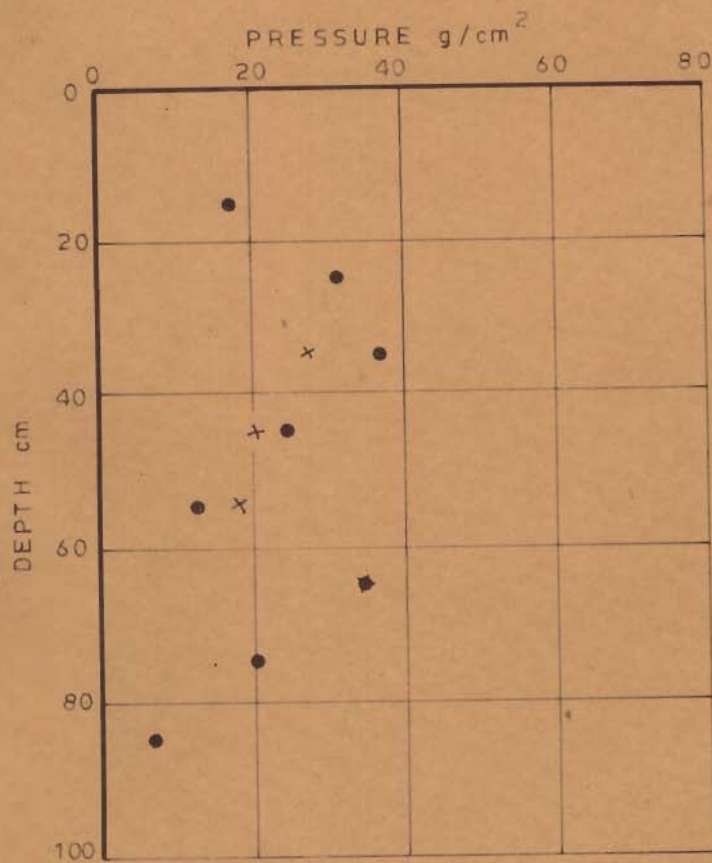


FIG. 3.18 - VALUES OF DYNAMIC INCREMENTS IN REPRODUCIBILITY TESTS - TEST 3

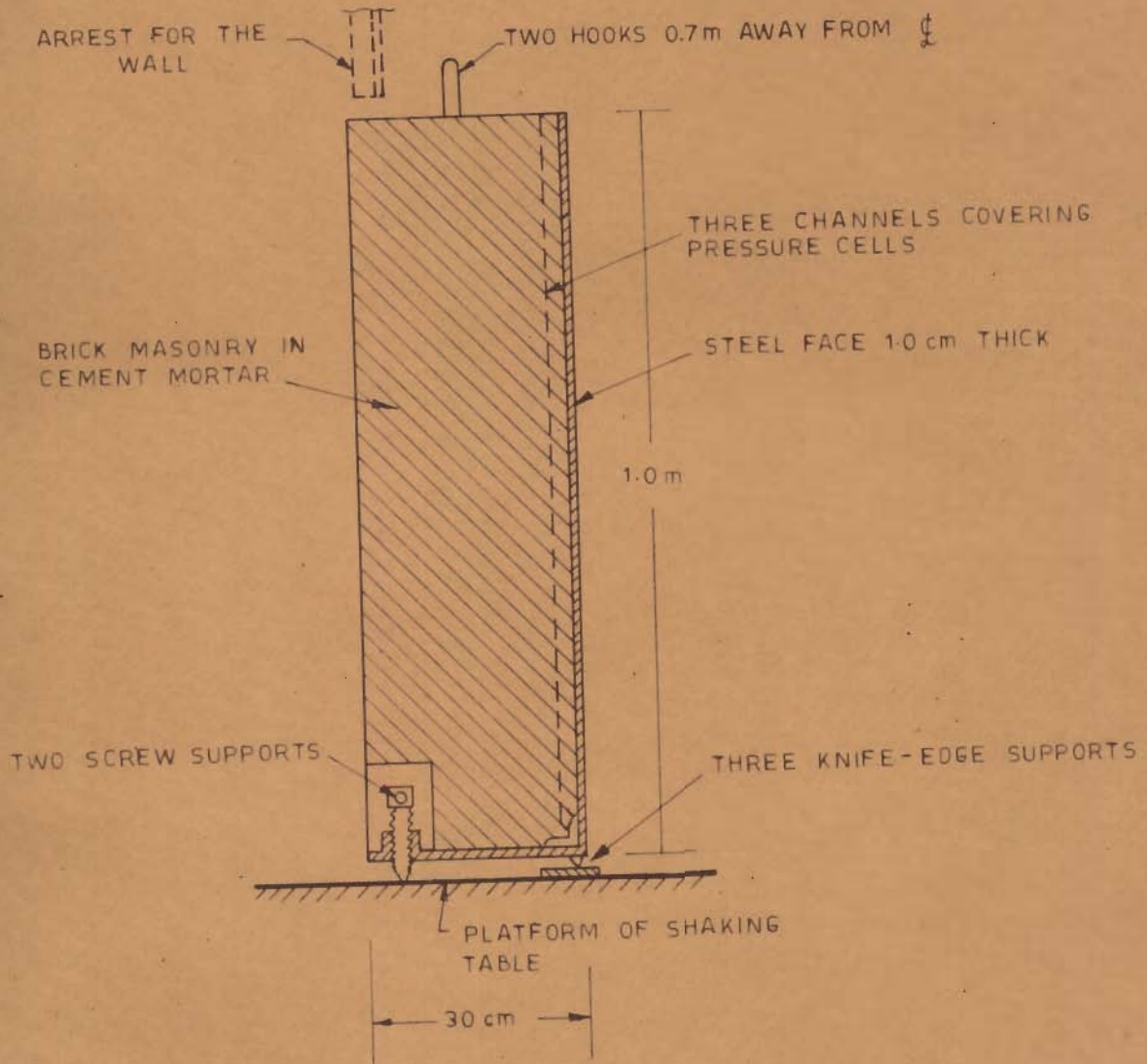


FIG. 4.1_ CROSS SECTION OF TEST WALL



FIG. 4.2 TEST SET-UP, RIGID WALL

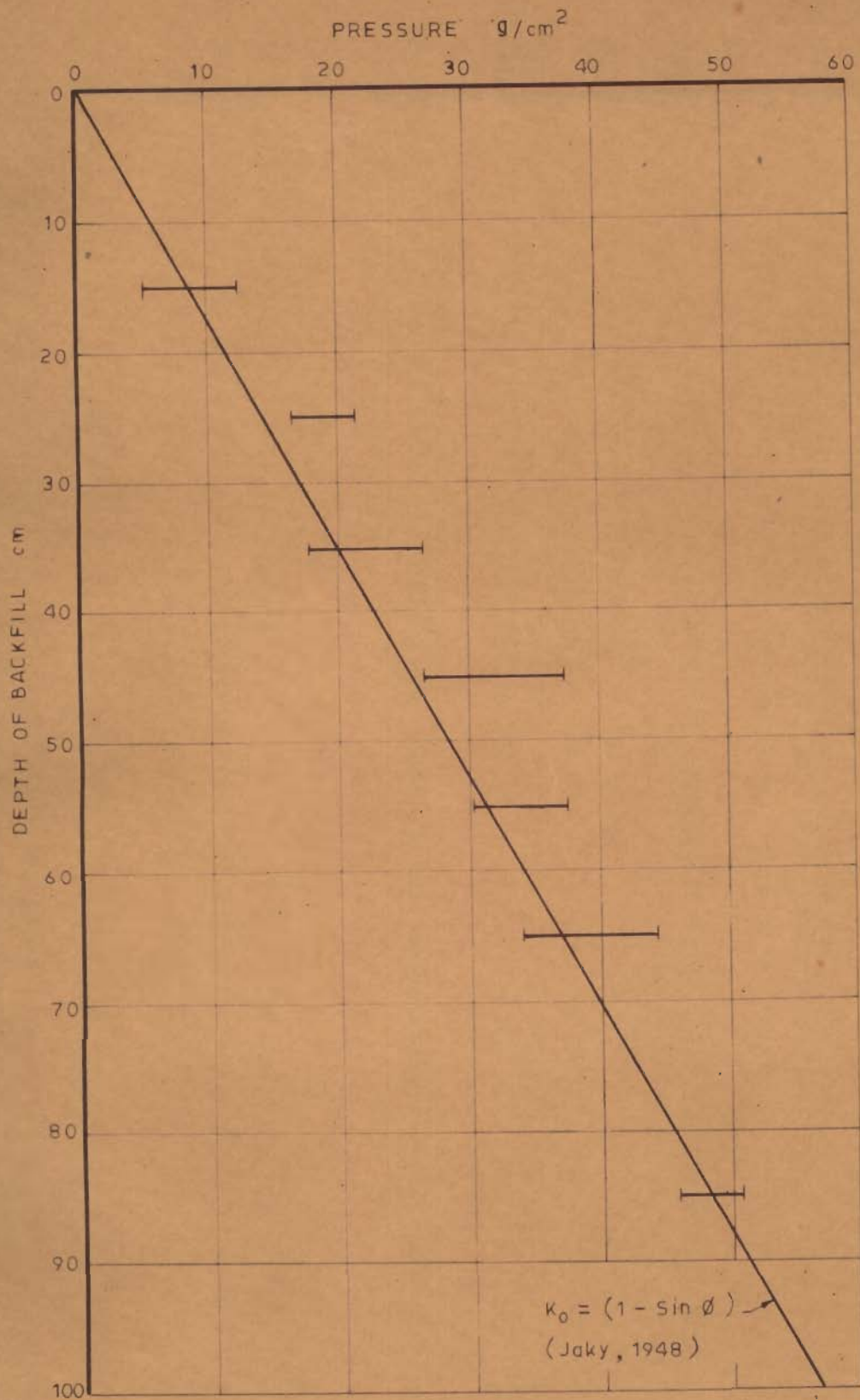


FIG. 4.3 - AT-REST PRESSURES ON THE WALL

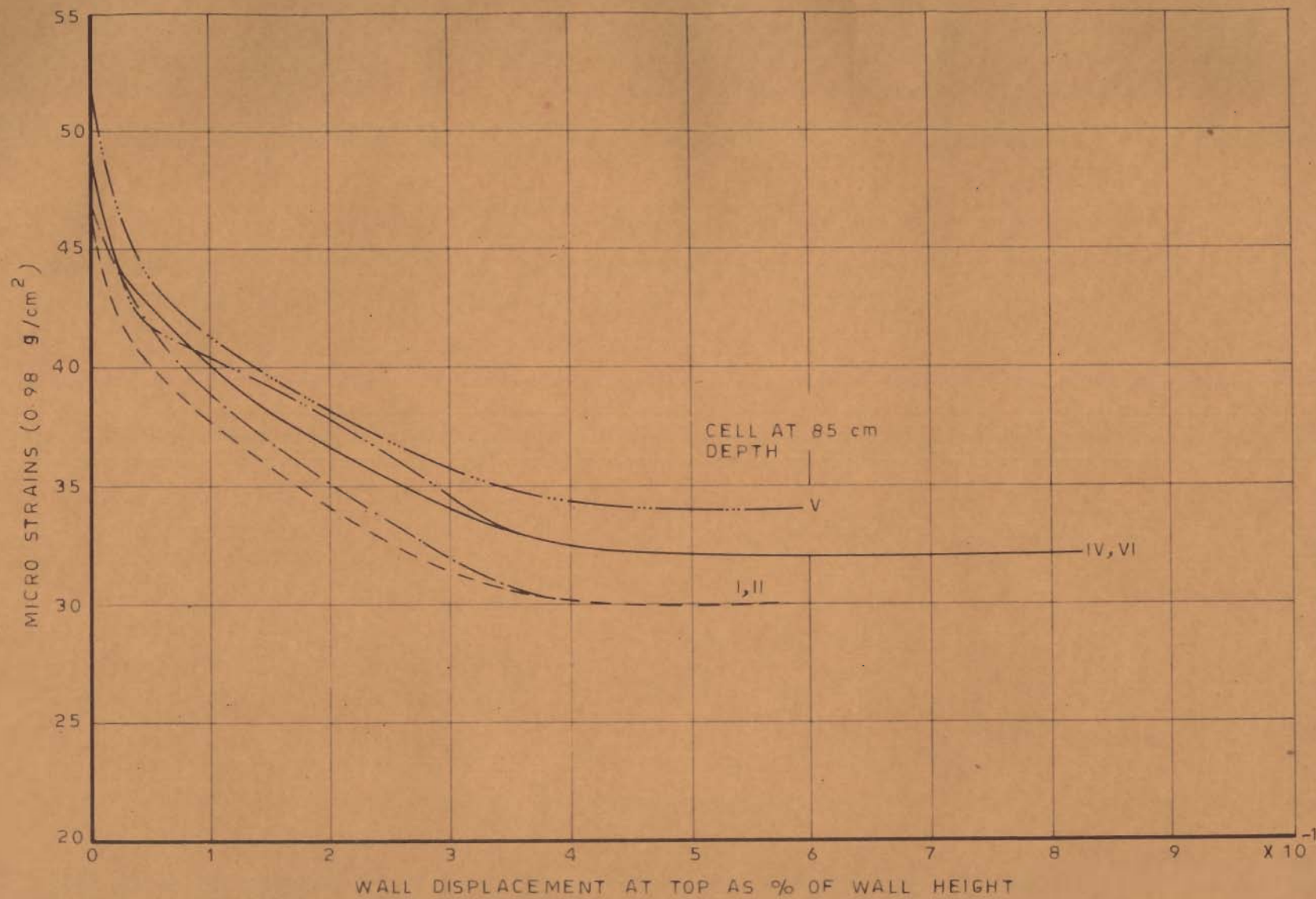


FIG. 4.4 _ REDUCTION LATERAL PRESSURE WITH WALL MOVEMENT

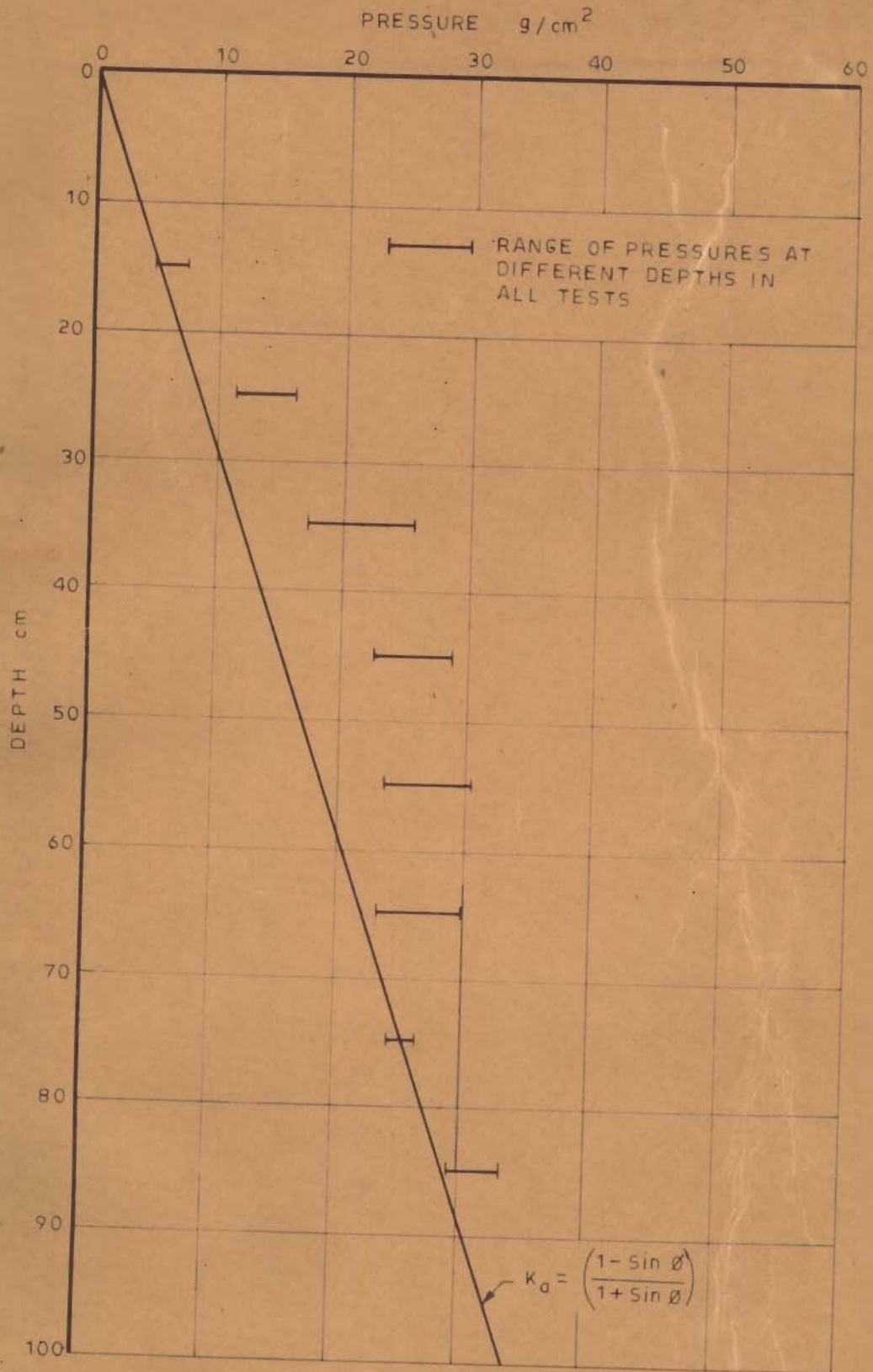


FIG. 4.5_ ACTIVE EARTH PRESSURES MEASURED

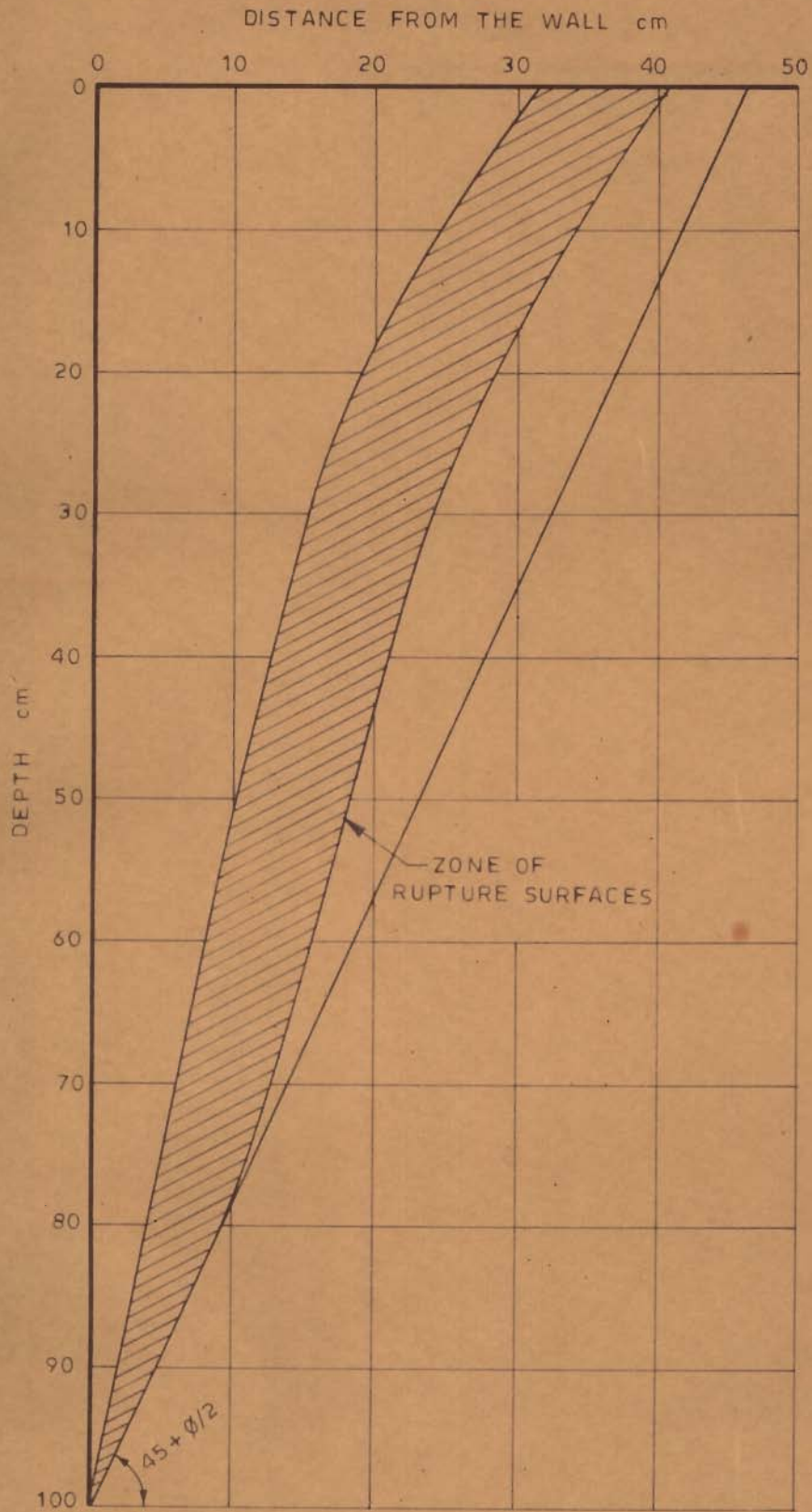


FIG. 4.6 - ZONE OF RUPTURE SURFACES

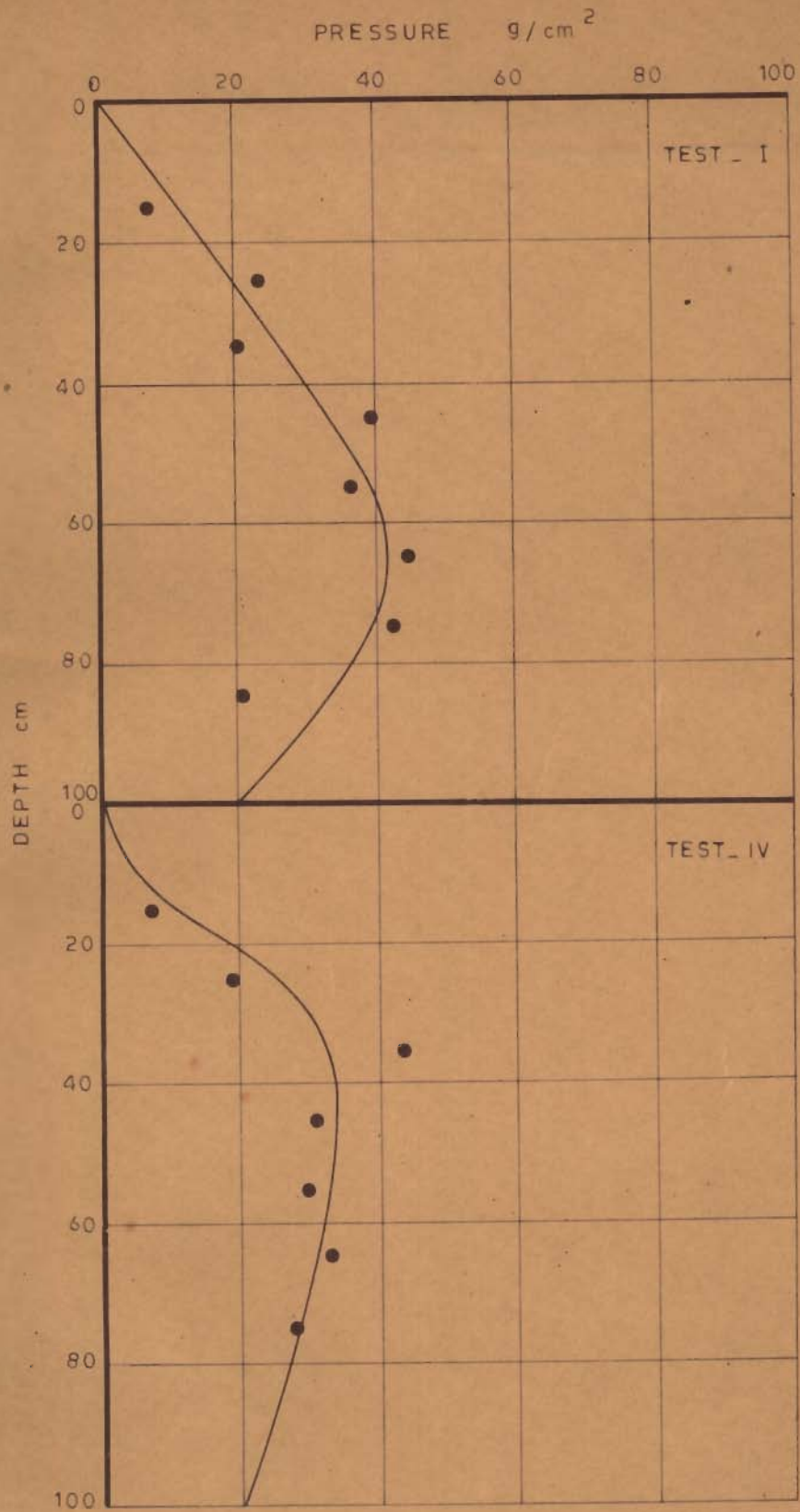


FIG 4.7_DYNAMIC INCREMENT DISTRIBUTION
TEST I AND IV



FIG. 4.8 - DYNAMIC INCREMENT DISTRIBUTION TEST II AND V

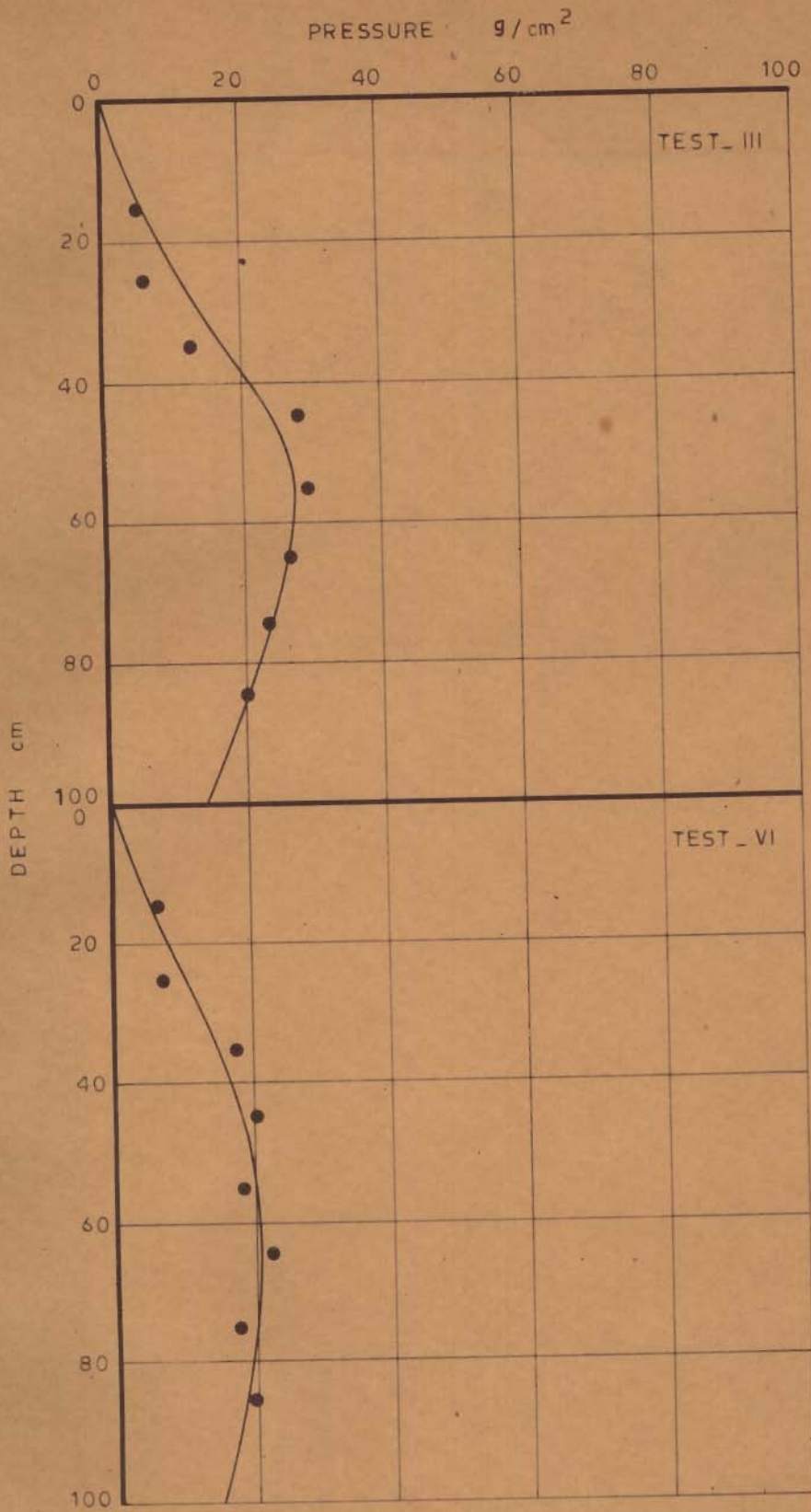


FIG. 4 9 - DYNAMIC INCREMENT DISTRIBUTION TEST III AND VI

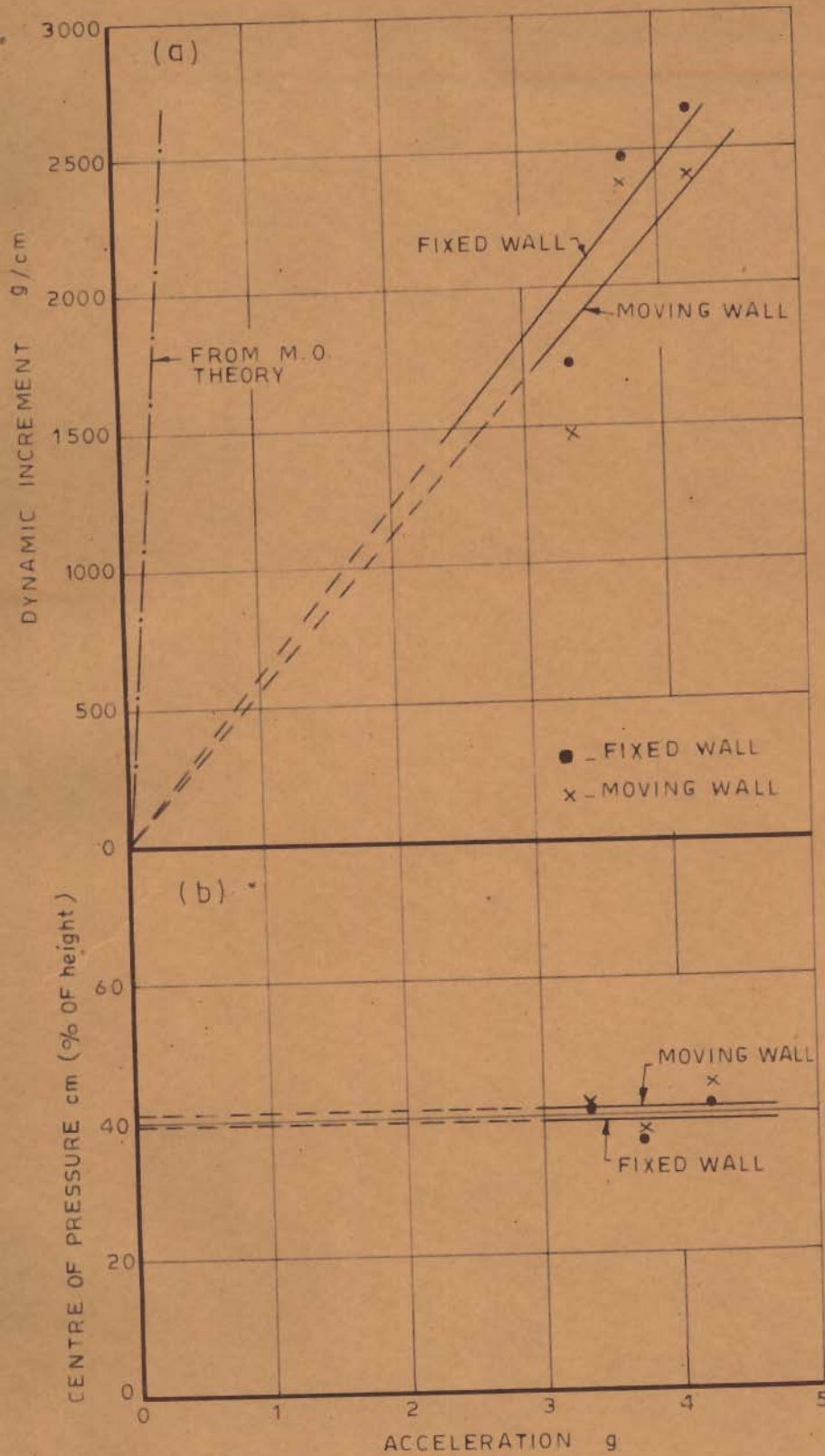


FIG. 4.10 - DYNAMIC INCREMENT AND CENTRE OF PRESSURE VS PEAK ACCELERATION

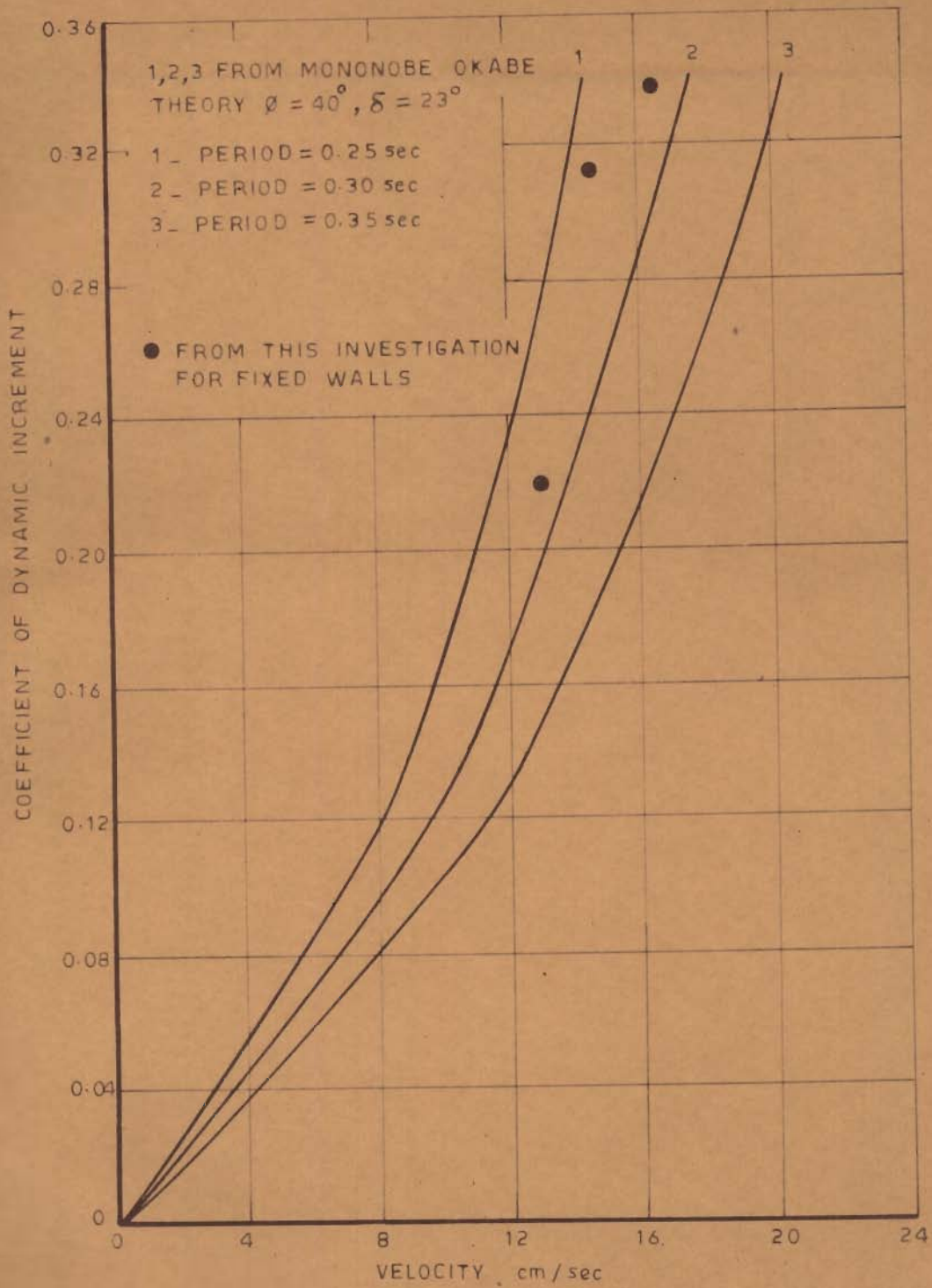


FIG. 4.11 - PEAK BASE VELOCITY VS COEFFICIENT OF DYNAMIC INCREMENT

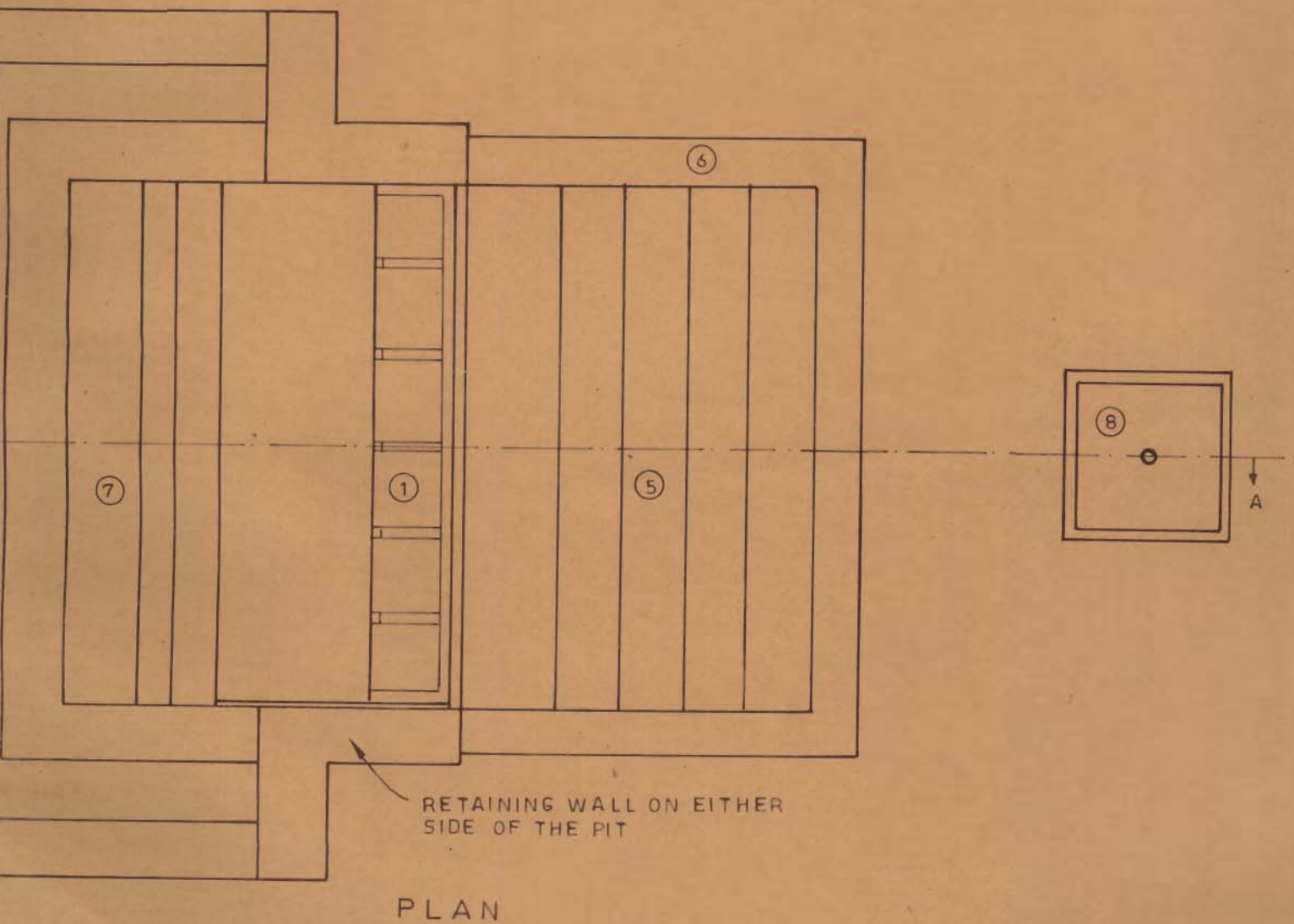
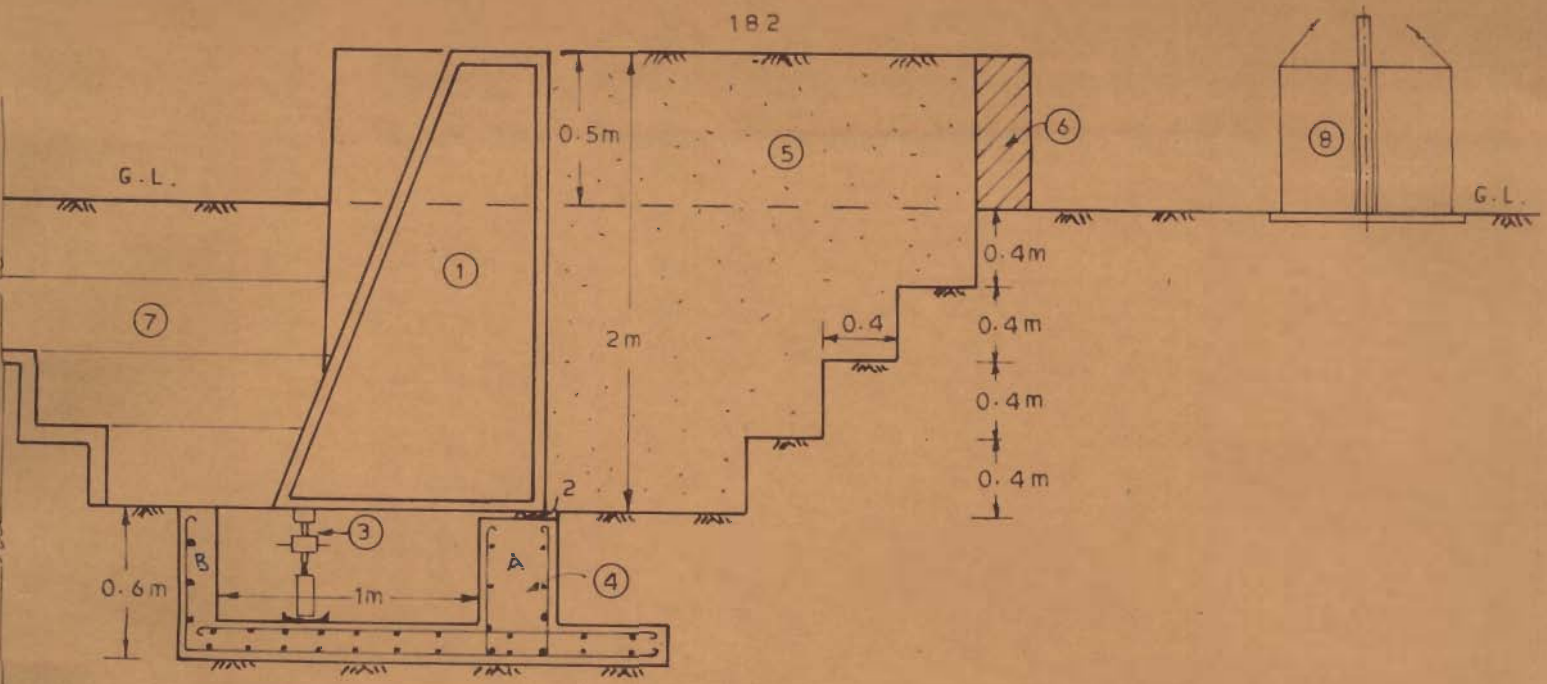
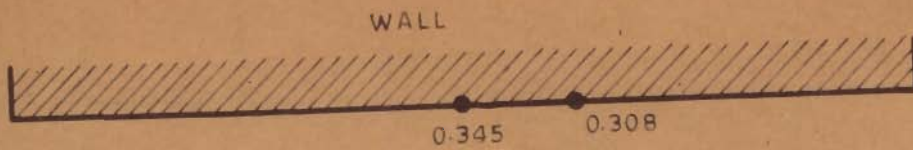


FIG. 5.1 _ TEST SET UP SCHEMATIC DIAGRAM



FIG. 5.2 TEST SET-UP WALL AND THE PIT



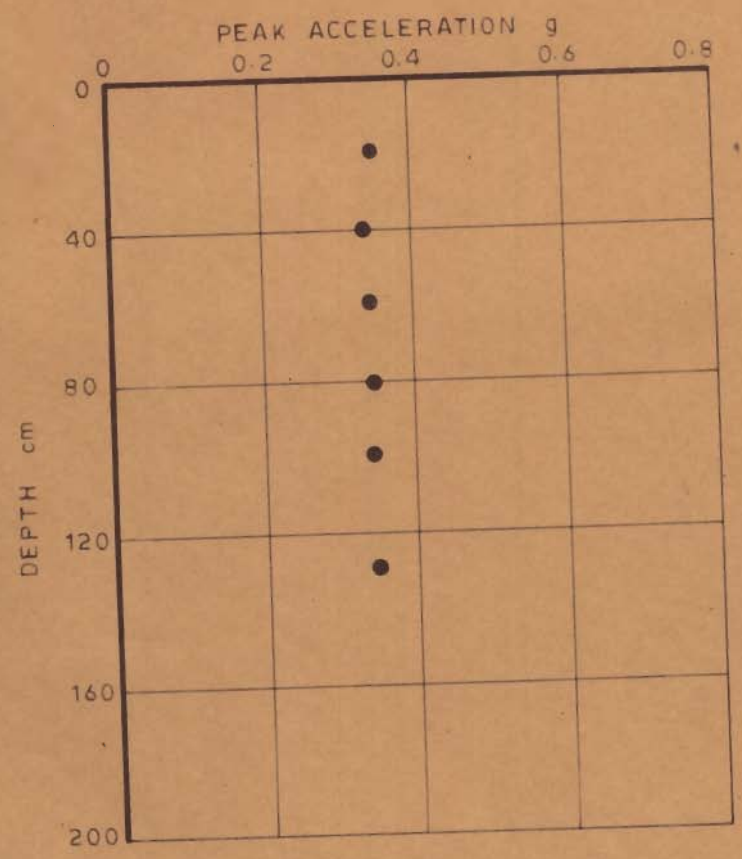
0.309 0.35

0.312

0.348

PLAN

● ACCELERATIONS IN THE PIT AT 20 cm DEPTH



b_ ACCELERATIONS WITH DEPTH AT THE CENTRE LINE OF THE PIT 50 cm FROM THE PIT

FIG. 5.3_ ACCELERATION IN THE PIT (Peak values)

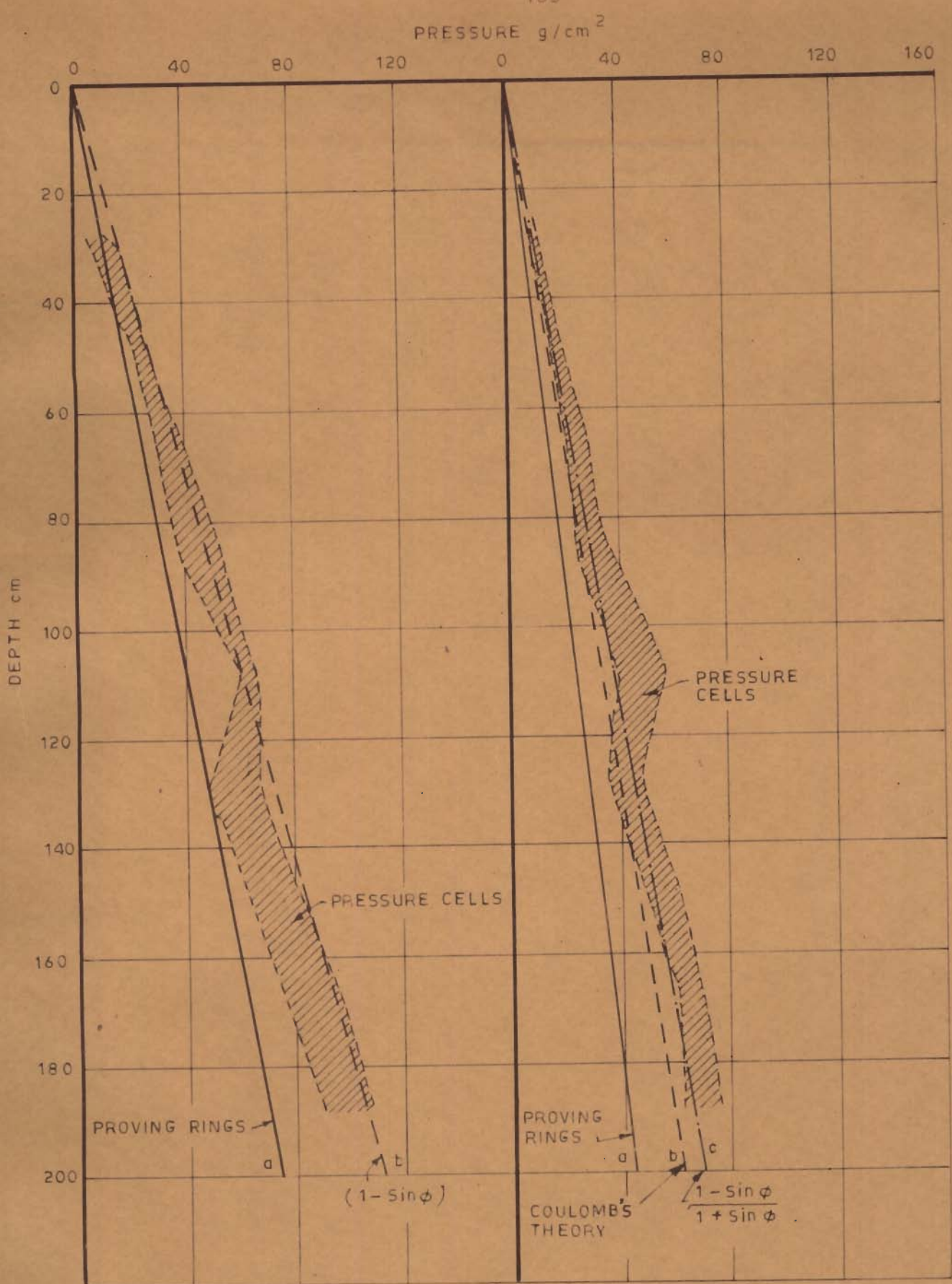


FIG. 5.4 _ AT-REST PRESSURES FIG. 5.5 _ ACTIVE PRESSURES

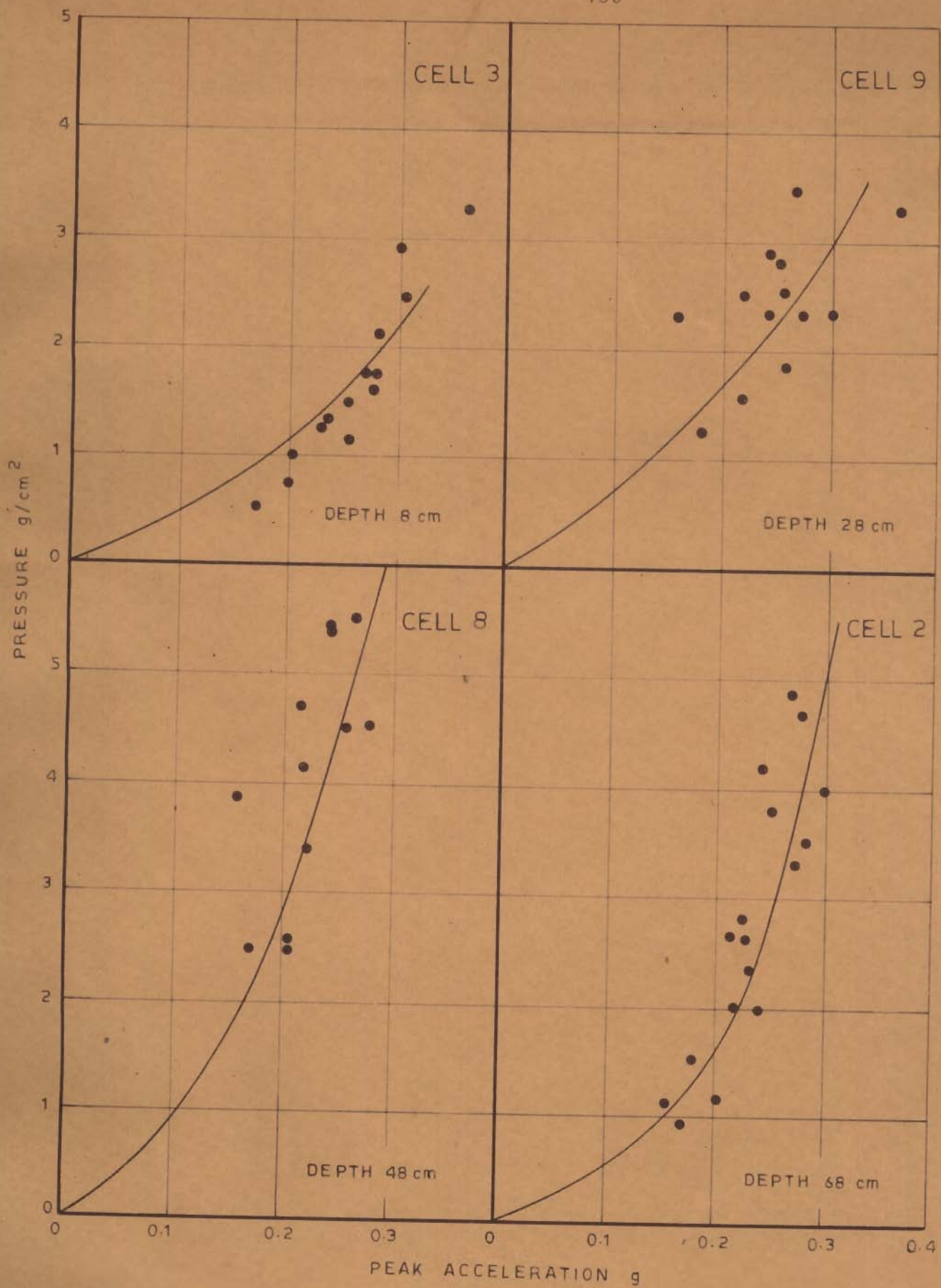


FIG. 5.6 - ACCELERATION VS DYNAMIC PRESSURE
CELL 3, 9, 8 AND 2

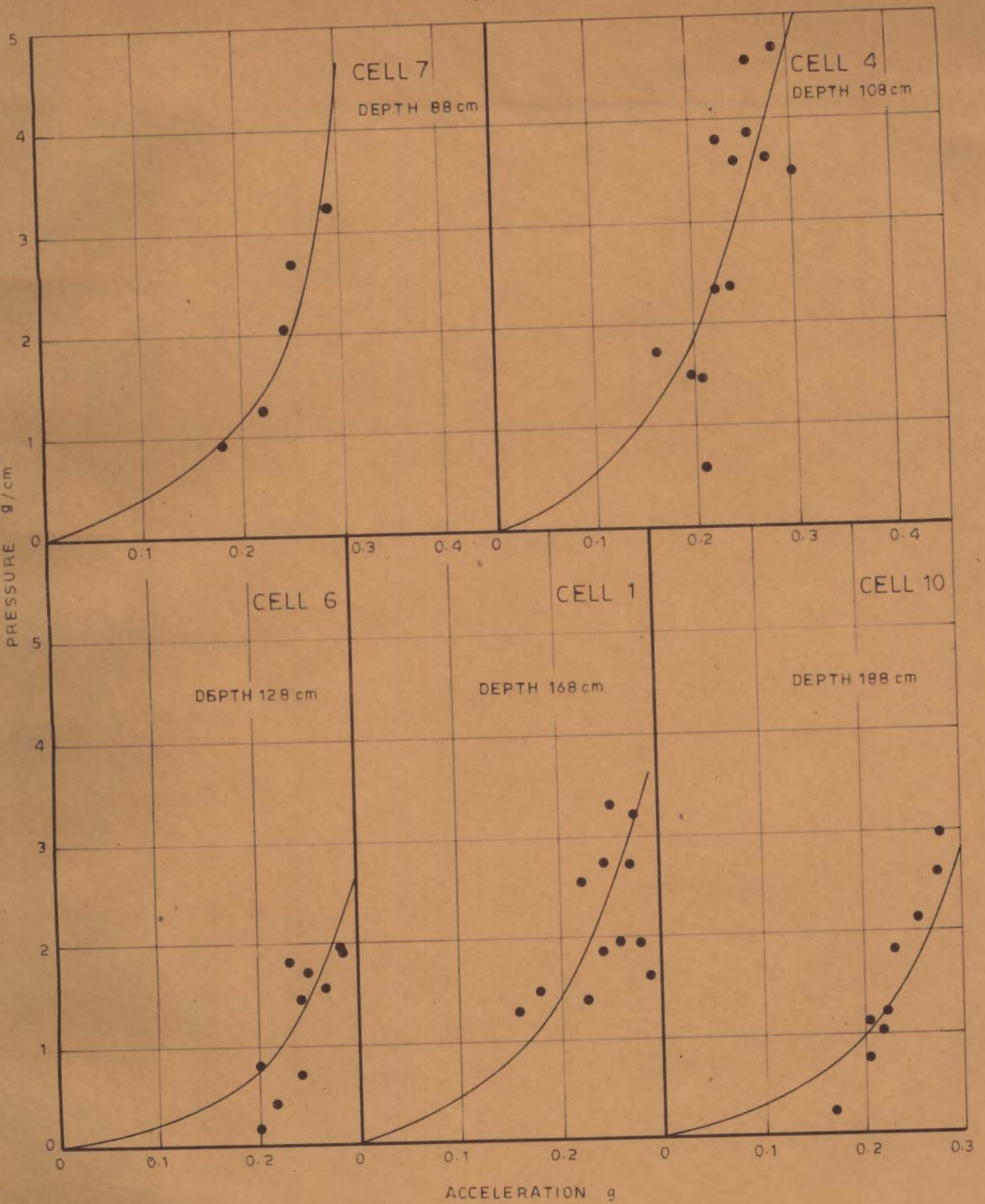


FIG. 5.6(cont'd) - ACCELERATION VS DYNAMIC PRESSURE
CELL 7, 4, 6, 1 AND 10

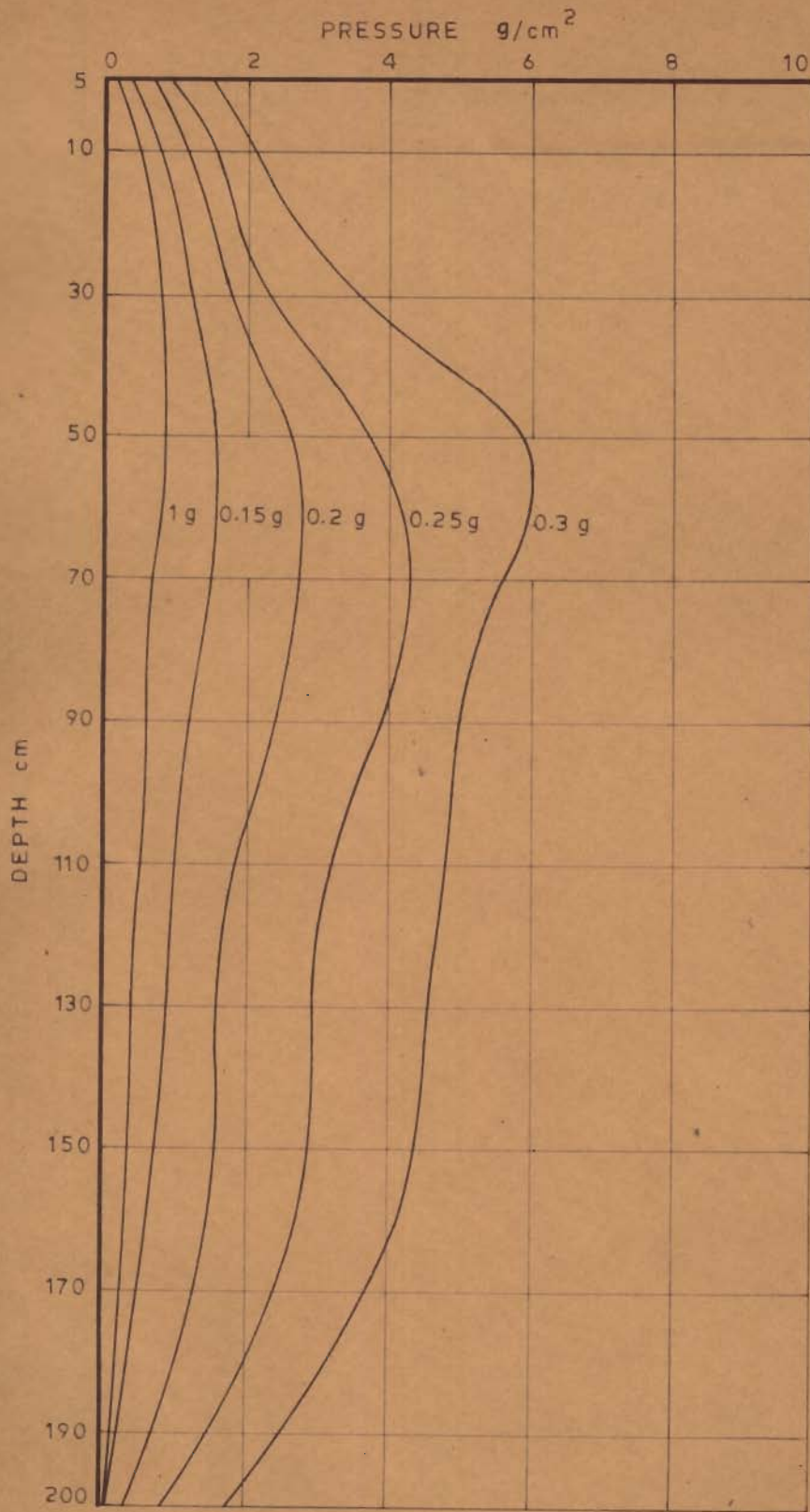


FIG. 5.7_DYNAMIC INCREMENT DISTRIBUTION

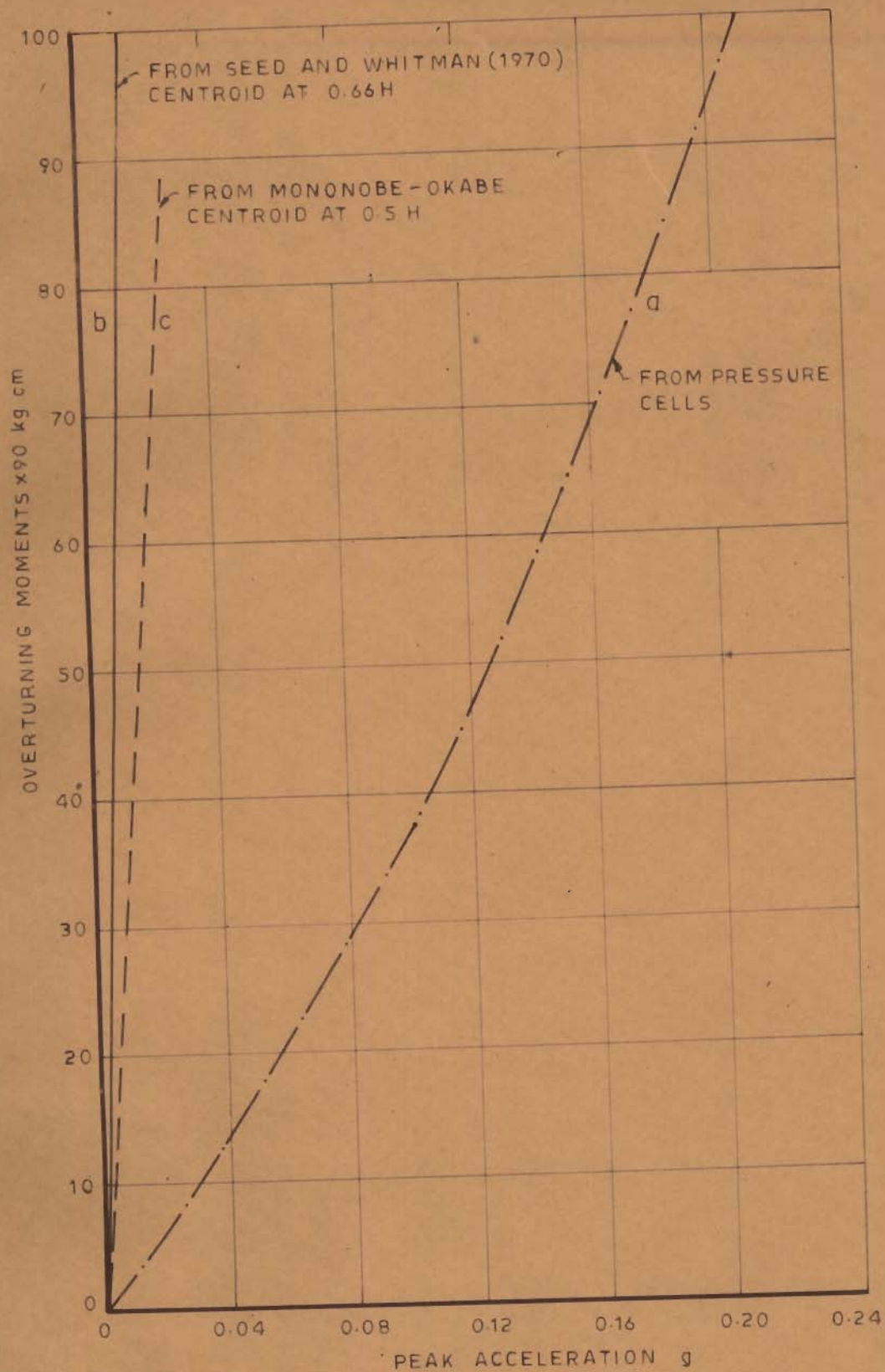


FIG. 5.8_ PEAK ACCELERATION VS OVERTURNING MOMENTS

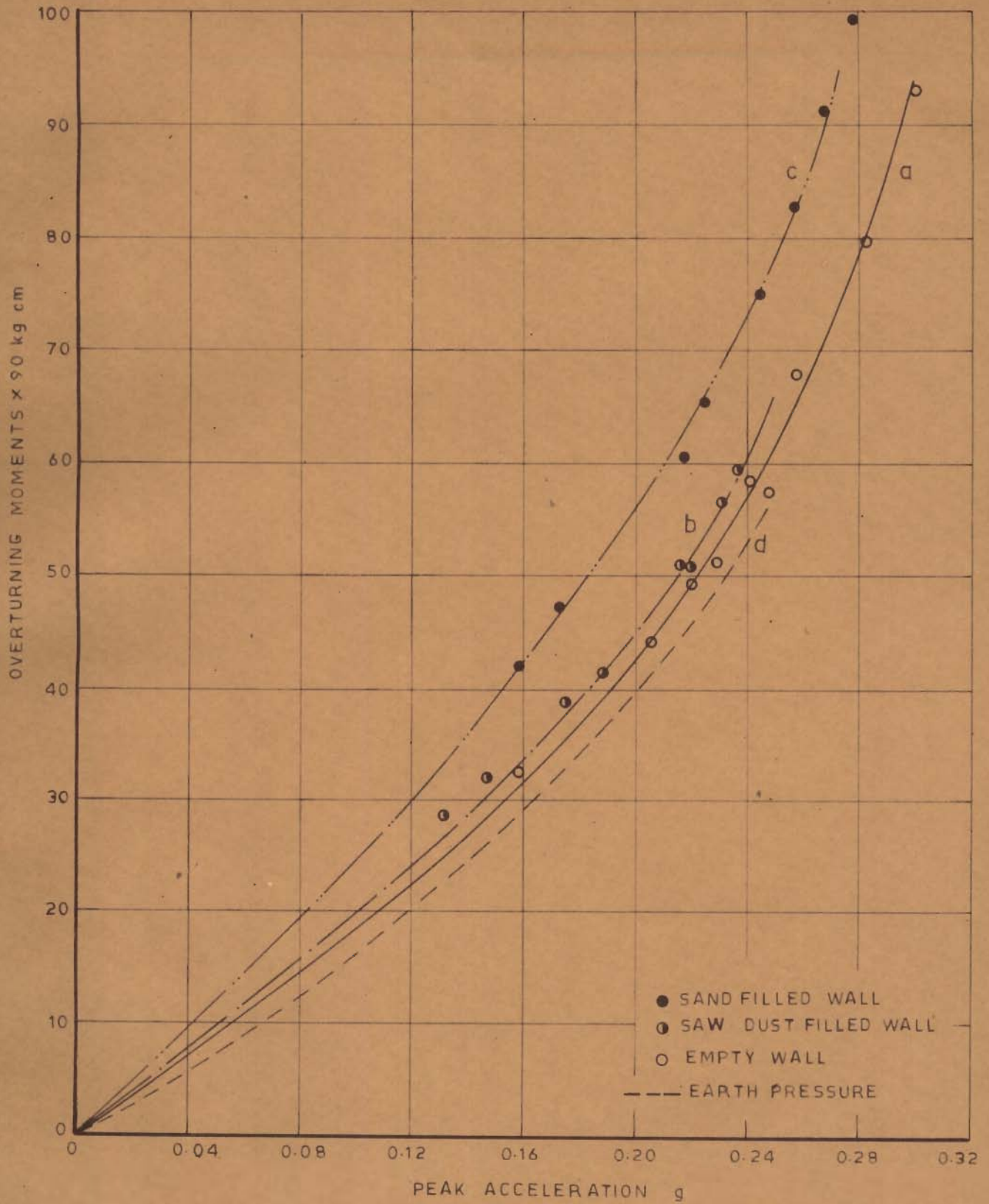


FIG. 5.9_ OVERTURNING MOMENTS VS PEAK ACCELERATION

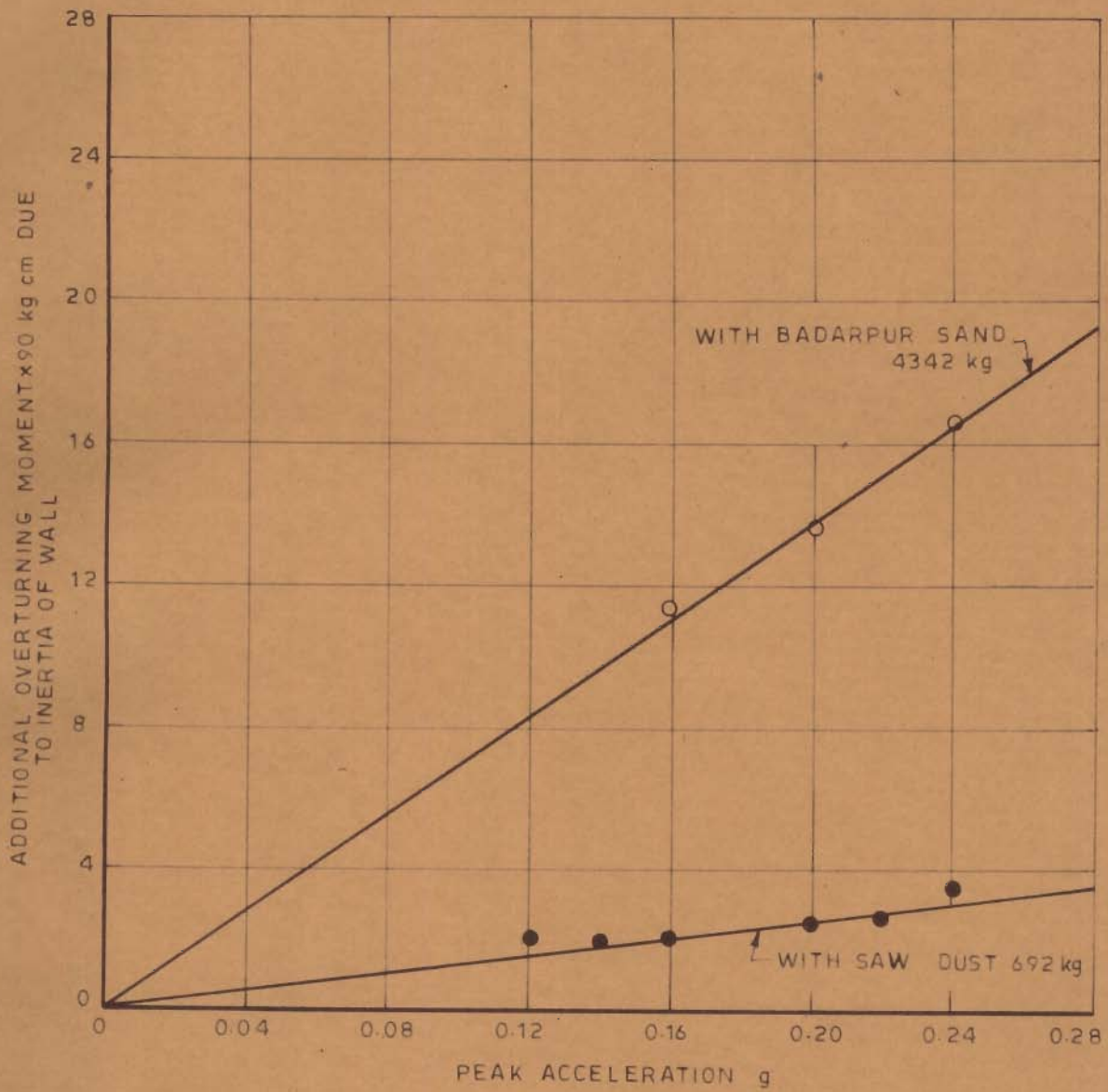


FIG. 5.10 - PEAK ACCELERATION VS INCREASE IN OVERTURNING MOMENT

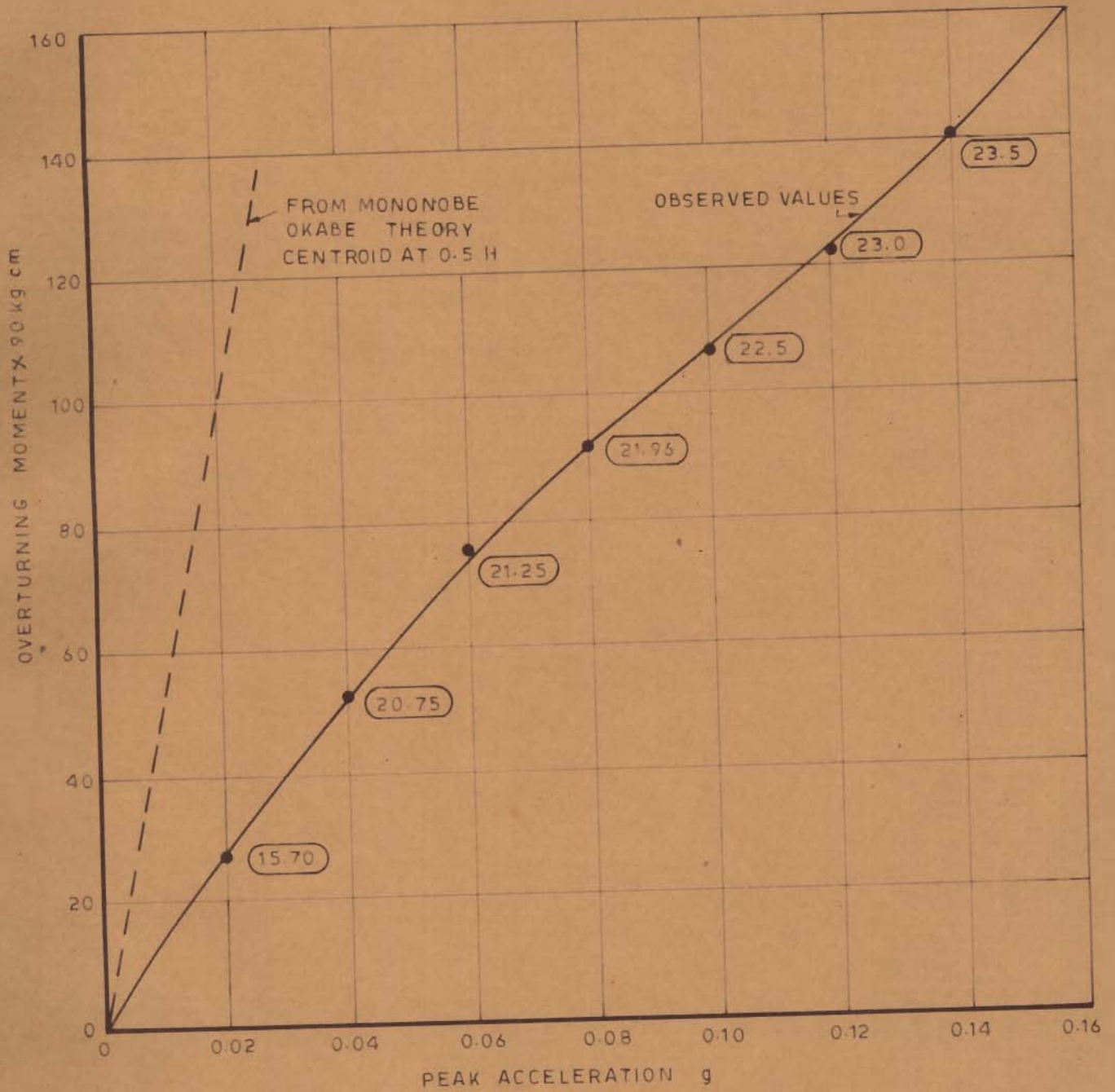


FIG. 5.11 - OVERTURNING MOMENT VS PEAK ACCELERATION
STEADY STATE VIBRATION

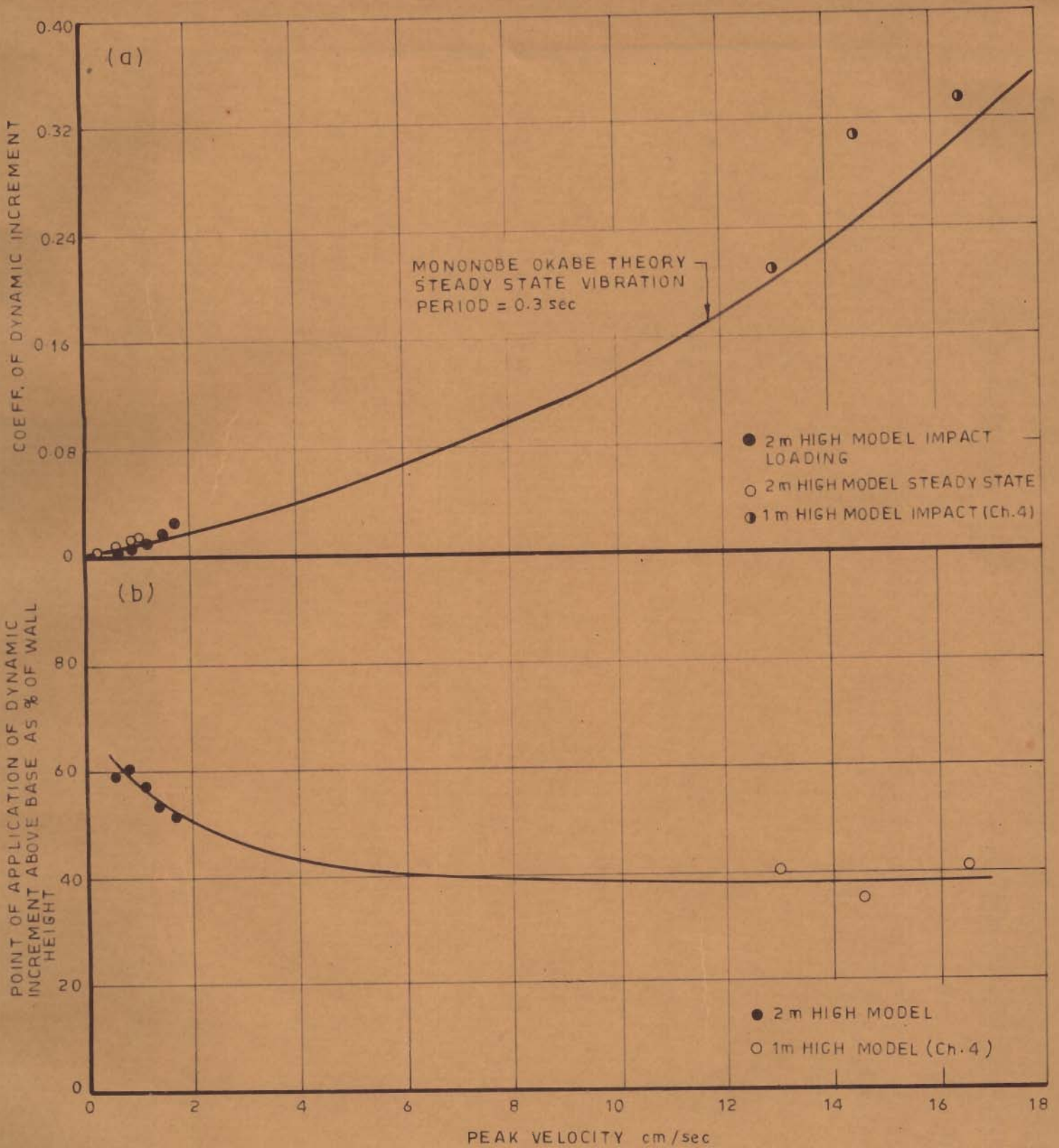


FIG. 5.12 - PEAK VELOCITY VS COEFFICIENT OF DYNAMIC INCREMENT AND ITS POINT OF APPLICATION

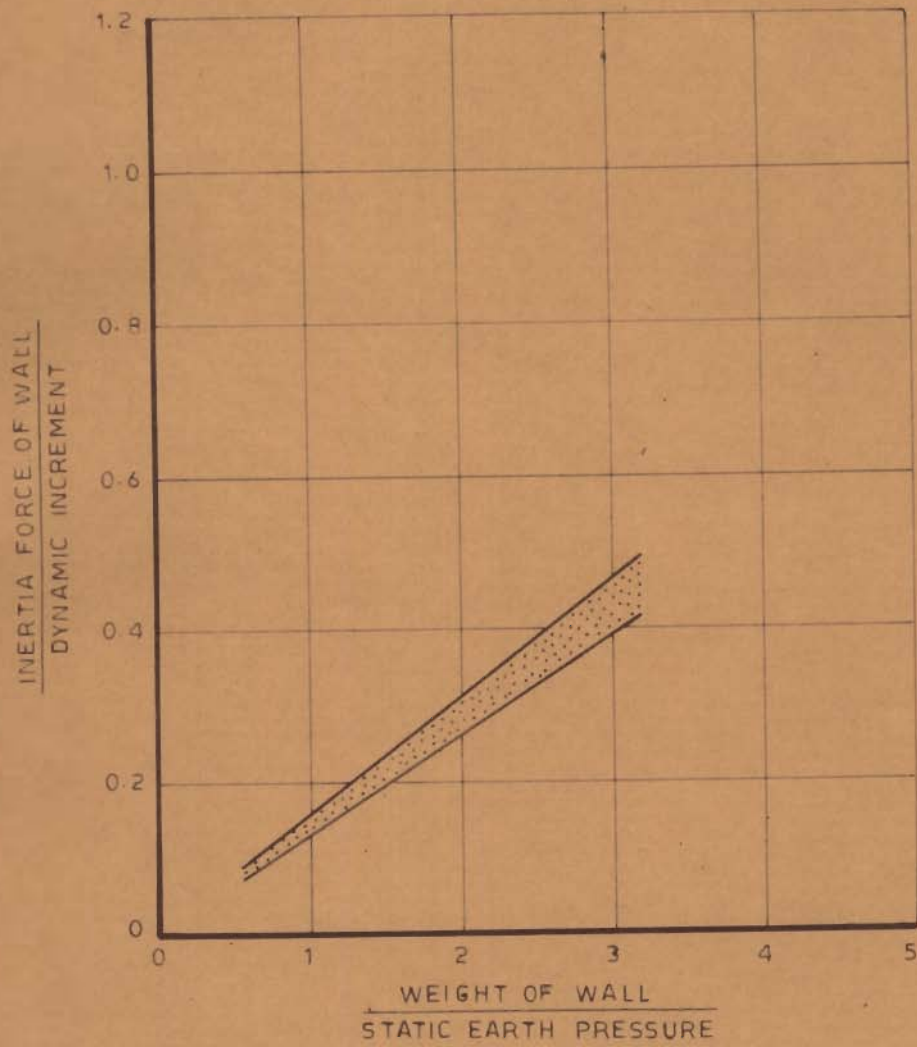


FIG. 5.13 - INERTIA FORCES OF THE WALL

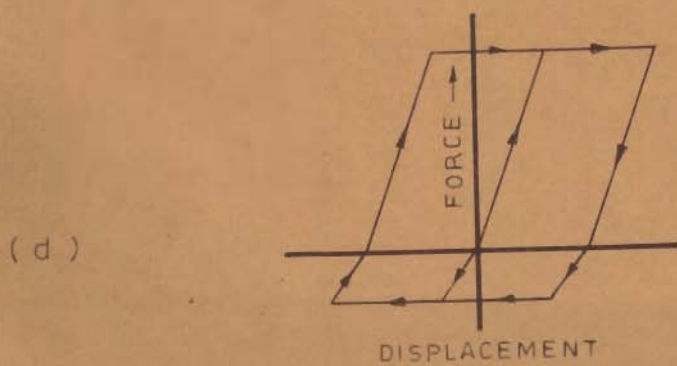
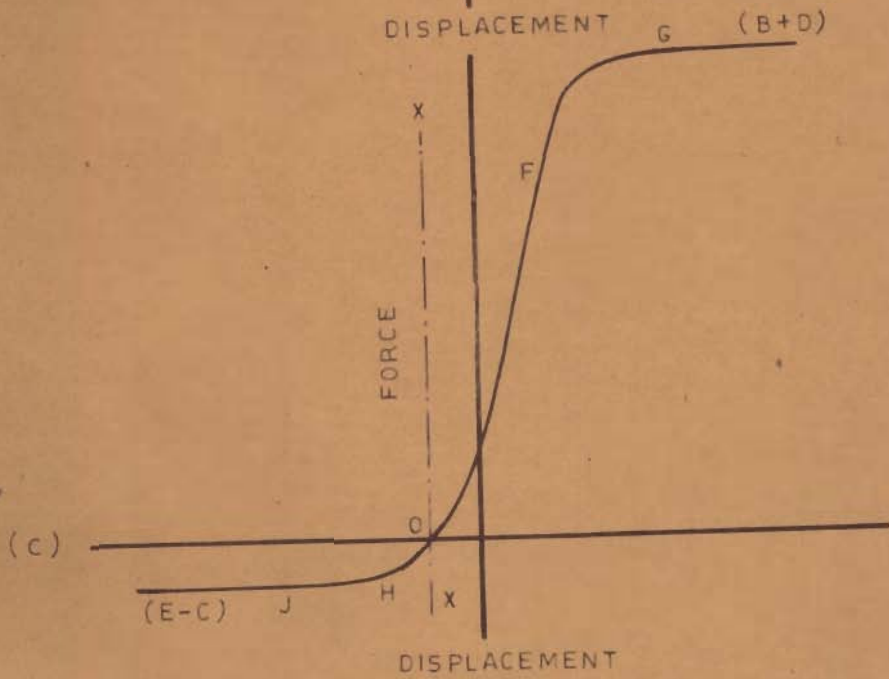
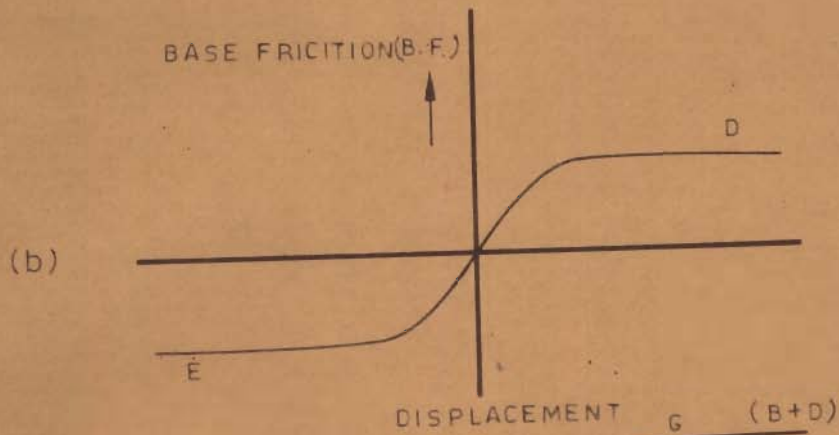
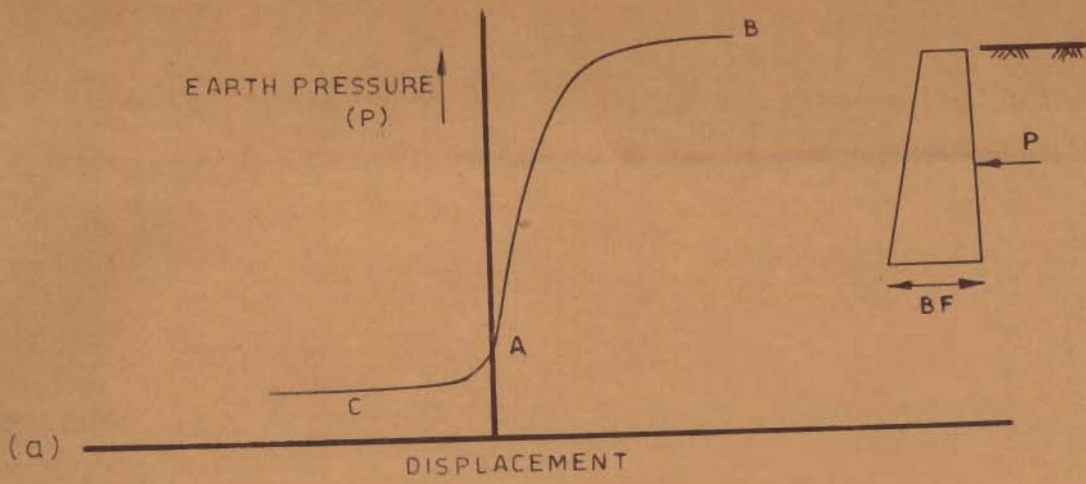
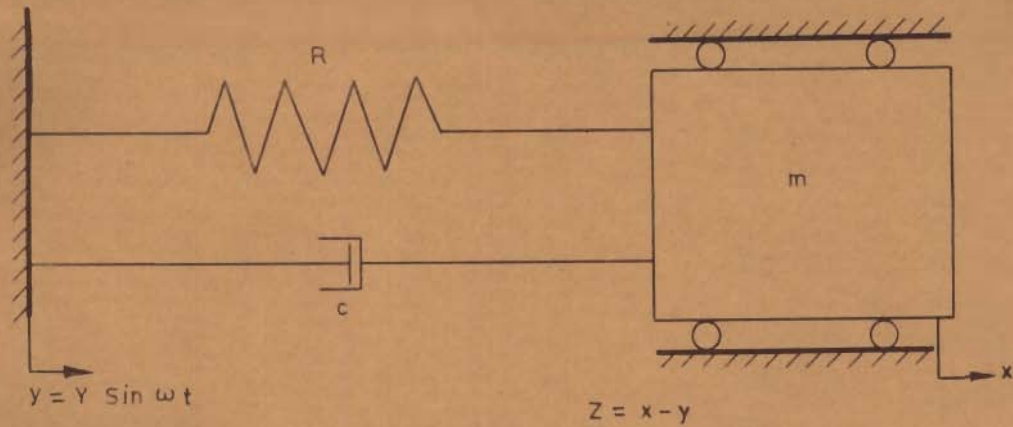
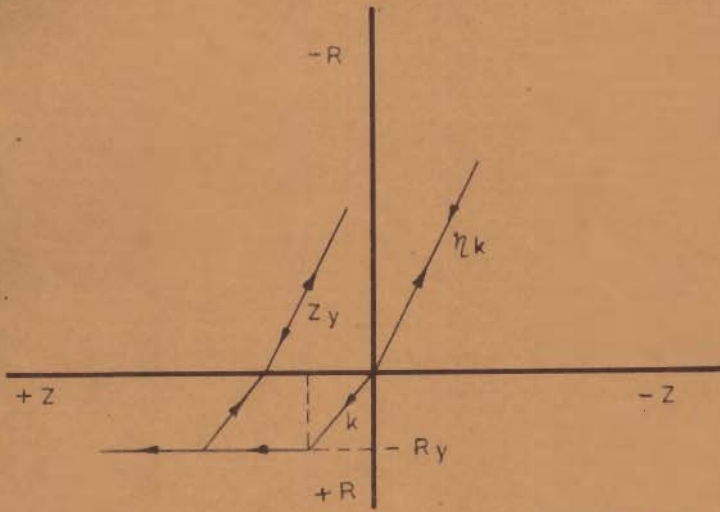


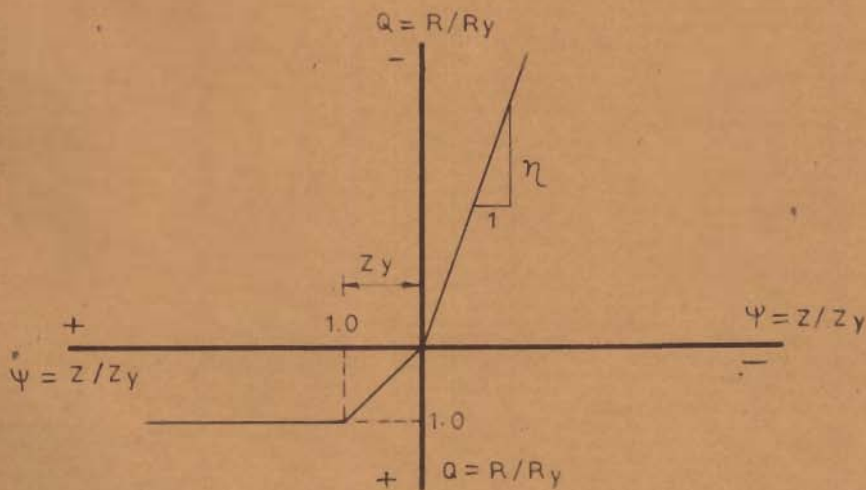
FIG.6.1 _FORCE VS DISPLACEMENT



a_MATHEMATICAL MODEL



b_ THE FORCE-DISPLACEMENT RELATIONSHIP



c_ DISPLACEMENT FORCE RELATIONSHIP

FIG. 6.2_ DETAILS OF MATHEMATICAL MODEL

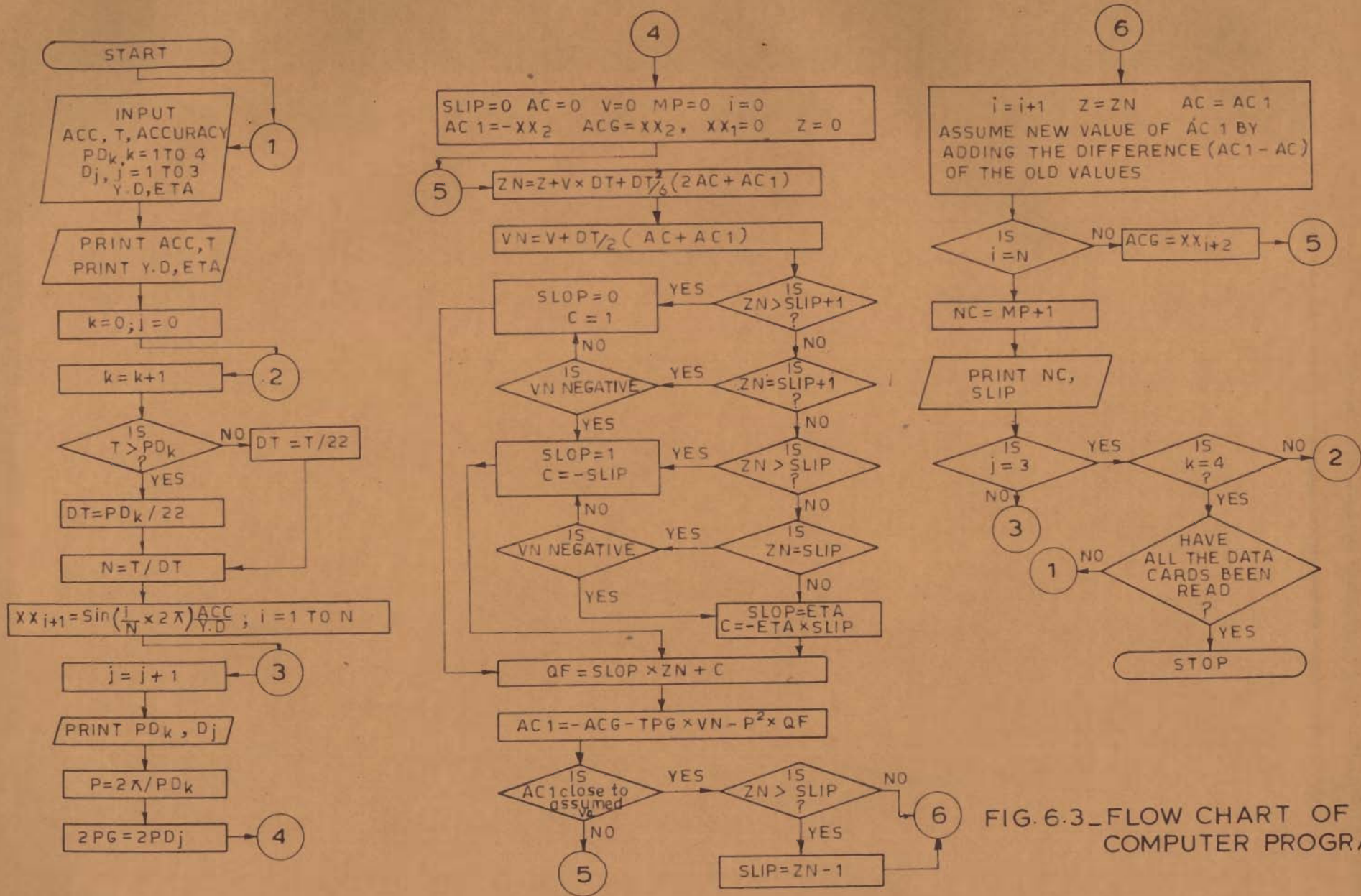


FIG. 6.3 - FLOW CHART OF THE COMPUTER PROGRAM

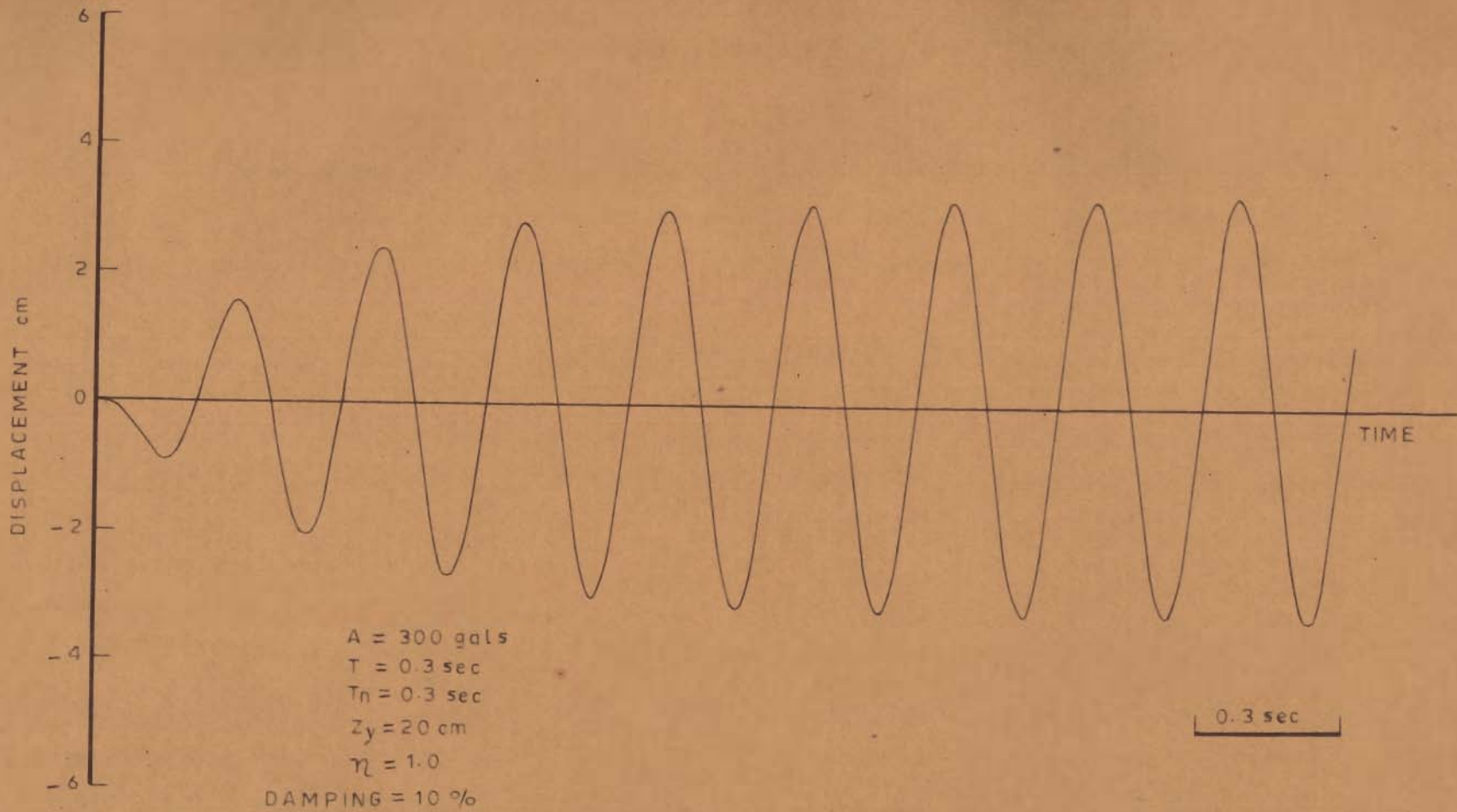


FIG. 6.4 _ RESPONSE OF ELASTIC SYSTEM BY LINEAR ACCELERATION METHOD

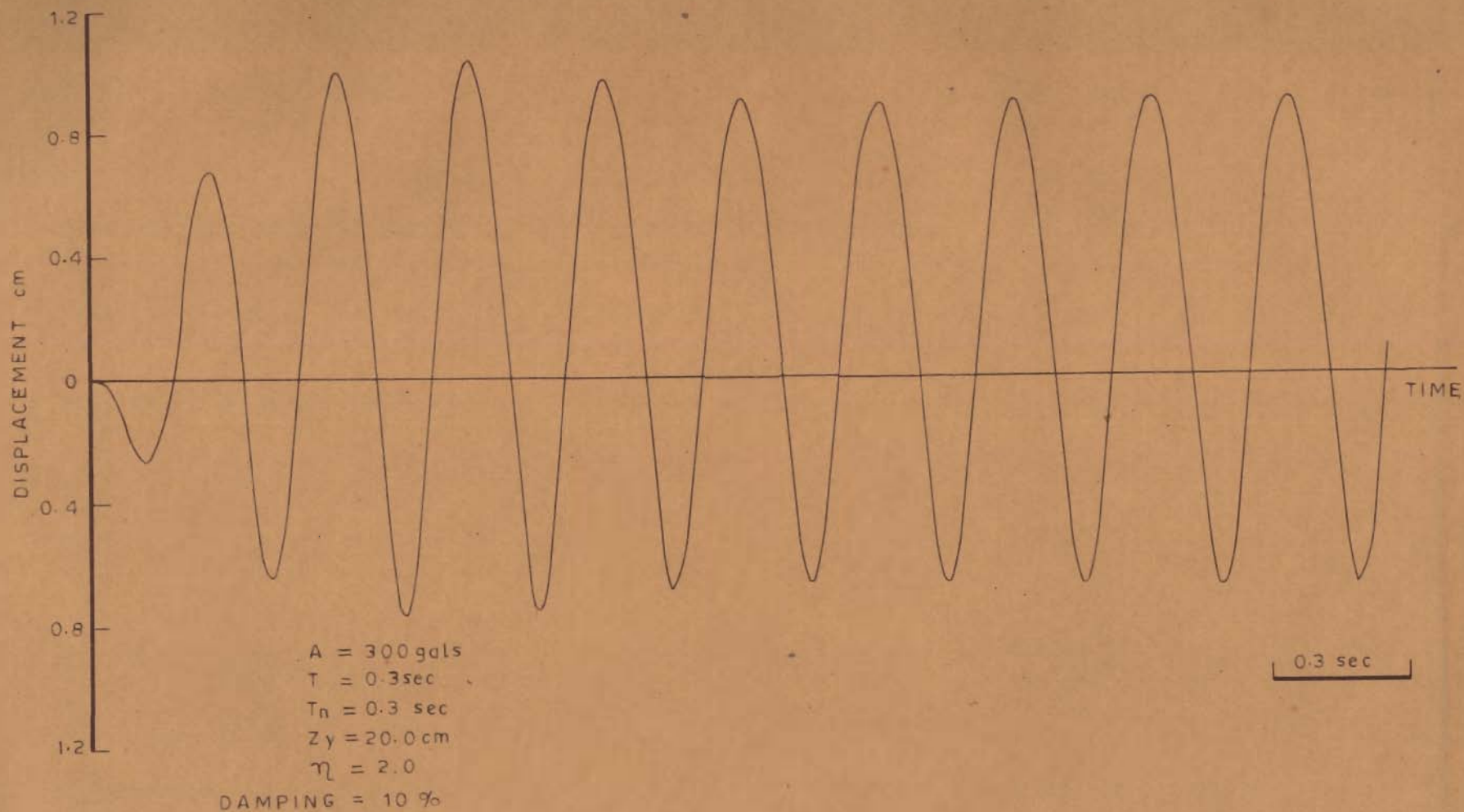


FIG. 6.5 - RESPONSE OF AN ELASTIC SYSTEM WITH DIFFERENT STIFFNESSES ON TENSION AND COMPRESSION SIDES

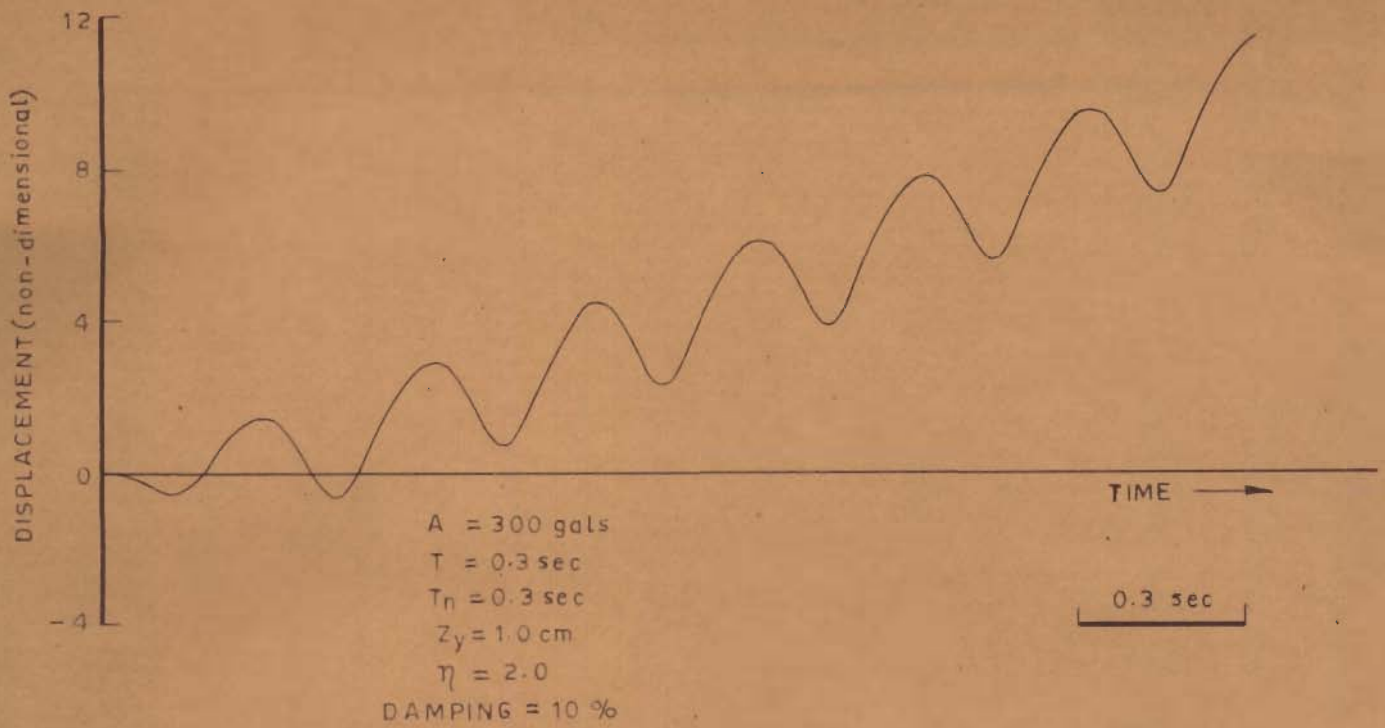


FIG. 6.6_ DISPLACEMENT VS TIME

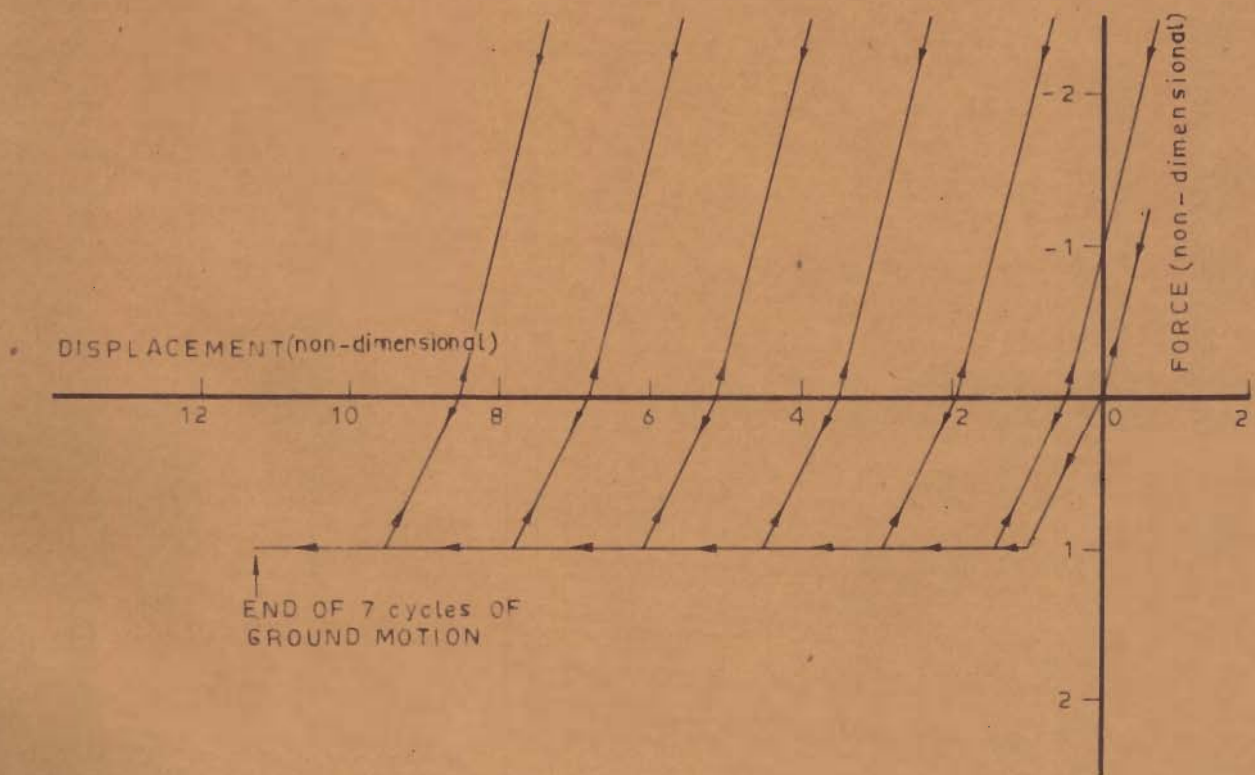


FIG. 6.7_ DISPLACEMENT VS NET SOIL RESISTANCE

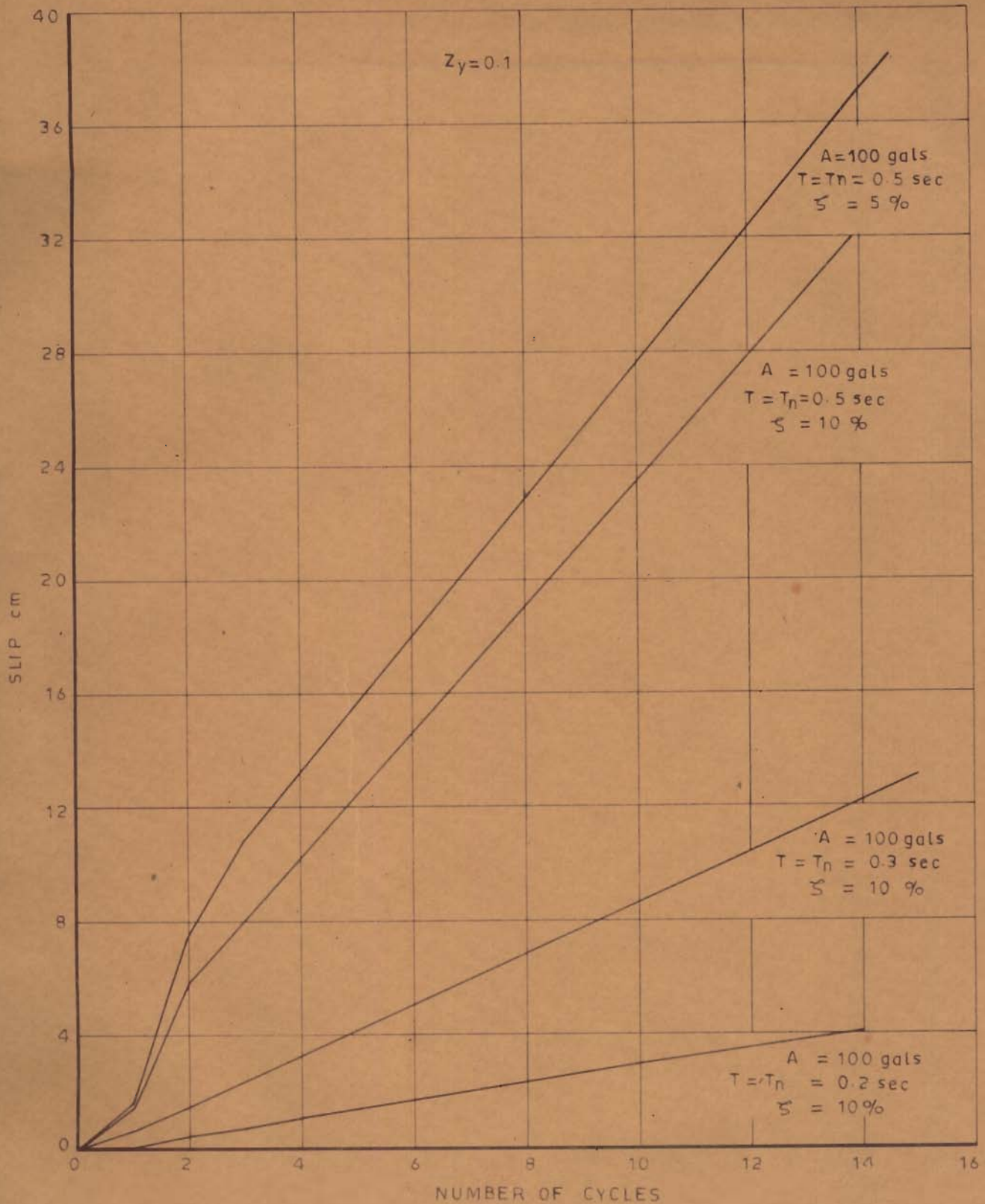


FIG. 6.8 - NUMBER OF CYCLES VS. SLIP

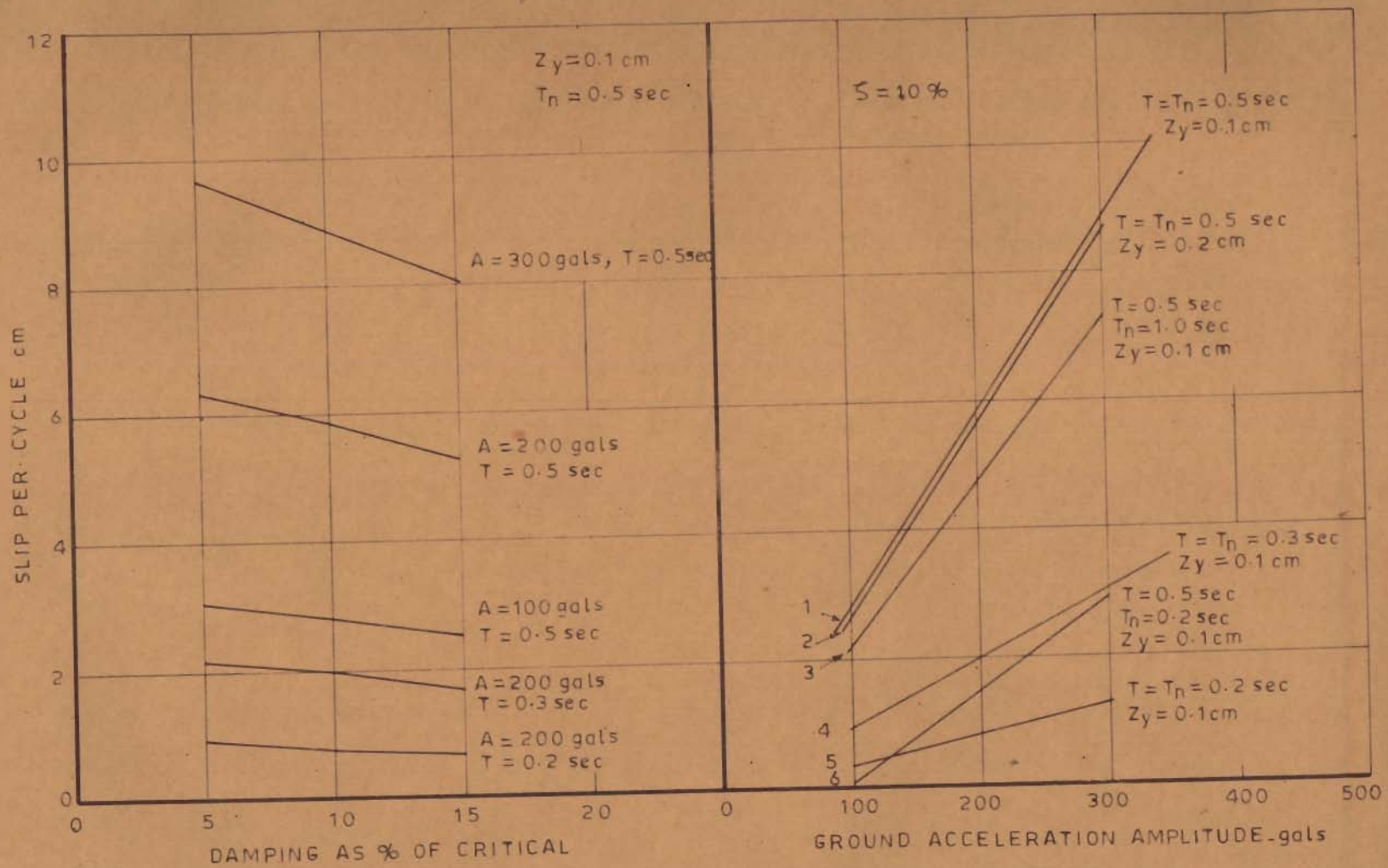


FIG. 6.9 - EFFECT OF DAMPING ON SLIP

FIG. 6.10 - EFFECT OF ACCELERATION AMPLITUDE ON SLIP

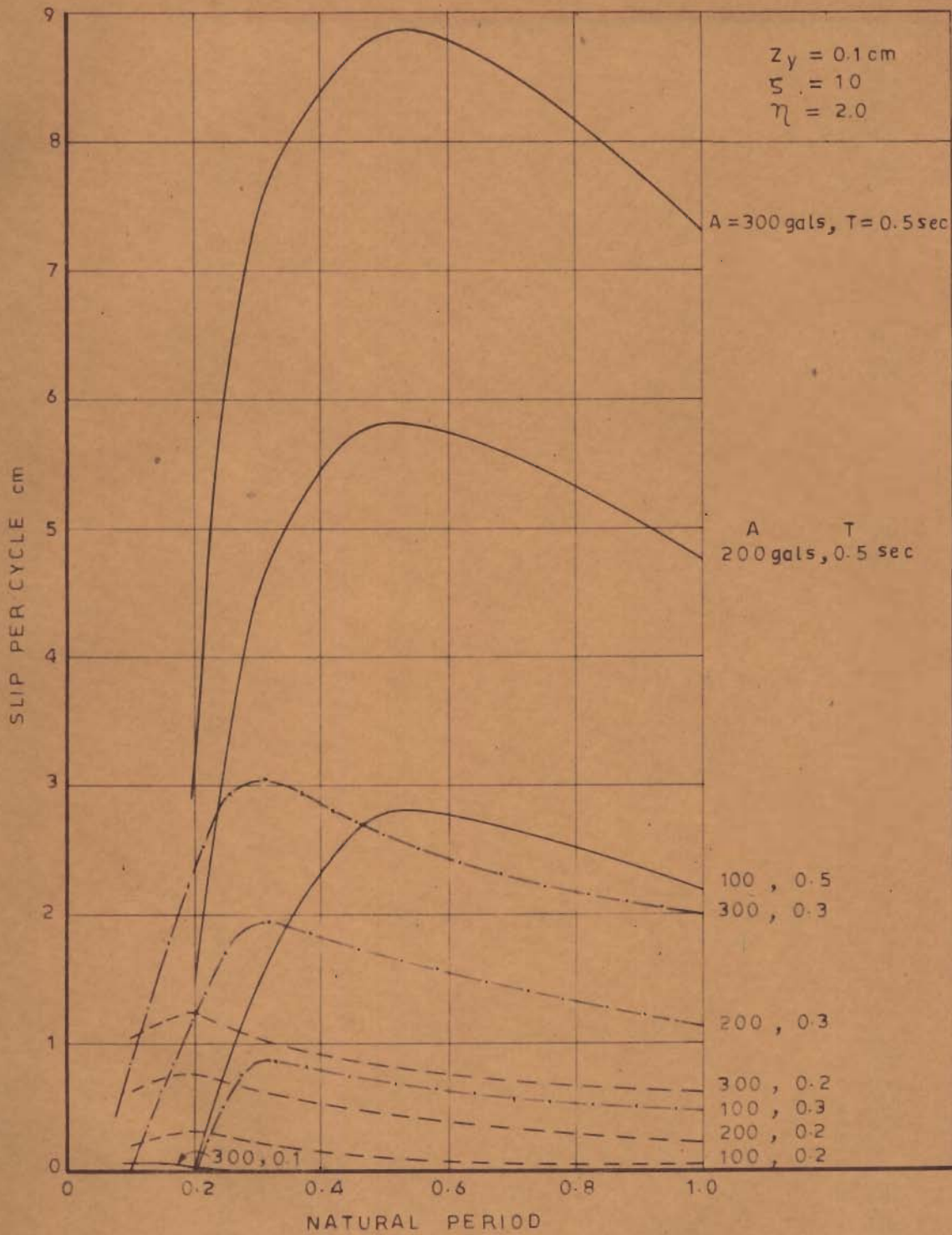


FIG. 6.11_ NATURAL PERIOD VS SLIP PER CYCLE

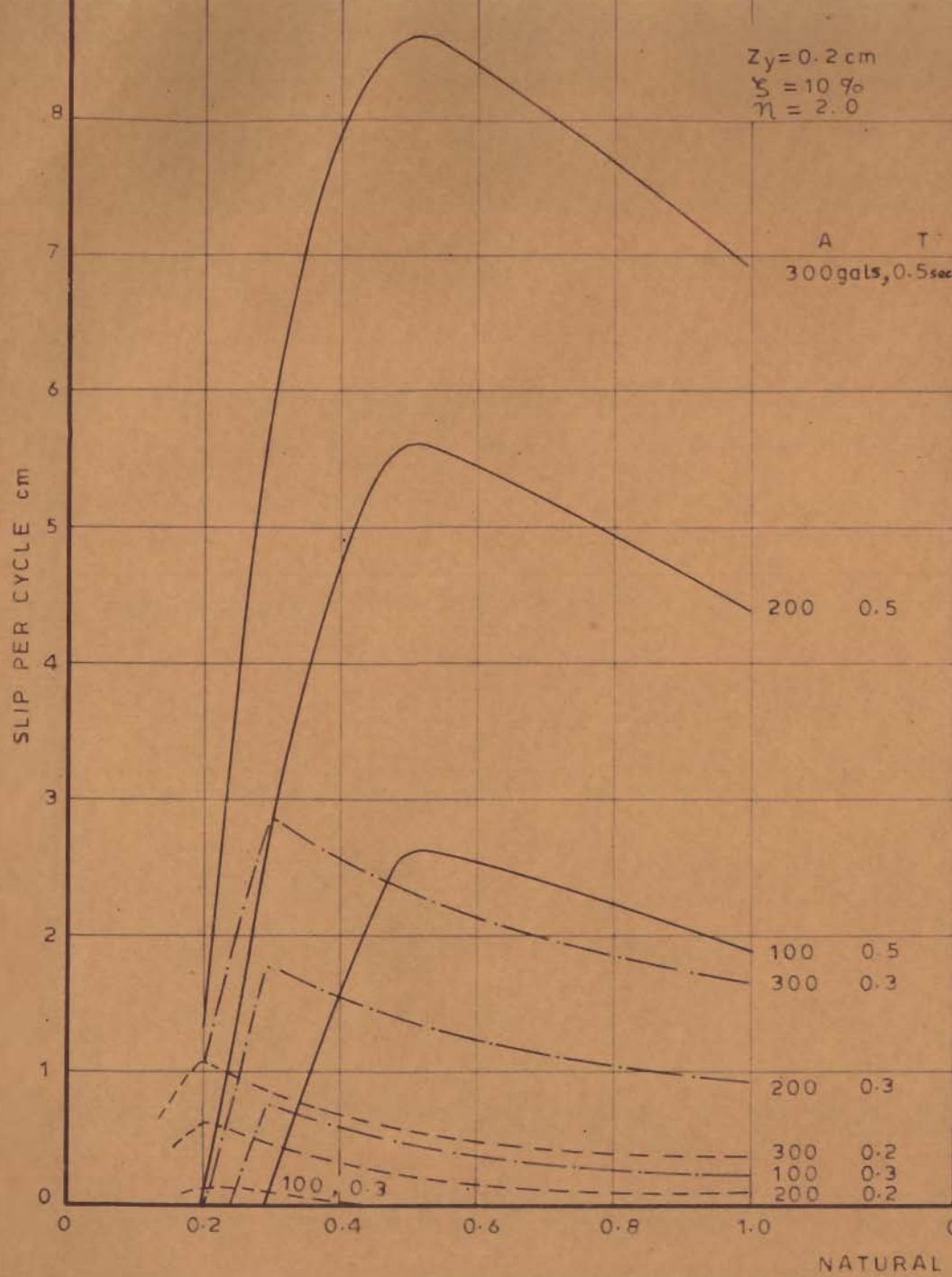


FIG. 6.12

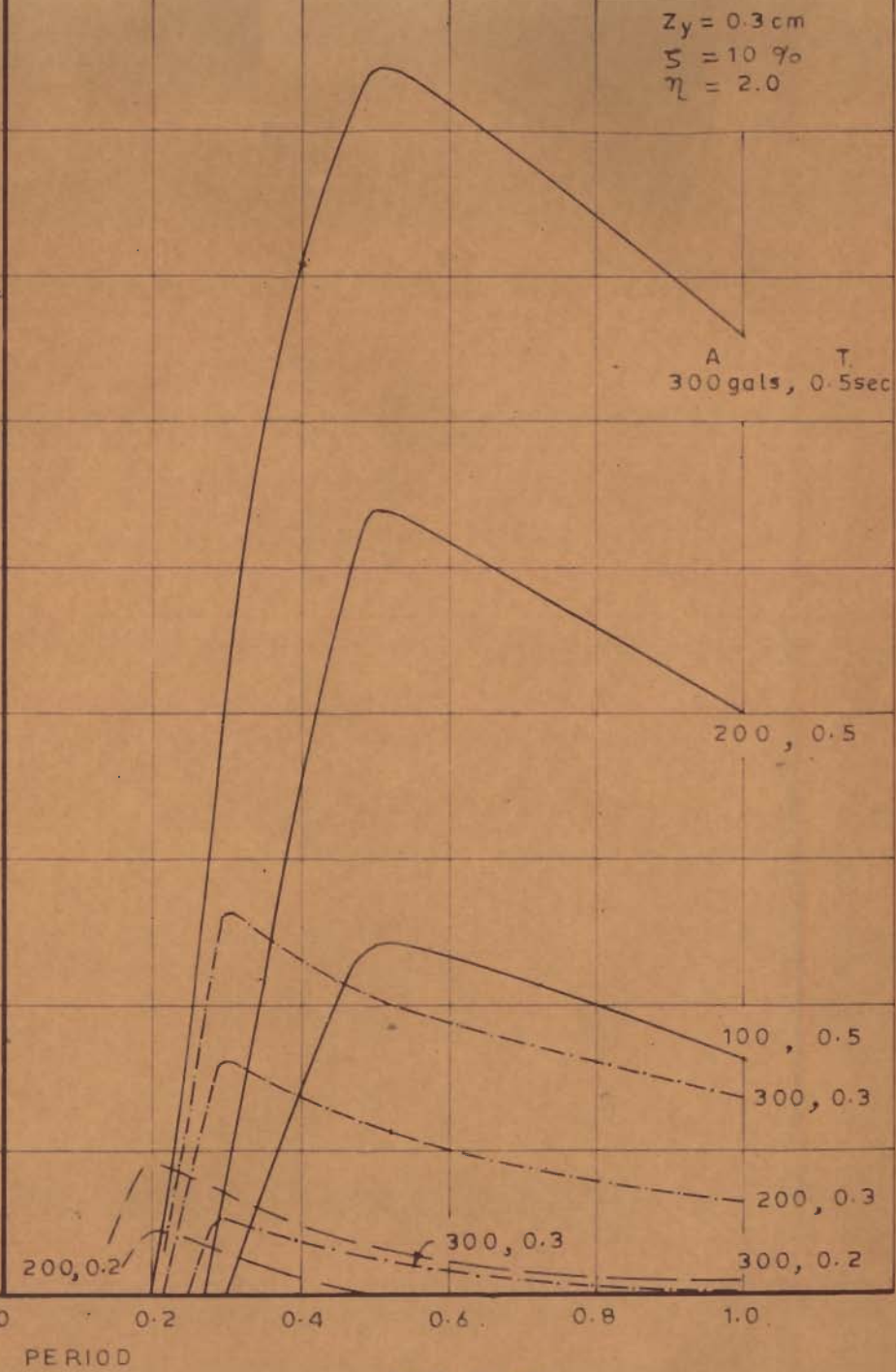
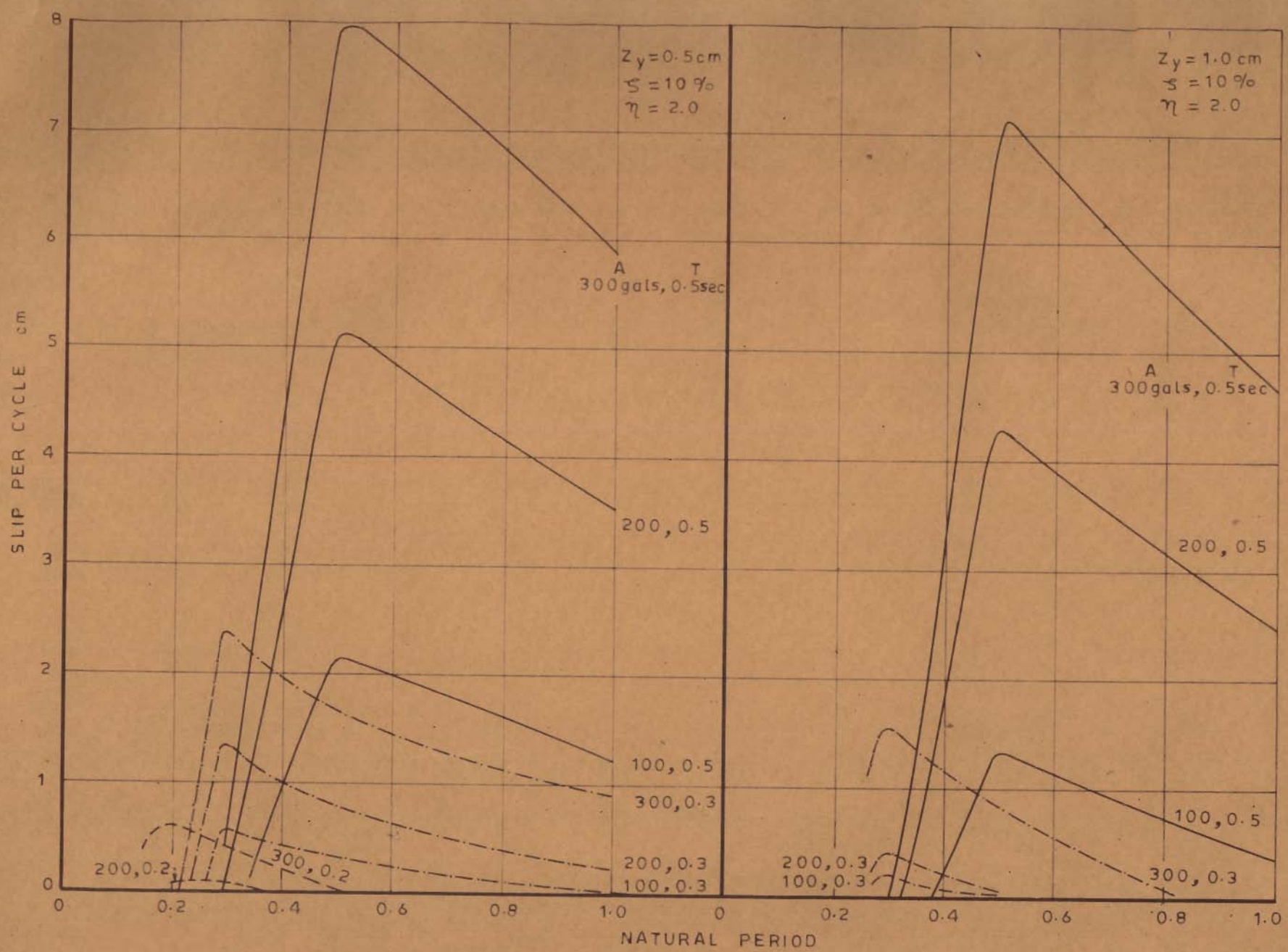


FIG. 6.13

NATURAL PERIOD VS SLIP PER CYCLE



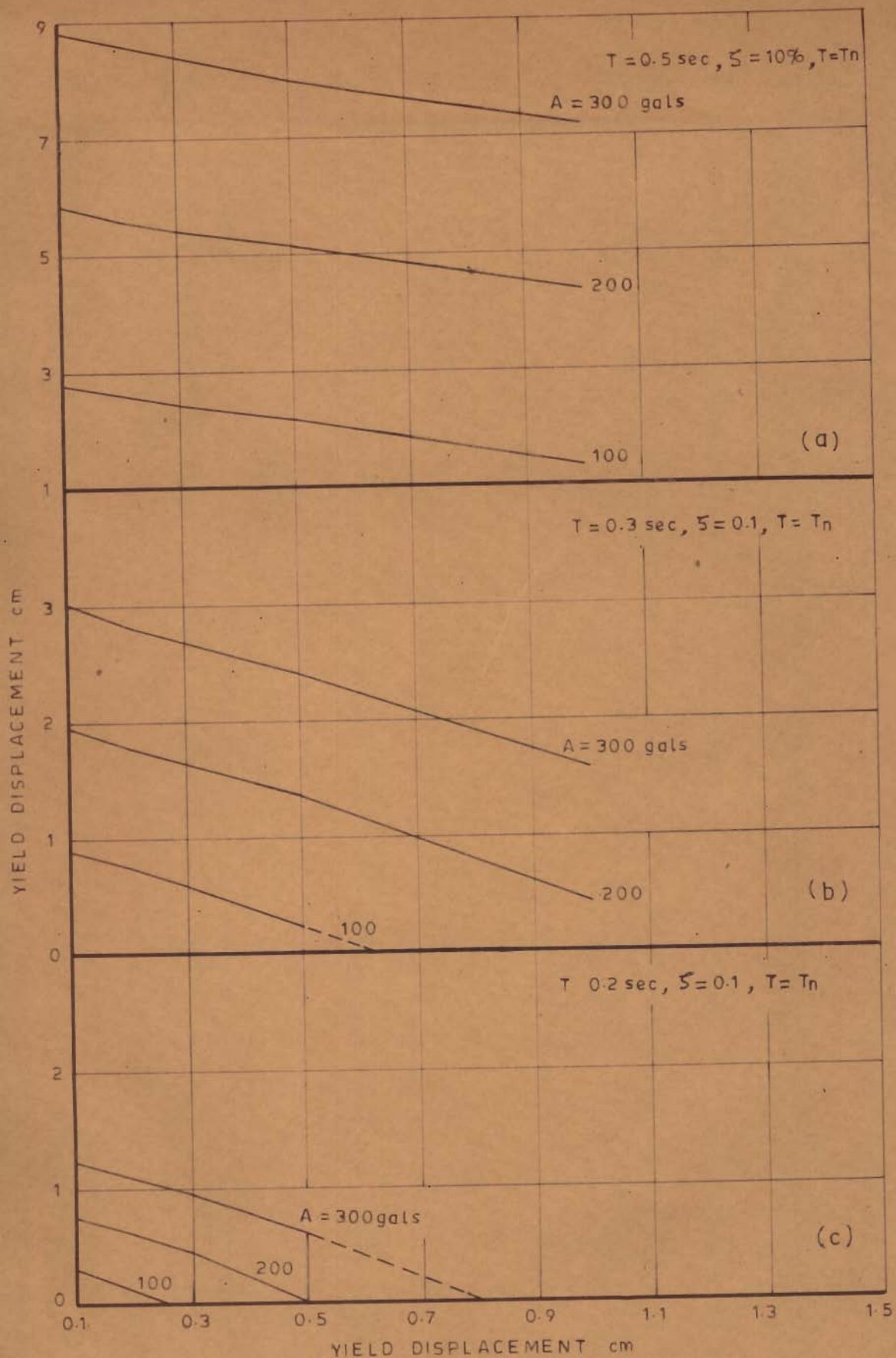


FIG. 6.16 - EFFECT OF YIELD DISPLACEMENT, ACCELERATION LEVEL AND FORCING FREQUENCY ON SLIP

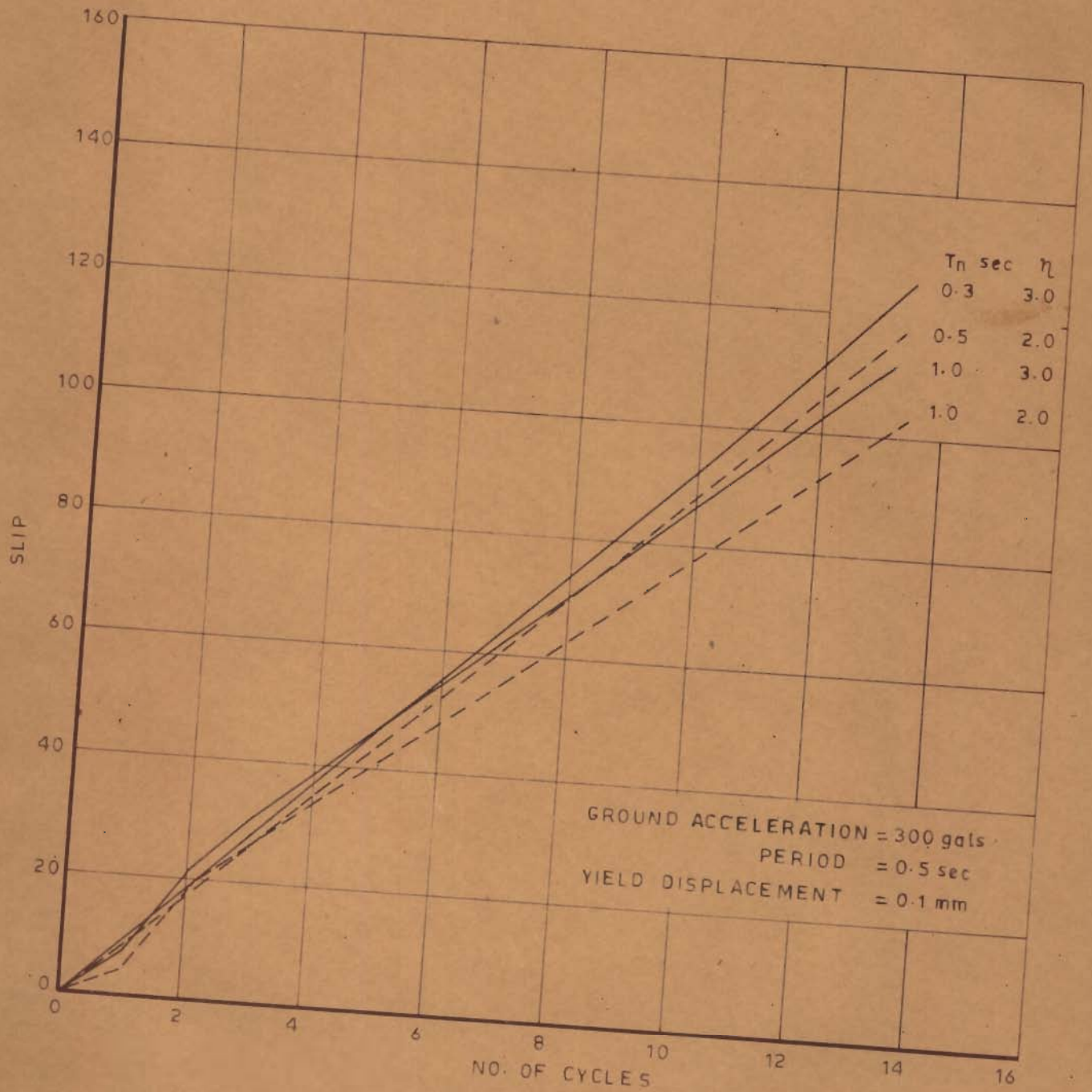


FIG. 6.17 - NUMBER OF CYCLES VS SLIP

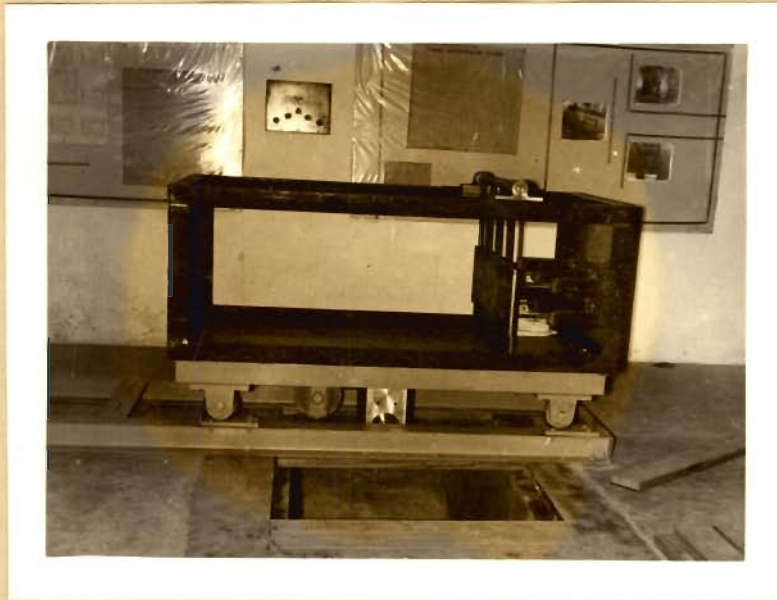
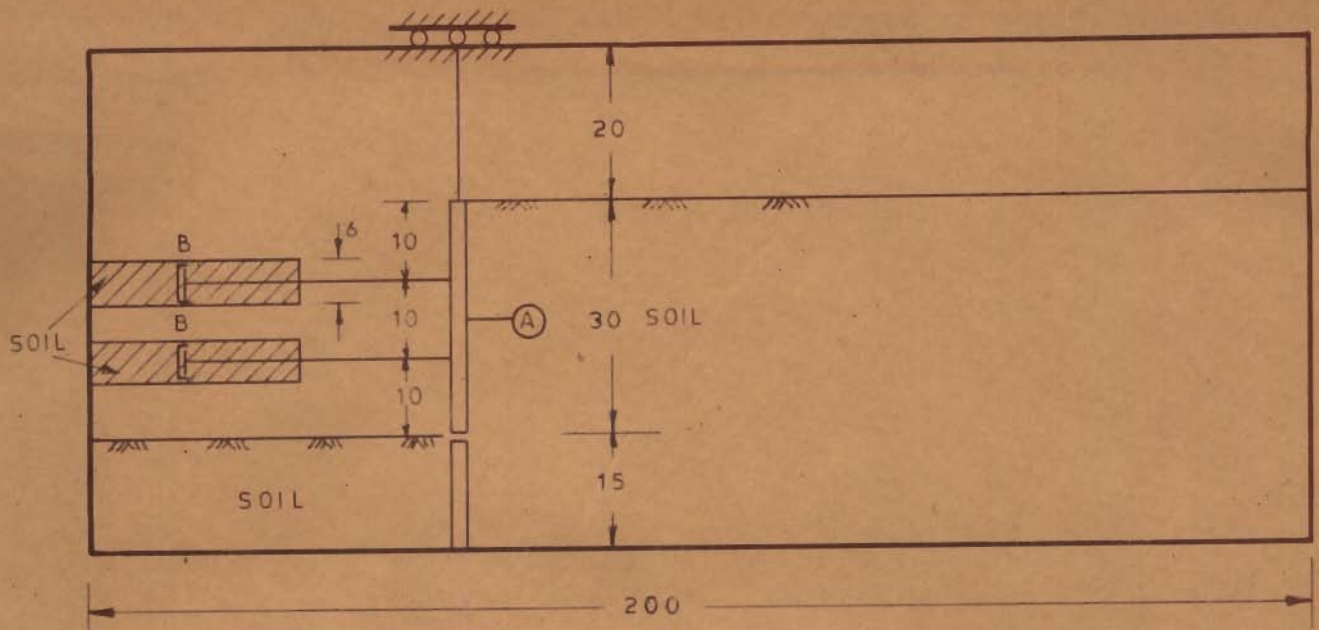
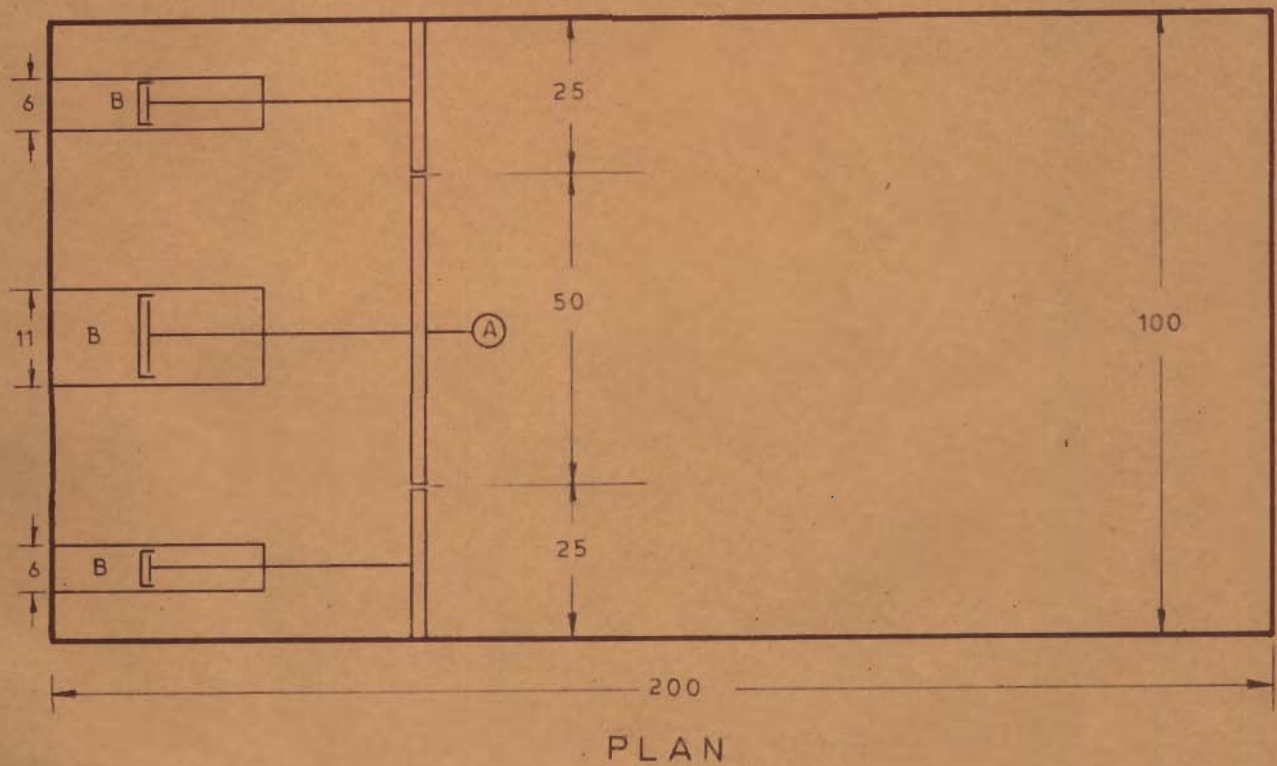


FIG. 6.18 EXPERIMENTAL SET-UP



SECTIONAL ELEVATION

ALL DIMENSIONS IN cm



PLAN

FIG. 6.19_ SCHEMATIC DIAGRAM OF EXPERIMENTAL SET UP FOR FINDING SOIL VIBRATING WITH WALL

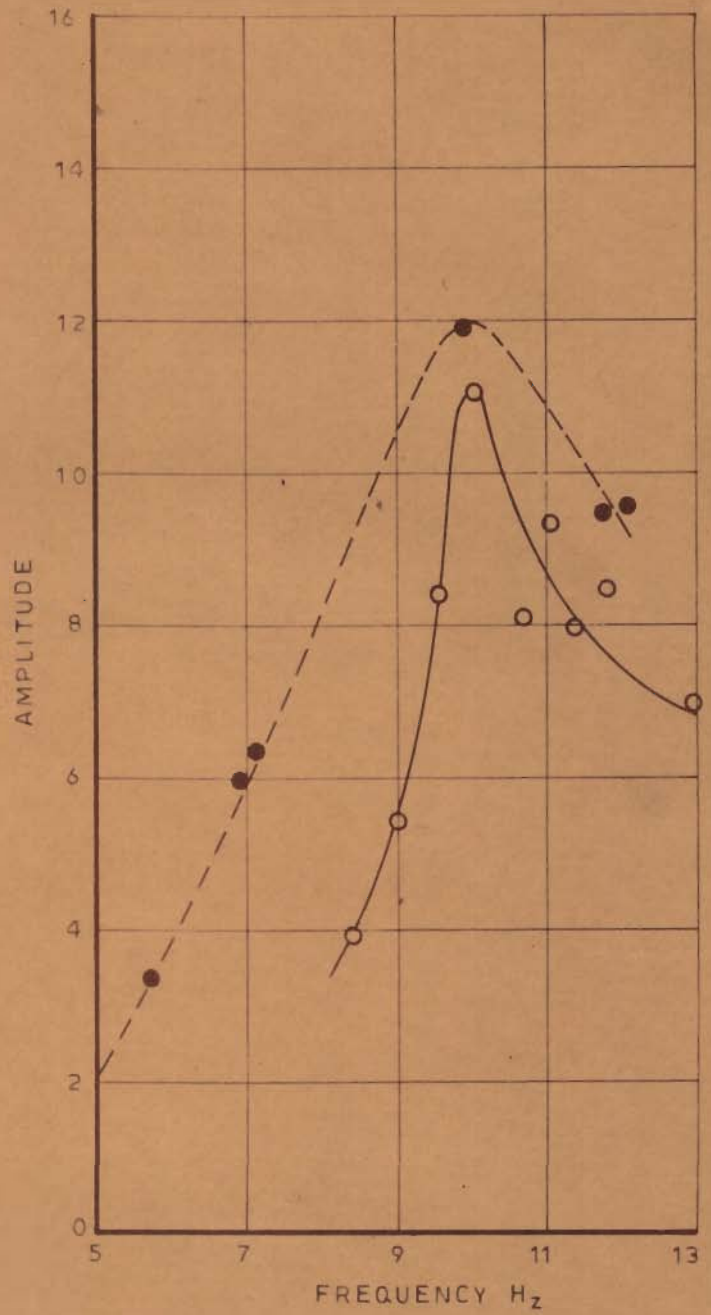
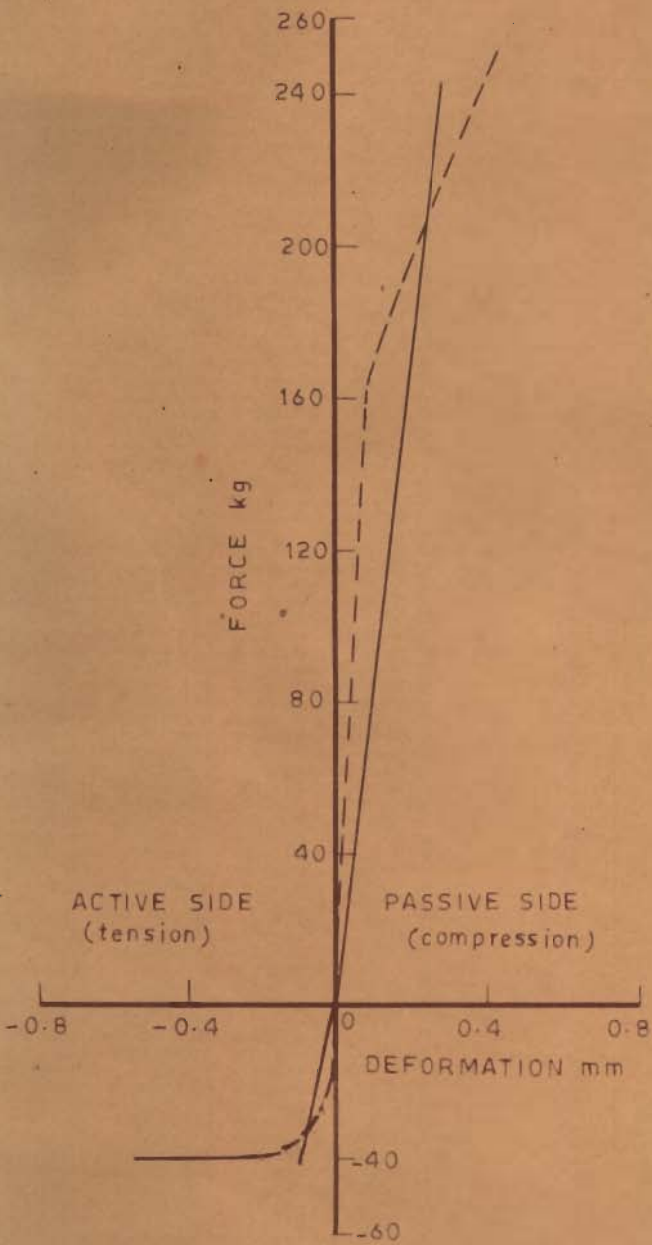
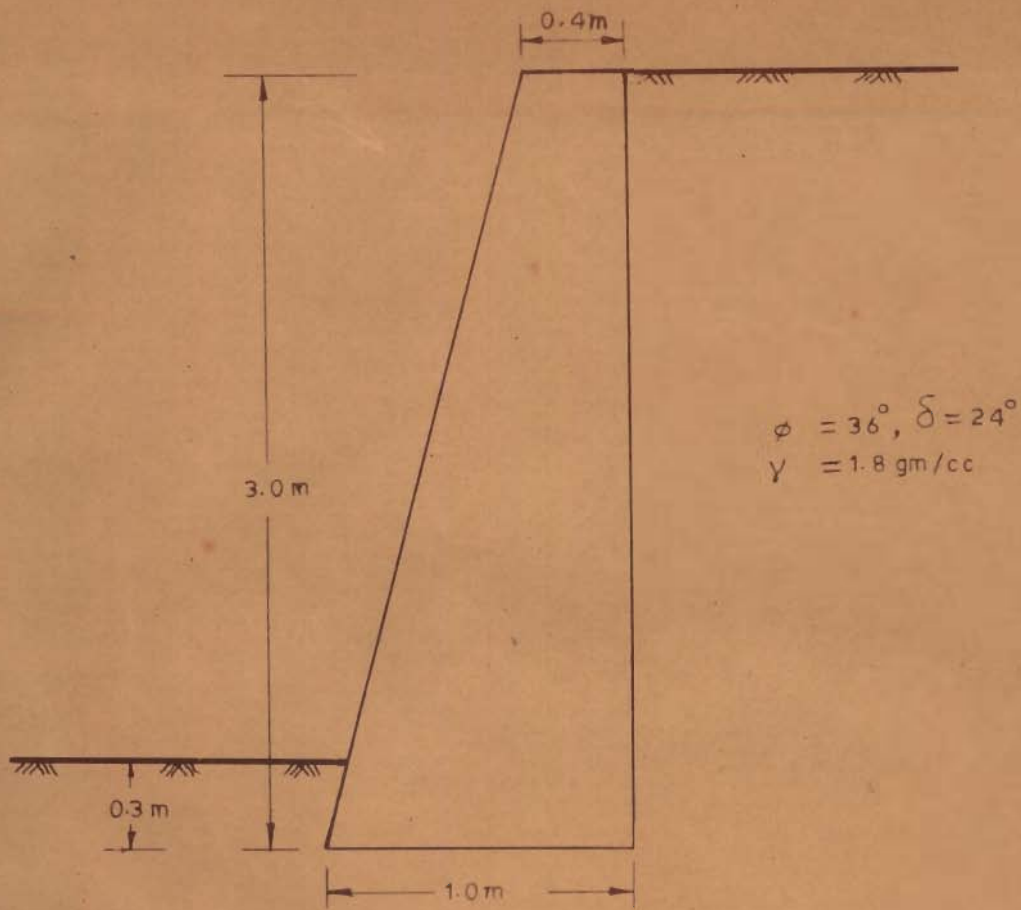
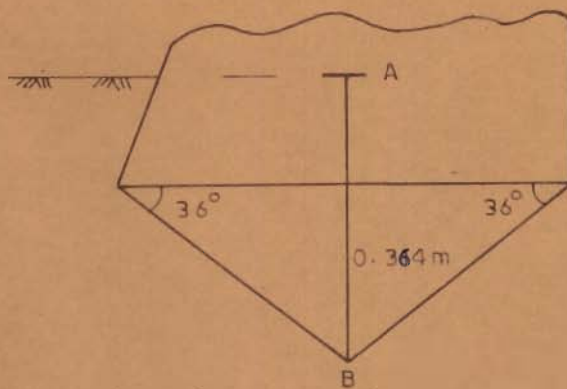


FIG. 6.20_LOAD DEFORMATION CURVE EXPERIMENTALLY DETERMINED

FIG. 6.21_FREQUENCY VS AMPLITUDE OF MODEL WALL



(a)



(b)

FIG. 6.22 _ THE PROBLEM OF RETAINING WALL ANALYSED

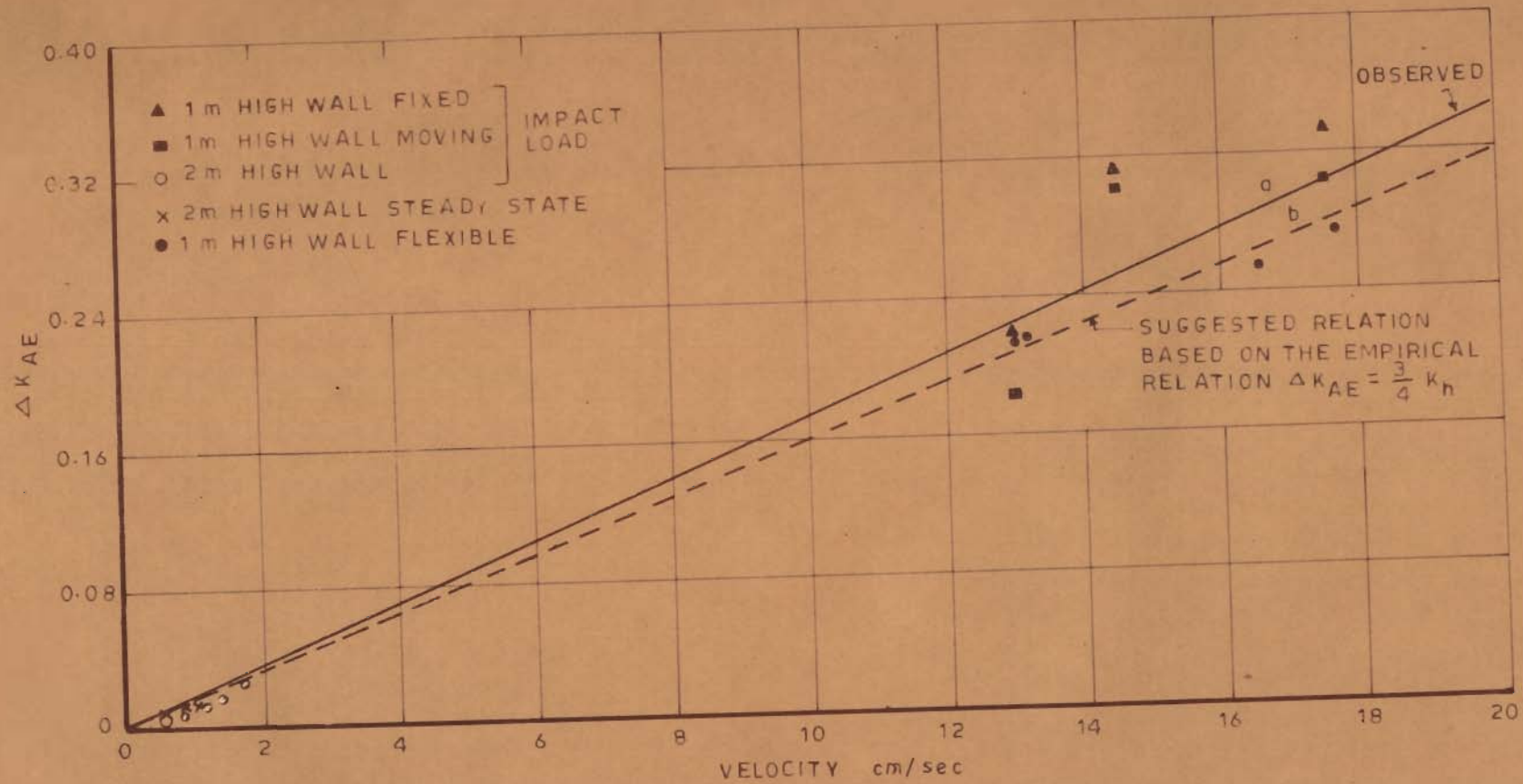


FIG. 7.1 - COEFFICIENT OF DYNAMIC INCREMENT AT VARIOUS VELOCITIES

VITA

Name	P. NANDAKUMARAN
Born	On 1st May 1943 at Calicut, Kerala, India
Education	Holy Child Convent, Kunnankulam, Kerala, 1948-1952
	District Board Upper Primary School, Nilambur. 1952-1954
	Govt Manavedan High School Nilambur. 1954-1958
	Guruvayurappan College, Calicut. 1958-1959
	Engineering College, Trichur. 1959-1964
	University of Roorkee. 1965-1967
Degrees	B. Sc. (Engineering) Civil, 1964
	M. E. (Hon's), Civil 1967
Experience	Lecturer in Civil Engrg, N. S. S. College of Engineering, Palghat -8 April 1964-Nov 1964
	Technical Teacher Trainee, University of Roorkee, Dec. 1964 - Jan. 1968
	Lecturer in Soil Dynamics, School of Research and Training in Earthquake Engineering, University of Roorkee, Roorkee Jan. 1968-June 1972
	Reader at School of Research and Training in Earthquake Engineering, University of Roorkee, Roorkee July 1972 onwards
Professional Societies Membership	1. Indian Geotechnical Society 2. Indian Society of Earthquake Technology

Publications

Narain, J., Saran, S. and Nandakumaran, P. (1969), "Model Study of Passive Pressures in Sand" Jl. SM and F divn. Proc. ASCE, Vol 95, No. SM 4, July, 1969.

Nandakumaran, P., Dhiman, H. C. (1970) "A Miniature Earth Pressure Cell for Dynamic Studies" Journal Indian National Soc. of Soil Mech. and Found. Engg. Vol 9, No. 1, 1970

Chandrasekaran, V. and Nandakumaran, P. (1970), "Importance of Soil and Foundation During Earthquakes", Bulletin Ind. Soc. of Earthquake Tech. March, 1970.

Nandakumaran, P., Prakash, S. and Mitra, P. K. (1970), "Yield Acceleration of Cohesionless Slope Under Steady State Vibrations" Proc. International Geotechnical Conf. Shiraz, Iran, September, 1970.

Prakash, S., Chandrasekaran, V. and Nandakumaran, P. (1970), "Behaviour of Battered Piles Under Lateral Loads", International Geotechnical Conf. Shiraz, Iran, September, 1970.

Nandakumaran, P. and Prakash, S. (1970), "The Problem of Retaining Walls in Seismic Zones" IV Symp on Earthquake Engg., Vol. 1, November, 1970.

Prakash, S., Chandrasekaran, V. and Nandakumaran, P. (1970), "Stability of Slopes During Earthquakes" IV Symp. on Earthquake Engineering Vol. 1, November, 1970.

Prakash, S., Nandakumaran, P. and Chandrasekaran, V. (1971), "Earthquake Considerations for Foundation Design Around Delhi Region", Proc. Seminar on Foundation Problems in and Around Delhi Region, Indian Geotechnical Society, January, 1971

Narain, J, Saran, S. and Nandakumaran, P. (1971) "A Study of Rupture Surface in Cohesionless Backfill of a Rigid Wall" Indian Geotechnical Journal Vol.1 No.1, January, 1971.

Prakash, S, Chandrasekaran, V. and Nandakumaran, P. (1971), "Behaviour of Foundations on Saturated Sand Masses", Indian Geotechnical Journal Vol.1, No.4, Sept., 1971.

Prakash, S, Chandrasekaran, V, Nandakumaran, P. and Krishen Kumar (1972), "Model Studies on Rockfill Dams at Pandoh", Proc. 42nd Annual Research Session Central Board of Irrigation and Power, Madras Vol.1, Publ. No. 116, June, 1972.

Prakash, S, Nandakumaran, P. and Chandrasekaran, V. (1972) "Some Oscillatory Tests on Clay" Second Southeast Asian Conf. on Soil Mech. and Found. Engg., Hong Kong, Nov. 1972.

Prakash, S. and Nandakumaran, P. (1973), "Dynamic Earth Pressure Distribution on Rigid Walls"; Symp on Earth and Earth Structures Subjected to Earthquake and other Dynamic Loads, Roorkee, March, 1973.

Prakash, S, Nandakumaran, P. and Joshi, V.H. (1973), "Design, Fabrication and Performance of an Oscillatory Shear Box", Indian Geotechnical Journal, April, 1973.

Krishna, J, Arya A.S., Sekaran, A.R.C., Chandra, B, Thakkar, S.K. and Nandakumaran, P, "Feasibility Study of a Nuclear Power Plant in Alluvial Deposit", Fifth World Conf. on Earthquake Engineering, Rome, June 1973.

Nandakumaran, P. and Joshi, V.H. (1973), "Static and Dynamic Active Earth Pressures Behind Retaining Walls", Bulletin, Ind. Soc. of Earthquake Tech. Sept., 1973.